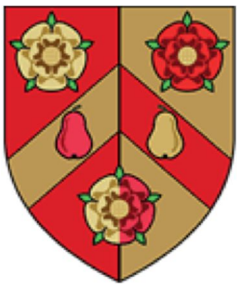
The repair mechanisms of DNA damage induced by G-quadruplexes stabilisation in BRCA1/2-deficient cells



Hugo Benainous

University of Oxford

Wolfson College



A thesis submitted for the degree of

Doctor of philosophy

Michaelmas Term 2020

Abstract

Mutations in the breast cancer type 1 or 2 susceptibility protein *(BRCA1* or *BRCA2* respectively) predispose to the onset of breast and ovarian cancer. Indeed, cells lacking homologous recombination (HR) rely mainly on error-prone mechanisms to repair DNA double-strand breaks (DSBs) and have an inherently increased sensitivity to replication stress. These defects can be exploited therapeutically with chemicals such as poly [ADP-ribose] polymerase (PARP) inhibitors. Among this family of inhibitors, olaparib has been approved by the Food and Drug Administration (FDA) in January 2018 as a maintenance treatment for breast cancer patients with *BRCA* defects. However, tumours ultimately develop resistance to olaparib treatment, stressing the need to develop new approaches to target resistant tumours. G-quadruplexes (G4s) are thermodynamically stable secondary DNA structures resulting from the folding of guanine-rich DNA sequences. During replication, unresolved G4s due to small molecules stabilisation, can induce fork stalling, ultimately leading to DSBs formation. Among these small molecules, pyridostatin (PDS) has been shown to effectively stabilise G4 structures. In BRCA-deficient cells HR is impaired, thus PDS leads to DSBs accumulation and genomic instability. Surprisingly, we observed that DSBs induced by PDS could be repaired in BRCA2-deficient cells. We identified classical non-homologous end joining (cNHEJ) as a repair mechanism for PDS-induced DNA damage in our cell

models including those with HR-deficient background using two chemical inhibitors of the DNA-dependent protein kinase catalytic subunit (DNA-PKcs), a protein ensuring effective cNHEJ functions. Indeed, we described that PDS and DNA-PKcs inhibitors have a synergistic effect in BRCA-deficient cells. Furthermore, we showed that PDS-induced lesions seem retained longer in BRCA-deficient cells that have acquired resistance to PARP inhibitors via the loss of the p53 binding protein 1 (53BP1). Whether this is due to the roles of 53BP1 in regulating cNHEJ activity or end resection remains to be elucidated. In summary, our results provide new insights into G4 ligands-induced DNA damage and their repair in HR-defective models. This knowledge could be further exploited towards a new therapeutic approach to treat mutated BRCA carriers with breast cancer that have developed PARP inhibitors resistance.

Acknowledgements

I would like to acknowledge Cancer Research UK (CRUK) and Medical Council Research (MRC) for allowing me to conduct research in the Oxford Institute for Radiation Oncology and supporting me financially via the MRC industrial strategy studentship. I would like to thank my supervisor Madalena Tarsounas, my co-supervisors Andy Ryan and Kristijan Ramadan and Merck KGaA, our industrial partner, for their supervision.

I thank people in our team for their valuable daily interactions, especially Rebecca for her supervision during the first months of my DPhil and constant advice until the end of the degree.

I would like to thank my high school philosophy teacher Stephane and my former boss Christophe, both essential mentors who shaped my passion for science and pushed me towards higher education.

A special thanks to my family and my friends Clement, Timo, Florian, Daniëlle and Quentin for the brainstorms, the unconditional support, the joy and the laughs they brought along the way.

Finally, a massive thanks to my partner Lottie for her tremendous help and support in every aspect of this unforgettable Oxford experience.

Declaration

I declare that the work presented in this thesis is wholly my own, except where stated otherwise, and that no portion of this work has been presented previously for another qualification at this or any other University.

Number of words

The thesis contains 32,035 words, excluding figures.

Nomenclature

Human genes are displayed in upper case and italic (e.g. *BRCA1*).

Mouse genes are displayed in italic with only the first letter in uppercase (e.g. *Brca1*).

Proteins are displayed in upper case (e.g. BRCA1).

Latin terminology is displayed in italic (e.g. *Saccharomyces cerevisiae*).

List of abbreviations

3'-UTR	3' Untranslated Region
5'-UTR	5' Untranslated Region
53BP1	p53 Binding Protein 1
Å	Angstrom
a-EJ	alternative End Joining
ATM	Ataxia Telangiectasia Mutated
ATR	ATM- and RAD3-related
ATRIP	ATR-Interacting Protein
BARD1	BRCA1-Associated RING Domain Protein 1
bp	base pair
BLM	Bloom syndrome protein
BRCA1	Breast cancer type 1 susceptibility protein
BRCA2	Breast cancer type 2 susceptibility protein
BSA	Bovine Serum Albumin
CD	Circular Dichroism
CDK2	Cyclin Dependent Kinase 2
CDK4	Cyclin Dependent Kinase 4
CHK1	Checkpoint Kinase 1
cGAS	cGAMP synthase

cNHEJ	classical Non-Homologous End Joining
CtIP	C-terminal binding protein 1-Interacting Protein
D-loop	Displacement loop
DDR	DNA Damage Response
ddH_2O	double distilled H_2O
dHJ	double Holliday Junction
DMEM	Dulbecco's Modified Eagle's Medium
DNA	deoxyribonucleic acid
DNA-PKcs	DNA-dependent Protein Kinase catalytic subunit
DNA2	DNA Replication Helicase/Nuclease 2
dNTP	Deoxyribonucleotide Triphosphate
DOX	Doxycycline
DSBs	Double-Strand Breaks
dsDNA	double-stranded DNA
DSS1	Deleted in Split hand / Split foot protein 1
EdU	5-ethynyl-2'-deoxyuridine
EJ	End Joining
FANCJ	Fanconi anemia group J protein
FBS	Foetal Bovine Serum
FDA	Food and Drug Administration
G4s	G-quadruplexes

HR	Homologous Recombination
HU	Hydroxyurea
IF	Immunofluorescence
IFN	Interferon
IMDM	Iscove's Modified Eagle's Medium
ISG	Interferon Stimulated Genes
KAP1	KRAB [Krüppel-Associated Box Domain]-Associated Protein 1
KRAS	Kristen Rat Sarcoma viral proto-oncogene
LIG4	DNA Ligase IV
MEF	Mouse Embryonic Fibroblasts
MLH1	MutL Homolog 1
MMEJ	Microhomology-Mediated End Joining
MMR	Mismatch Repair
MMS	Methyl Methanesulfonate
MRE11	Meiotic Recombination 11
mRNA	messenger Ribonucleic Acid
mTOR	mammalian Target Of Rapamycin
MSC	MSC2490484A or M3814
NBS1	Nijmegen Breakage Syndrome 1
NMM	N-Methyl Mesoporphyrin IX
NMR	Nuclear Magnetic Resonance

p53	tumour protein p53
PALB2	Partner And Localiser of BRCA2
PARP	Poly [ADP-Ribose] Polymerase
PAXX	Paralog of XRCC4 and XLF
PBS	Phosphate-Buffered Saline
PBST	0.05% Tween 20 in PBS
PCNA	Proliferating Cell Nuclear Antigen
PDS	Pyridostatin
PIKK	Phosphatidylinositol 3-kinase-related kinases
POT1	Protection of Telomeres 1
ppi	pixels per inch
PQS	Putative G-Quadruplex Sequences
PTX	Paclitaxel
RER	Ribonucleotide Excision Repair
RNA	Ribonucleic Acid
RNA-seq	RNA-sequencing
ROS	Reactive Oxygen Species
RPA	Replication Protein A
RT	Room Temperature
RTEL1	Regulator of Telomere Elongation Helicase 1

SEM	Standard Error of the Mean
SDS-PAGE	Sodium Dodecyl Sulfate-polyacrylamide gel electrophoresis
SDSA	Synthesis-Dependent Strand Annealing
shRNA	short hairpin RNA
siRNA	small interfering RNA
SMARCAL1	SWI/SNF related, matrix-associated, actin-dependent
SMC1	Structural Maintenance of Chromosomes 1
SSA	Single-Strand Annealing
SSB	Single-Strand Break
ssDNA	single-stranded DNA
TOP1	Topoisomerase I
TOP2	Topoisomerase II
TOPBP1	DNA Topoisomerase II-Binding Protein 1
TMS	Telomestatin
UV	Ultraviolet
XLF	XRCC4-Like Factor
XRCC4	X-Ray Repair Cross Complementing 4
WB	Western Blot
WT	Wild Type

List of figures

Figure 1: DNA damage response to genotoxic stress 2

Figure 2: Schematic representation of cNHEJ and HR..... 8

Figure 3: Alternative end joining DNA repair mechanisms 11

Figure 4: Schematic representation of replication fork stalling and restart 13

Figure 5: Schematic representation of G-quadruplexes structures..... 21

Figure 6: G-quadruplexes biological roles and potential application 34

Figure 7: Toxicity of DNA-PKcs inhibitors on BRCA2-deficient human cells..... 39

Figure 8: Efficiency and specificity of DNA-PKcs inhibitors in DLD1 cells 40

Figure 9: Effect of DNA-PKcs inhibitors in combination with PDS on BRCA-deficient human cell viability..... 44

Figure 10: Effect of DNA-PKcs inhibitors in combination with olaparib on BRCA-deficient human cell viability..... 45

Figure 11: PDS synergy with NU7441 or MSC relies mainly on DNA-PKcs activity 47

Figure 12: Effect of DNA-PKcs inhibitors in combination with CX5461 on BRCA-deficient human cell viability 48

Figure 13: Effect of PDS in combination with NU7441 or MSC on BRCA-deficient human cell survival 50

Figure 14: PDS-induced DNA damage can be partly repaired in a *BRCA2*-independent manner 53

Figure 15: DNA-PKcs inhibitor NU7441 impairs the recovery of BRCA2-deficient cells upon PDS treatment 55

Figure 16: Effect of DNA-PKcs inhibitor NU7441 on BRCA2-deficient cells upon olaparib treatment 56

Figure 17: Effect of PDS in combination with olaparib on BRCA2-deficient human cell viability 58

Figure 18: Effect of G4 ligands, olaparib and NU7441 on cNHEJ-deficient human cell 60

Figure 19: Recovery of BRCA1-deficient mouse cells upon PDS treatment is impaired by NU7441 64

Figure 20: Recovery of BRCA-deficient mouse cells upon olaparib treatment 65

Figure 21: Recovery of olaparib resistant BRCA-deficient mouse cells upon PDS or olaparib treatment 66

Table of content

1 Introduction 1

1.1 Genome instability and tumorigenesis 1

1.2 DNA damage signalling and repair 4

1.3 Replication stress 12

1.4 BRCA-deficient tumours and therapeutics 16

1.5 G-quadruplexes 20

2 Results 36

2.1 Characterisation of novel DNA-PKcs inhibitor MSC 36

2.2 G4s ligands or olaparib in combination with DNA-PKcs inhibitors 41

2.3 PDS- and olaparib-induced DNA damage recovery in BRCA-deficient cells… 51

2.4 PDS treatment on cells with various cNHEJ defects 59

2.5 PDS- and olaparib-induced DNA damage recovery in BRCA1-deficient and olaparib resistant cells. 61

3 Discussion 69

3.1 MSC seems more potent than NU7441 69

3.2 G4s ligands synergise with DNA-PKcs inhibitors 70

3.3 PDS-induced DNA damage can be partly repaired in BRCA-deficient cells..... 72

3.4 Cells with cNHEJ defects have an increased sensitivity to PDS..... 75

3.5 PDS-induced DNA damage is retained in olaparib resistant cells 76

4 Conclusion and outlook 79

5 Material and methods 85

5.1 Cell lines and growth conditions..... 85

5.2 Immunoblotting 86

5.3 Antibodies..... 88

5.4 Western blot quantification..... 89

5.5 FACS analysis 89

5.6 Cell viability assays and combinations 90

5.7 Clonogenic assay 90

5.8 Preparation of metaphase chromosome spreads 91

5.9 Transfection with siRNA 92

6 References 94

7 Appendix 142

7.1 Supplementary Figures 143

1 Introduction

1.1 Genome instability and tumourigenesis

Deoxyribonucleic acid (DNA) was initially isolated by the Swiss biologist Friedrich Miescher in 1869 and its molecular structure uncovered by the combined efforts of Francis Crick, James Watson, Maurice Wilkins and Rosalind Franklin in 1953[1]. DNA carries the genetic information encoding for proteins that maintain growth, homeostasis and reproduction. These biological processes were considered as fundamental characteristics to define life[2] and are shared among all known living organisms. The human body is constituted of approximately 10^{13} cells, each containing about 6 billion nucleotides[3], the building block of the DNA double helix.

The large amount of genetic material stored in cells is constantly challenged by genotoxic stress, leading to thousands of DNA lesions in every human cell every day[4]. This type of cellular stress can have external or internal origin **(Figure 1)**. Exogenous sources can be found in everyday life in the form of carcinogenic chemicals (such as cigarette smoke or burnt aliments), ultraviolet (UV) radiation or X-rays (medical origin or radioactivity)[5]. Endogenous DNA lesions can be caused by the oxidative stress induced by various biochemical processes (such as aerobic respiration, releasing reactive oxygen species (ROS))[6] or during DNA replication when base deamination or base mis-incorporation occurs[7,8].

The majority of DNA lesions are single-strand DNA (ssDNA) breaks (SSB)[8] and can eventually be converted into DSBs. A single DSB occurrence can induce cellular death[9] and is therefore considered as the most toxic form of DNA lesions. In turn, DNA damage can lead to replication stress[10,11], genomic instability[8], severe chromosomal aberrations[12,13] and cell death. These are common hallmarks of tumour predisposition[14].

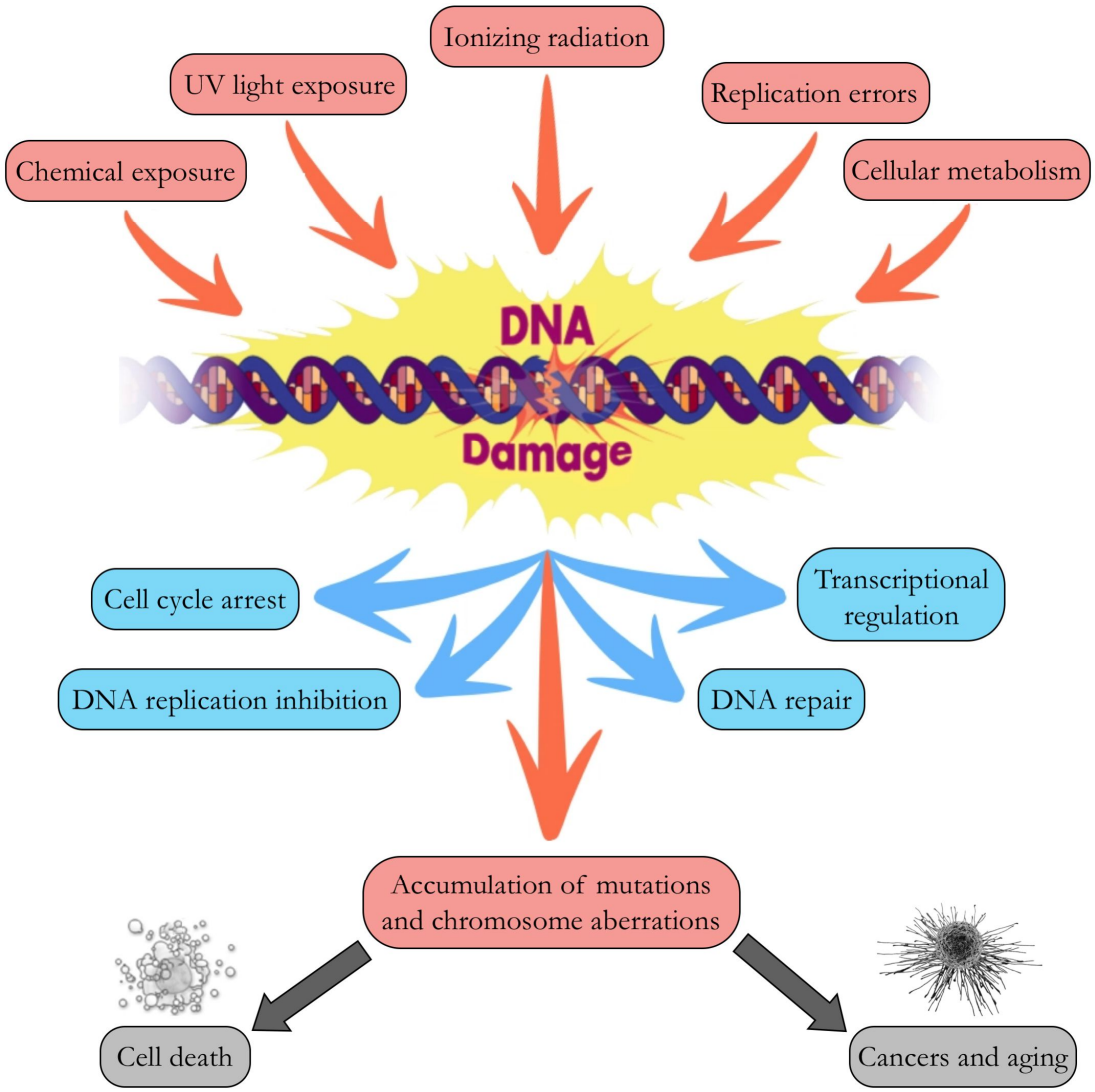


Figure 1: DNA damage response to genotoxic stress

Adapted from[15]

In order to avoid such a dramatical fate and protect genome integrity, evolution has equipped cells with various mechanisms to fix DNA alterations or, if damage is too severe, trigger cellular death[16]. Both pathways prevent the spread of compromised DNA to daughter cells. However, inappropriate or inaccurate repair of the DNA can act as a double-edged sword. Whilst restoring DNA continuity by ligating both ends of a DNA break together, part of the genetic code in the vicinity of the break can be lost or altered, ultimately resulting in DNA mutation[17].

Fortuitously, not all mutations have an impact on cells integrity. Indeed, most of the human genome is composed of untranscribed regions, protein coding regions account only for a small percentage of the whole genome (around 2%)[18] and mutations can be silent if the amino acid sequences remain unchanged during translation. Furthermore, only a subset of genes have the potential to induce tumourigenesis. Among them, there are genes that encode proteins involved in cell cycle regulation, DNA damage repair, cellular death or more broadly to maintain genome stability. Any abnormal function of such genes can favour cancer onset and therefore they are designated as tumour suppressors. A well characterised tumour suppressor is the gene encoding the tumour protein p53 (*TP53*) which has a critical role in genome integrity, is frequently mutated in cancer and is broadly considered as "the guardian of the genome"[19]. Another class of genes, known as oncogenes, have the potential to induce tumourigenesis when dysregulated. They differ from

tumour suppressors regarding that their biological roles are not primarily involved in the maintenance of genome integrity. For instance, the Kristen rat sarcoma viral proto-oncogene (*KRAS*) encodes for a GTPase involved in cell growth, is frequently observed mutated across different cancer types and a single mutation within its gene can cause malignancy[20]. For these reasons, somatic mutations in tumour suppressors or oncogenes can favour tumourigenesis onset or push tumours towards a more advanced cancer stage. These are usually referred to as "driver" mutations[21].

In order to ensure the faithful maintenance of genome stability upon DNA lesions, a complex network of proteins constituting the DNA damage response (DDR) is activated to promote and tightly regulate the DNA repair machineries[22].

1.2 DNA damage signalling and repair

Upon DNA damage, the DDR initiates the recognition of DNA lesions followed by a signalling cascade which, in turn, recruits and promotes the appropriate repair mechanism. In order to increase the time available for the repair and facilitate protein recruitment to the site of damage, the cell-division cycle is slowed down or paused during this process. Cell cycle arrest is equally important to avoid further issues from the encounter between the DNA lesions (plus bound proteins) and the

replication machinery[22]. A key protein orchestrating DDR signalling is ataxia telangiectasia (AT) mutated (ATM). This phosphatidylinositol 3-kinase-related (PIKK) kinase was initially discovered mutated in patients with AT[23], a rare inherited disorder characterised by neuronal degeneration, immunodeficiency, chromosome instability and cancer predisposition. Patients with AT appeared to have a poor tolerance to radiotherapy[24], later explained by a profound radiosensitivity of the patients cells[25], which was suggested to be linked to defects in DNA repair[26]. Upon DSBs, ATM phosphorylates hundreds of proteins[27] mainly involved in DNA repair, chromatin remodelling, cellular death and cell cycle checkpoint activation[28]. A critical substrate activated by ATM is the tumour suppressor p53. ATM can phosphorylate p53 at serine 15 which, in turn, induces its stabilisation and triggers cell cycle arrest in G1 or promotes cellular death via apoptosis or senescence[29,30]. The gene encoding p53 (*TP53*) was frequently found mutated in a broad range of cancers including serous ovarian carcinomas and breast adenocarcinomas[31]. ATM is recruited to DNA damage site by Nijmegen breakage syndrome 1 (NSB1, also known as nibrin), associated with meiotic recombination 11 (MRE11) and RAD50 to form the MRE11-RAD50-NBS1 (MRN) complex[32]. Once recruited on chromatin ATM phosphorylates the histone variant H2AX on serine 139[33], usually referred to as yH2AX. ATM spreads H2AX phosphorylation on chromatin around the DSBs[34], forming a signalling platform for further protein recruitment. Indeed, H2AX was reported to be highly phosphorylated upon

DSBs[35], thus γH2AX is frequently used as a DSBs marker in DNA damage studies. MDC1 then interacts with γH2AX[36] and is further stabilised on chromatin via ATM phosphorylation[37]. In turn, MDC1 triggers a signalling cascade that results in DNA damage repair factors recruitment on chromatin, such as 53BP1[38].

In mammalian cells, the integrity of the DNA is maintained by two major DSBs repair pathways, HR[39,40] and cNHEJ[41,42] **(Figure 2)**. HR is considered as an error-free mechanism, relying on the sister chromatid as a template for accurate repair[43], thus occurring during S and G2 phases of the cell cycle, when sister chromatids become available. Initially, the MRN complex is recruited to damage sites and interacts with the C-terminal binding protein 1-interacting protein (CtIP) to initiate DNA end processing[44,45]. Indeed, CtIP promotes the endonuclease activity of MRE11 which creates a nick in the DNA and is then followed by 3' to 5' exonuclease activity, removing nucleotides towards DNA end. Meanwhile, the 5' to 3' long range resection of the DNA is conducted by other exonucleases such as EXO1, BLM-DNA2 or BLM-WRN complex[46-52]. This process of creating single-stranded DNA tails, designated as DNA end resection, is central in DSB repair choice, as resected DNA ends become committed towards homology-based repair. CtIP is phosphorylated by ATM[45,53] and interacts with BRCA1[54-59] leading to resection enhancement. However, CtIP-mediated resection can still happen independently of ATM or BRCA1[60,61]. BRCA1's function in resection and more

broadly in HR-related processes require its association with its interacting partner "BRCA1-associated RING domain protein 1" (BARD1)[62-64]. The single-stranded DNA (ssDNA) tails arising from nucleolytic processing become a specific substrate for the replication protein A (RPA) which forms a heterotrimer on ssDNA[65], providing protection from further degradation. BRCA2 is then recruited, in complex with BRCA1, BARD1 and partner and localiser of BRCA2 (PALB2)[66,67], to displace RPA and load RAD51 on ssDNA[54,62,66-69]. The interaction between RPA and BRCA2 is mediated via its interacting partner, the deleted in split hand / split foot protein 1 (DSS1). RAD51 proteins are then assembled with ssDNA into nucleofilaments, allowing the search for DNA template in either sister chromatid or similar substrate[69,70]. This process results in the creation of a displacement loop (D-loop). The resolution of the D-loop can be achieved through synthesis-dependent strand annealing (SDSA)[71] or via the formation of a DNA structure called a double Holliday junction (dHJ)[72]. Following DNA repair and synthesis, the double Holliday junction can be dissolved by various resolvases such as SLX1-SLX4 and MUS81-EMS1[73-76] or BLM and GEN1[77]. While both pathways lead to accurate repair, resolution of the dHJ can lead to cross-over recombination[71,78-80].

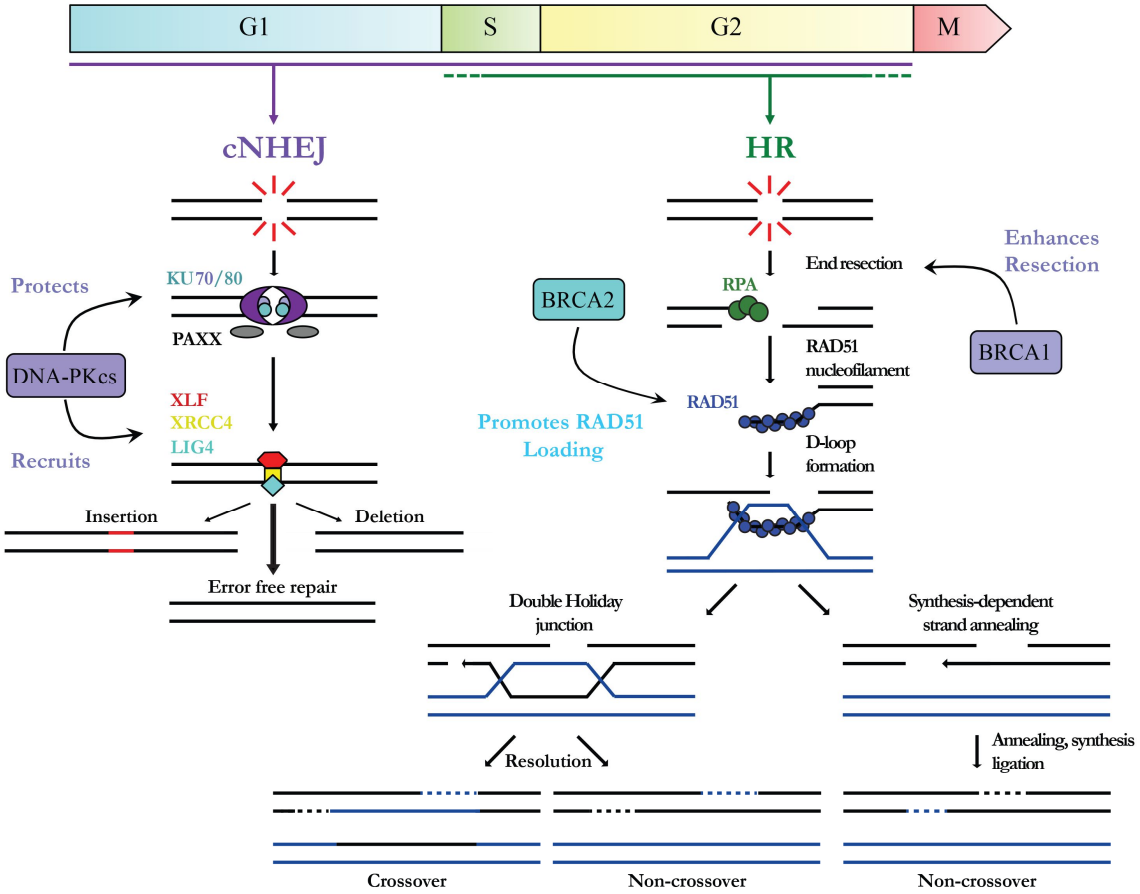


Figure 2: Schematic representation of cNHEJ and HR

cNHEJ is the prevalent DSBs repair mechanism in G0/G1 and remains active throughout the entire cell cycle except during mitosis[81,82]. cNHEJ machinery is also required when programmed DSBs are generated during lymphocyte maturation by V(D)J recombination[83,84] and class-switch recombination (CSR)[85]. These processes are essential to generate a high diversity of antigen receptor repertoires in lymphocyte B and T cells. For this reason, defects in NHEJ factors lead to severe immunodeficiency in both mice and humans[86-89]. Mechanistically, broken DNA ends are first recognised and protected by two highly abundant proteins, Ku70 and

Ku80, forming a scaffold for the recruitment of DNA-PKcs[90], another crucial PIKK of the DDR. Recently, PAXX has been characterised as a paralogue of the X-Ray repair cross complementing 4 protein (XRCC4) and the XRCC4-like factor (XLF), stabilising DNA-PKcs on chromatin[91]. DNA-PKcs phosphorylates Ku70/80 and itself in order to facilitate the recruitment of downstream proteins, including the DNA ligase IV (LIG4)[92,93]. These proteins form the XRCC4-LIG4-XLF complex which ultimately ligates DNA ends together[94-97]. Despite being mainly characterised to repair blunt or near-blunt DNA ends, a subset of DSBs that require further end processing can still be repaired through cNHEJ. Indeed, the nuclease Artemis is phosphorylated by DNA-PKcs and can promote some end processing[89,98-101]. Whilst cNHEJ is a fast and efficient process as it does not require an appropriate template for the repair, the low homology of DNA ends (0 to few nucleotides) can cause errors. It is believed that insertions and deletions frequently occur as the outcome of the repair due to DNA degradation or processing[102]. However, it appears that cNHEJ is robust and reliable under normal circumstances[103,104]. Nevertheless, mutations in components ensuring the correct function of cNHEJ can result in highly toxic events[105,106], such as chromosomal rearrangements, when breaks from different chromosomes are ligated due to close proximity[107-109].

In order to avoid inefficient or error-prone repair, HR and cNHEJ are tightly regulated depending on the cell cycle phase and DNA end resection[110]. While BRCA1 promotes end resection and pushes towards HR, 53BP1 has been characterised as a negative regulator of end resection, therefore promoting cNHEJ[111-113]. The interplay between 53BP1 and BRCA1 upon DNA damage suggest that they are competing to dictate the DNA damage repair choice[111,112,114-116]. When the main DSBs DNA repair pathways, HR and cNHEJ, are unable to function, the DNA integrity can still be partly rescued by alternative end joining (a-EJ) DNA repair mechanisms depending on strands homology[117-120] (**Figure 3**). Single-strand annealing (SSA) relies on extensive CtIP-dependent DNA end resection, generating long 3' ssDNA overhangs[117,121]. After DNA end resection, complementary sequences between the two ssDNA are annealed by the recombination protein RAD52[122] and the remaining ssDNA overhangs, referred to as flaps, are likely cleaved by the ERCC1-XPF complex[123]. Similarly, microhomology-mediated end joining (MMEJ) relies on microhomology annealing following end resection[124]. The polymerase theta (POLQ) has an important role during the annealing step and is synthetically lethal with BRCA1[125,126]. The concept of synthetic lethality occurs when a combination of two or more genes are disrupted and / or dysregulated leading to cell death while the single deficiency on their own does not impact cell viability. It means that POLQ and BRCA1 synthetic lethality suggests that MMEJ is the main backup mechanism upon HR loss. Even

if DNA breaks with low or no homology (0-2 nucleotides) can be directly repaired with end joining (EJ), the two other a-EJ repair mechanisms remove the non-complementary ssDNA overhangs, likely resulting in relatively large genomic deletions.

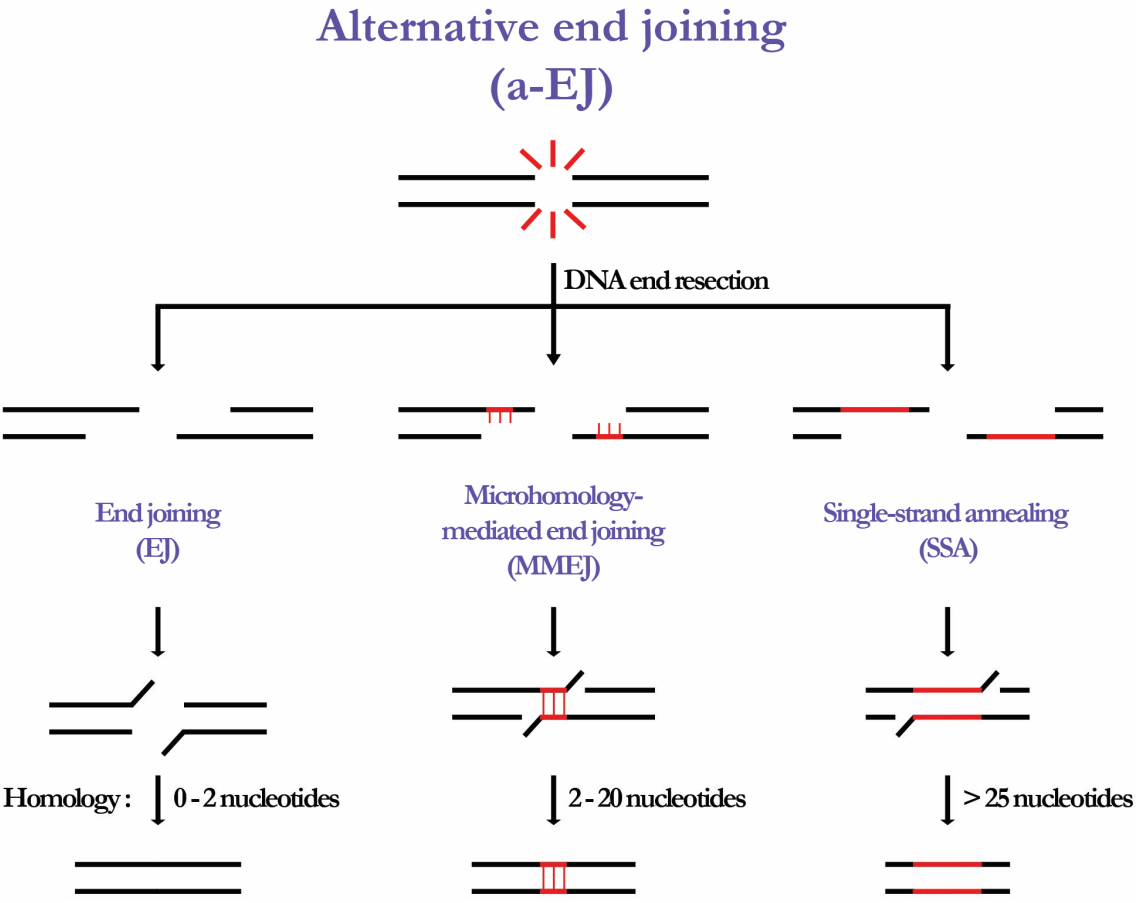


Figure 3: Alternative end joining DNA repair mechanisms

Adapted from[120].

Whilst the efficient signalling and repair of DNA lesions is crucial to avoid genomic instability, it is equally important to prevent the emergence of mutations and DNA

damage in the first place. A common source of DNA damage arises during DNA replication when various issues can cause the replication fork to stop. When unaddressed, the stalled replication forks ultimately collapse, leading to DSBs formation. Therefore, promoting the protection and the restart of the replication forks is essential to limit DNA damage onset.

1.3 Replication stress

DNA replication is a fundamental biological process that duplicates the DNA during cell division. The complete and reliable replication of the DNA is essential to transmit accurate genomic copies to the daughter cells and prevent genomic instability. Unfortunately, many factors can cause the replication machinery to be disrupted, slowed down, arrested or unable to finish replication. Such abnormal functions and their underlying causes usually constitute the concept of replication stress[11].

When the replication machinery, composed of the replication-associated proteins, called the replisome, encounters an unusual DNA structure, the replication fork is likely to stop, forming what is referred to as stalled replication fork. Such structures are called replication barriers and can arise in the form of secondary structured DNA, ongoing transcription machinery, DNA lesions, heterochromatin or other protein adducts on DNA[127]. Additionally, depletion of the deoxyribonucleotide

triphosphate (dNTP) pool, fuel for DNA polymerases, can slow down the replication fork and lead to fork stalling when sustained. This was shown using hydroxyurea (HU) which inhibits dNTP synthesis[128]. Stalled replication forks undergo extensive resection by nucleases and can eventually collapse leading to DSBs, thus compromising genome integrity[129]. Incomplete replication can lead to highly detrimental chromosomal aberrations in mitosis. Indeed, the part of the genome that is not duplicated will be lost in one of the daughter cells and chromosomes that remain linked together by non-replicated DNA can cause more issues when pulled apart in anaphase[130]. In order to prevent the fork collapsing, allowing for normal replication and maintenance of genome integrity, many mechanisms have evolved to signal and manage replication stress (**Figure 4**).

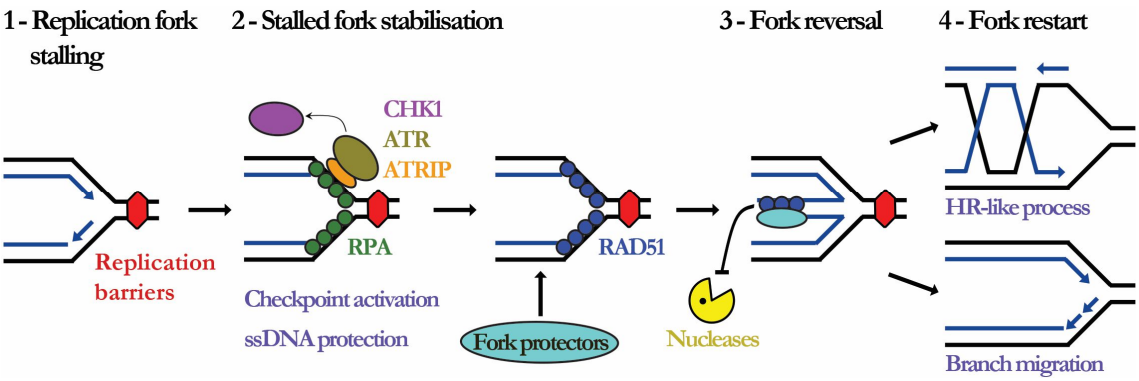


Figure 4: Schematic representation of replication fork stalling and restart

Adapted from[131]

Upon replication fork stalling, the protein orchestrating the cellular response is ATM- and RAD3-related (ATR), the third major PIKK protein involved in DDR with ATM and DNA-PKcs[132]. The extensive resection occurring at stalled replication forks leads to long ssDNA tracts that rapidly become coated by RPA trimers, stabilising the structure and protecting ssDNA. The ATR interacting protein (ATRIP) recognises and binds to RPA which, in turn, recruits ATR on DNA[133]. ATR is further activated by the DNA topoisomerase II-binding protein 1 (TOPBP1), which interacts with ATRIP as well[134,135]. Upon activation, ATR can phosphorylate and activate checkpoint kinase 1 (CHK1)[136,137]. This induces the degradation of cell division cycle 25A (CDC25A), a protein that activates the cyclin-dependent kinases 2 (CDK2) and 4 (CDK4), both essential proteins for the G1 / S transition of the cell cycle. The decrease of CDK activity induces the slow down and eventually the arrest of cell cycle progression[138-140]. This creates enough time for the repair or to activate cell death, if the damage is too severe to be fixed. ATR interaction with the protein SWI/SNF related, matrix-associated, actin-dependent (SMARCAL1) can also help protect the replication fork and avoid fork collapse[141].

Proteins involved in HR also play a key role in protecting and promoting the restart of stalled replication forks[142]. Indeed, in HU treated cells, BRCA1 and RAD51 formed foci in S phase that colocalise with the proliferating cell nuclear antigen

(PCNA)[143], a cofactor of DNA polymerase and essential for the replication fork progression[144,145]. Subsequent studies have shown that RAD51 localisation to replication fork induces an HR-like mechanism involving RAD51-mediated strand invasion which is, in turn, able to restart the fork[128,129]. Moreover, both BRCA1 and BRCA2 are able to protect the replication fork against extensive nucleolytic degradation by various nucleases[146-149]. Stalled replication forks can form four-way junctions by annealing of the parental and newly synthesised strands, a process referred to as fork reversal. This allows the protection of the fork and promotes the repair and / or restart of the replication fork[150] via HR-like process or branch migration[131]. Evidence has shown that the reverse fork strand is likely recognised by nucleases in absence of BRCA1 or BRCA2, inducing extensive resection and eventually DNA damage[151-153]. These results suggest that BRCA1, BRCA2 and RAD51 protect stalled replication forks against nucleolytic degradation. Interestingly, CtIP was recently described as another protector of stalled replication forks against the DNA replication helicase/nuclease 2 (DNA2) induced resection in a BRCA-independent manner[154]. Moreover, HR-like processes can help to overcome replication barriers and promote replication fork restart[155].

Regarding the crucial roles of BRCA proteins in HR and at stalled replication forks, cells and tumours lacking these factors display an increased sensitivity to replication

stress and DNA damage. Such vulnerabilities can be exploited with various therapeutic approaches to treat cancer patients carrying *BRCA* defects.

1.4 BRCA-deficient tumours and therapeutics

BRCA1 has been initially identified in familial breast cancer by linkage analysis in 1990[156]. The following year, findings validated this observation and further associated *BRCA1* with hereditary familial ovarian cancer[157,158]. Subsequently, mutations in *BRCA1* were found in familial breast and ovarian cancers[159,160]. Allelic loss of *BRCA1* can occur as well in somatic breast and ovarian cancers[161,162]. Besides genomic mutation, the activity of *BRCA1* can be altered due to promoter hypermethylation in both breast and ovarian tumours[162]. Similarly, *BRCA2* was identified, during the same period, as another breast cancer susceptibility gene, being mutated in familial breast cancers[163-165]. For these reasons, *BRCA1* and *BRCA2* were originally characterised as tumour suppressor genes. A study conducted in mice revealed that both *Brca1* and *Brca2* are essential during embryogenesis and their disruption leads to embryonic death early in development. Such phenotype was partially rescued in *Tp53* null background[166]. This restoration of embryonic viability was also observed in mice carrying truncated *Brca1* allele and simultaneously depleted with *Trp53bp1* (gene encoding for 53BP1 in mice)[167] as well as in $Atm^{-/-}$ or $Chek2^{-/-}$ background[168]. These results imply that loss of

heterozygosity in mutant carriers likely arises at later stage of development unless supported by further mutation(s) alleviating its lethality. Apart from the phenotype similarity between *Brca1*- and *Brca2*-null mice[166,169,170], embryos lacking both *Brca1* and *Brca2* were not further impaired compared to *Brca1*-null[166]. These observations were among the first to suggest that both proteins might be involved in the same pathways. In a cohort of 237 families with multiple cancer cases, the risk of developing breast cancer during lifetime was estimated above 80% for mutated *BRCA1* or *BRCA2* carriers. For ovarian cancers the lifetime risk was 40-65% in mutated *BRCA1* carriers and 20% in mutated *BRCA2* carriers[171]. These estimations were reinforced in a panel of 1,008 Ashkenazi Jewish women with inherited mutation in either *BRCA1* or *BRCA2*. In this cohort of patients, the lifetime risk to develop breast cancer was 82% and 77% for ovarian cancer. A third study conducted in the United States on nearly two thousand families (from various ethnicities) showed similar results, with a breast cancer lifetime risk of 46% in mutated *BRCA1* carriers and 43% in mutated *BRCA2* carriers. Ovarian cancer lifetime risk was 39% in mutated *BRCA1* carriers and 22% in mutated *BRCA2* carriers[172]. Besides breast and ovarian cancers, *BRCA* mutations have been found in other types of cancer such as prostate, pancreatic and stomach cancers[173-175].

Consistently with the crucial roles of BRCA proteins in DSBs repair and replication stress management, cells lacking the appropriate function of either BRCA1 or BRCA2 display elevated genomic instability. Furthermore, HR-deficient cells rely

mainly on error-prone mechanisms to repair DSBs, such as a-EJ[125,126,176]. Even heterozygous mutations in either *BRCA1* or BRCA2 can have a substantial impact on cell integrity such as a reduced fork protection and HR efficiency[177]. Moreover, a recent study have addressed *BRCA* heterozygosity in human primary epithelial cells and reported an elevation of DNA damage and a decrease in the replication checkpoint response and apoptosis[178]. Thereby, introducing more stress in cells with such defects was initially considered as a promising approach to push towards cellular death[179]. Indeed, early studies in mice demonstrated the increased sensitivity of BRCA-deficient cells against irradiation[169,180,181] and oxidative DNA damage (such as induced by hydrogen peroxide treatment)[182]. Subsequent results showed that BRCA-deficient cells were markedly more sensitive to many DNA damaging agents such as platinum drugs[183,184], etoposide and methyl methanesulfonate (MMS)[185,186]. Platinum drugs are routinely used in clinic as chemotherapy against a broad range of tumours and demonstrated promising outcome in mutated *BRCA* carriers[187,188]. Potent chemicals have been designed to specially target and kill BRCA-deficient cells, including the highly promising class of PARP inhibitors. Among this family of inhibitors, olaparib has been shown to specifically induce replication stress and DNA damage in HR-compromised cells and tumours alone[189,190] or in combination with platinum drug[191]. Unfortunately, platinum resistance can arise in tumours treated with cisplatin, including BRCA-deficient ones. Such resistance seems mostly driven by a secondary mutation

happening in either *BRCA1* or *BRCA2* that restores the reading frame of the protein[192-194], likely restoring appropriate protein activity, thus inducing PARP resistance as well[194].

Olaparib has been approved by the FDA in 2015 as monotherapy for patients with advanced BRCA-mutated ovarian cancer[195]. Olaparib application was further extended for the treatment of breast cancer patients with BRCA defects in 2018[196]. Several PARP inhibitors have been approved by the FDA such as niraparib, rucaparib and talazoparib (also named BMN-673)[197-200]. However, tumours can develop direct resistance to PARP inhibitors treatment[201], arising through various mechanisms including additional mutations that restore HR functions[201-204], DNA end resection or restoration of stalled fork stability[153,205,206]. Indeed, depletion of 53BP1 leads to PARP inhibitors resistance in *Brca1*-mutated mouse tumours[207] and is correlated with poor prognosis in clinics[114]. More recently REV7, c20orf196 (SHLD1), FAM35A (SHLD2) and FLJ26957 (SHLD3), described as the shieldin complex, were reported as 53BP1 interactors and induced PARP inhibitors resistance upon depletion[202,208-210]. In BRCA1-mutated cells, the depletion of 53BP1 promotes DNA end resection leading to a partial restoration of RAD51 foci formation and therefore HR-mediated repair[111]. Moreover, recent work showed that PALB2 was able to be recruited at resected DSBs in 53BP1-depleted / BRCA1-null cells, restoring HR function[211]. Thanks to cutting-edge CRISPR screening, genes involved in PARP inhibitors resistance have been more broadly

mapped[176,212,213]. These extensive efforts towards the understanding of PARP inhibitors resistance mechanisms are stressing the need to develop new approaches to treat olaparib resistant tumours.

1.5 G-quadruplexes

The inherent ability of guanylic acid to self-aggregate was observed more than a century ago[214]. Later on, the molecular basis of such an aggregate was determined by fibre diffraction leading to a model in which guanines form four stranded helixes based on the stacking of four planar guanines, named G-quartet, stabilised by Hoogsteen hydrogen-bonding interactions[215-217]. Such four stranded structures were found to stably emerge, under physiological conditions, when using short G-rich sequences originated from eukaryote telomeric DNA[218-220]. Indeed, telomeric DNA is mainly composed of the repetitive G-rich sequence (TTAGGG)n, located at the end of chromosomes[221] and usually single-stranded[222]. These findings suggested a potential occurrence *in vivo* and structures featuring the stack of at least two G-quartets were designated as G-quadruplexes (G4s) (**Figure 5A**). G-quartets are further stabilised by centrally located monovalent cations with the stability preference as follow, $K^+ > Na^+ > NH4^+ >> Li^+$[223-225]. Subsequently, a wide variety of G4s topologies and structures have been identified using circular dichroism (CD)

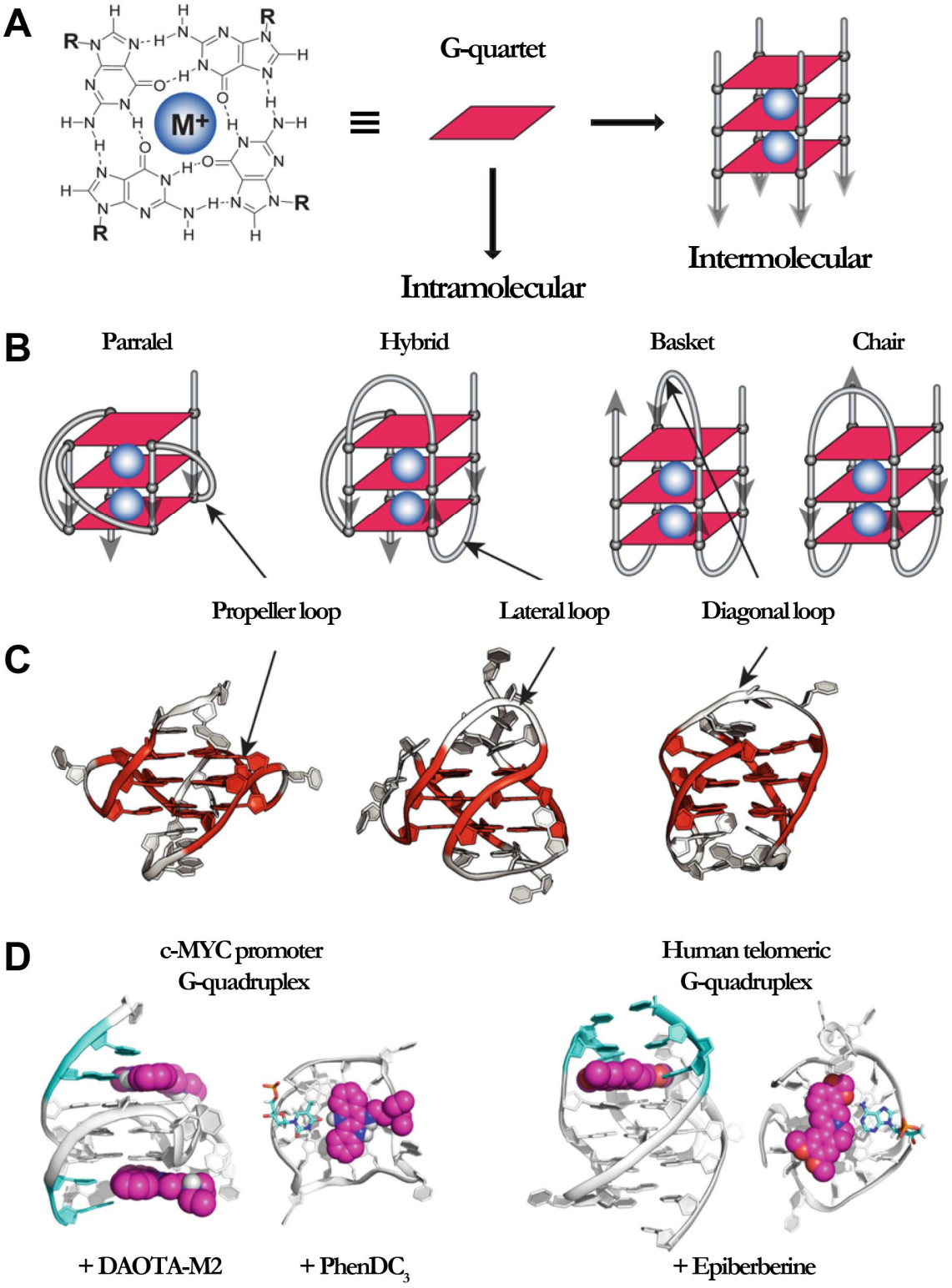


Figure 5: Schematic representation of G-quadruplexes structures

(A) Schematic representation of a G-quartet and an intermolecular G-quadruplex composed of three G-quartets and four DNA strands (tetramolecular). The stabilizing monovalent cation (M^+) is represented

by a blue sphere. (B) Schematic illustration of several intramolecular G-quadruplexes with different loop conformations and (C) their folding in a 3-dimensional representation. (D) NMR structure examples of two different G-quadruplexes in complex with G4 ligands[226-229]. Adapted from[230].

spectroscopy[231,232], nuclear magnetic resonance (NMR) spectroscopy[233,234] and X-ray crystallography[235-239]. CD spectroscopy is widely used to assign folds, monitor structural transitions and small molecule binding while NMR and crystallography methods can achieve more detailed structural resolution[240]. Indeed, early studies were able to reach a near- to sub-Å resolution of the G4 structure formed by the hexanucleotide d(TG_4T) using X-ray crystallography[241,242]. The folding of nucleic acid sequences into G4s can arise from the association of one (unimolecular), two (bimolecular) or four (tetramolecular) separate strands of DNA and / or RNA[243-250]. The orientation of the guanine strands can be parallel, anti-parallel or hybrid[231,235,251] (and the number of G-quartets ranged from two to more than seven). G-quartets are connected by loops of various sizes and orientations consisting of the nucleotide sequences not involved in the G-quartets formation (**Figure 5B, C**). The length and composition of the loops affect the folding kinetics and structural stability of G4s[240,252,253]. Moreover, molecular dynamics simulations suggest that G4s folding is dynamic and conformational changes likely occur within the same G4, leading to different topologies[254,255]. Interestingly, short loops appear

to be over-represented in the human genome and more thermodynamically stable[256-258].

Despite the structural diversity of G4s, computational approaches have emerged to predict the G4 forming potential of DNA sequences, allowing to map their locations genome-wide. Originally, computational predictions suggested that, in the human genome, over 300,000 sequences harbour a potential G-quadruplex-forming sequence (PQS), a motif prone to fold into G4s structures[258,259]. Such analysis was based on the consensus sequence motif $G_{\geq 3}N_{1\text{-}7}G_{\geq 3}N_{1\text{-}7}G_{\geq 3}N_{1\text{-}7}G_{\geq 3}$, where G stands for guanine and N for any nucleotide. More recent *in silico* approaches, including machine learning models[260,261], have tried to refine the consensus sequence motif[262] reaching up to 765,000 estimated PQS with the algorithm G4Hunter[263]. However, these predictive models miss the importance of the chromatin structure and its associated proteins, the bimolecular and tetramolecular G4s, likely resulting in an underestimation of the actual PQS number. Genome-wide mapping of PQS have revealed their prevalence in the human genome and their conservation within different mammal species[264]. Surprisingly, such motifs are unevenly distributed across the human genome. Bioinformatic analysis revealed that PQS are highly enriched in telomeres, in the vicinity of promoter regions, and 5' untranslated regions (5'-UTR) implying a potential effect on transcription[264-266].

The first observation of G4s *in vivo* was achieved with an *in vitro* designed antibody targeting telomeric G4s structures in the macronuclei of the ciliate *Stylonychia lemnae*[267]. Alternative G4-specific antibodies were subsequently engineered for human cells[268,269]. Another approach to study G4s *in vivo* consists of the use of small molecules, called G4 ligands, that could specifically bind and stabilise G4s structures. The first reported G4 ligand to bind telomeric DNA was successfully used to inhibit telomerase activity, an enzyme that elongates telomeres[270].

Whole genome mapping of G4s was achieved as well, to a certain extent, using experimental approaches. Indeed, some G4 ligands were shown to induce DSBs in cells, which provided a good opportunity to isolate the site of DNA damage and map the DSBs using sequencing. For instance, the G4-interacting small molecule PDS induced DNA damage in MRC-5-SV40 cells. The regions where the DSBs occurred were subsequently isolated then sequenced using chromatin immunoprecipitation (ChIP-seq) of γH2AX, a marker for DNA damage[271]. It revealed that the isolated regions appeared enriched in predicted PQS sites. Later on, DSBs have been more precisely mapped in NHEK cells using DSBCapture, a sequencing-based method to map DSBs at a high resolution[272]. In this study, endogenous DSBs were found enriched three folds over random in PQS. Another approach to map DSBs induced by G4 ligands was performed using ChIP-seq of RAD51 in U2OS cells upon treatment with the ligand CX5461, leading to the

identification of nearly 3,000 genomic targets for this ligand[273]. These findings suggest that G4 ligands induce DSBs at the site of G4s and have supported the promising potential of G4 ligands applications in cellular models.

A large variety of small molecules targeting G4s structures have been generated, approaching a thousand of reported compounds in the G4 Ligands Database[274] (http://www.g4ldb.org/). The specificity and interaction strength of newly synthesised ligands are usually assessed by fluorescence resonance energy transfer (FRET) melting method. It consists of incubating the G4 ligand with different common G4-forming sequences from different genomic regions[275], such as human telomeric DNA[220], c-MYC[276,277], k-RAS[278], c-KIT[279,280] or double-stranded DNA (dsDNA). Effective and specific ligands must have a high affinity for at least one of the G4 sequences while having a low affinity for dsDNA. In order to increase the specificity for G4s over dsDNA, ligands are mainly composed of multiple aromatic rings and have an overall positive charge. The aromatic surface of planar ligands is believed to interact with the end of the G4s structures, as supported by the crystal structure of the small molecule daunomycin in complex with the G4 sequence d(TGGGGT)[281], while non-planar ligands could be interacting preferably with the loops. Studies investigating NMR structures of the c-MYC promoter G-quadruplex in complex with various G4 ligands (quindoline, TMPyP4, $PhenDC_3$ and DAOTA-M2) have shown that G4 ligands are more likely to bind on the top and / or the

bottom of this specific G4 structure[226,227,282]. Similarly, several G4 ligands (TMS derivative, epiberberine and platinum(II)-based tripod) have been described to intercalate between the upper loop and the first G-quartet of the human telomeric G-quadruplex structure[228,229,283,284] (**Figure 5D**). Complexes and crystals analysis are useful models to study the most favourable interactions although they miss the potential binding dynamics between the G4 ligand and its target. Indeed, molecular dynamics binding simulations suggest multiple kinetics between the G4 ligand CX5461 and several G4s[285], meaning that CX5461 is likely able to interact with various parts of the G4 structure, including the loops, before adopting its optimal conformation. Small ligands might even be able to intercalate between G-quartets. However, a reduced steric bulk is prone to increase the propensity of the ligand to intercalate with dsDNA[286]. Unfortunately, the molecular features that improve the affinity for G4s structures over dsDNA, reduce the solubility and often lead to poor pharmacokinetic and pharmacodynamic properties[287]. Nevertheless, numerous G4 ligands have shown efficacy *in vivo*, shedding light on the broad biological functions of G4s and their regulation.

Considering that G4s structures can have a high thermal stability, to a similar extent as dsDNA[240], enzymatic reactions seem to be required for their unfolding and regulation. Indeed, several DNA helicases can unfold G4s *in vitro*. The best characterised are WRN[288,289], BLM[289-291], FANCJ[292,293] and Pif1[294]. An elegant *in*

vivo system was engineered in *Saccharomyces cerevisiae* to investigate the role of pif1, a DNA helicase involved in genomic maintenance[295,296], upon the insertion of the G-rich minisatellite CEB1 in the yeast genome. This study revealed that pif1 has the ability to unwind G4s arising from the CEB1 sequence *in vitro* and to prevent CEB1 genomic instability *in vivo*[294]. Further findings showed that a subset of pif1-binding sites correlate with G4 motifs *in vivo* and that their genomic stability involves pif1 activity[297]. Moreover, the G4s unwinding ability of this protein was extended to multiple helicases of the Pif1 family across different species[298]. In human cells, BLM and FANCJ helicases also have the ability to prevent genomic instability at G4 motifs[293,299]. More structural studies have shown the direct interaction of a helicase with G4s thanks to the crystal structures of the helicase DHX36 with the c-MYC promoter[300,301]. The hypothesis that helicases can directly bind and unwind G4s *in vivo* was further reinforced by findings using G4 ligands. Indeed, the *in vitro* ability of FANCJ, Pif1 and BLM to unwind G4s was decreased by the G4 ligands telomestatin (TMS)[293], Phen-$DC_{3/6}$[302], and N-methyl mesoporphyrin IX (NMM)[290] respectively. Interestingly, BLM appeared to be trapped on the G4s structure upon the addition of NMM[290]. *In vivo*, wild type (WT) yeast treated with Phen-$DC_{3/6}$ exhibited a similar genomic instability as the Pif1-deficient yeast, which was further destabilised upon G4 ligand treatment[302]. In mouse embryonic fibroblast (MEF) cells deficient in DNA2, another helicase harbouring the ability to resolve G4s, treatment with the G4 ligands TMPyP4 and

TMS increased telomere fragility to a higher extent than in WT cells[303]. These results suggest that cells have multiple helicases to resolve G4s structures and that the activity of these helicases can be impaired by G4 ligands, likely due to steric hindrance, structural rearrangement or trapping. However, the helicases specificity for different G4s structures and the extent of their redundancy[304] remain to be fully elucidated. Defects in these helicases can lead to severe syndromes such as Bloom (BLM)[305], Werner (WNR)[306] or Fanconi anaemia (FA) syndrome[307]. The alpha-thalassemia X-linked mental retardation (ATRX) is also due to defects in the ATRX helicase[308] which has been reported to interact with G4s[309-312] and its depletion leads to increased fork stalling and DNA damage[313,314]. While it is unclear to which extent these syndromes are linked to G4 unfolding failure, small molecules targeting G4s and helicases remain an appealing approach to better understand the unfolding dynamic and eventually modulate such interactions.

The first reported biological role of G4s *in vivo* was observed at telomeres[267] and was initially believed to impair telomerase recruitment[270] and G4s were therefore considered as a negative regulator of telomere maintenance[315,316]. Indeed, RTEL1, BLM, WRN and other RecQ helicases that can unwind G4s are also involved in telomere maintenance[317-319]. However, it appears that telomeric G4s formation might, in turn, be useful to recruit telomerase and other proteins to telomeres[320,321].

Apart from telomeres, G4 motifs have also been found enriched in promoter regions[264,266] and can modulate the transcriptional activity of several genes. For instance, the expression of the oncogene *c-MYC* is regulated by a G-rich region known to form G4s *in vitro* upstream of its promoter[276,322]. When this region was mutated in a way to destabilise the resulting G4s structure, the transcriptional activity of c-MYC in HeLa cells increased by roughly 3-fold and was reduced as well upon treatment with the G4 ligand TMPyP2[277]. Similarly, the promoter of the oncogene *KRAS* has the ability to fold into G4s structures and the treatment of HEK-293 cells with TMPyP2 reduced its expression by approximately 20%[278]. In MRC-5-SV40 cells, G4s stabilisation by PDS altered the transcriptional level of several oncogenes and tumour suppressors harbouring PQS in their promoters, including *c-MYC*[271]. This was further reinforced by the finding that several indenoisoquinoline analogues appeared to be able to interact with the c-MYC promoter G4s, downregulating c-MYC expression in MCF-7 breast cancer cells[323]. Alteration of the G4s unwinding helicases BLM and WRN also lead to dysregulation of genes with promoters containing PQS.

During replication or transcription, RNA can bind to ssDNA and form stable RNA-DNA hybrids. Together with the displaced ssDNA, such noncanonical DNA structures are referred to as R-loops. While they have various regulatory roles in transcription and chromatin structure, they can also be a source of genomic

instability when they encounter the replication machinery and cause replication fork stalling.[324]. Early electron microscopy experiments reported that a plasmid containing G4s motifs was able to form R-loops in *Escherichia coli*[325]. Recent findings showed that various G4 ligands (including PDS) were able to increase the formation of R-loops in human U2OS cells in a transcription-dependent manner. Indeed, IF experiments showed colocalization between antibodies targeting G4s (BG4) and antibodies targeting R-loops (S9.6) few minutes following G4 ligands addition to media[326]. Elegant single molecule FRET assays showed that when PQS are located downstream of a transcription start site and fold into G4s on the displaced DNA strand of a R-loop, the mRNA production is enhanced[327]. This is likely due to the G4s stabilizing effects on the R-loops, allowing more transcription events to occur at the same site. However, G4s formation of the transcribed strand lead to a decrease of mRNA level, probably due to the impairment of the RNA polymerase complex progression[327-329]. Alternatively, certain G4s seem able to enhance transcription by promoting the recruitment of transcription factors. Indeed, the ubiquitous transcription factor SP1 has been shown to bind to G4s with a high affinity and SP1 binding sites strongly overlapped with PQS[330]. Moreover, the proto-oncogene KRAS has a region upstream of its transcription start site, called the nuclease-hypersensitive element, which can fold into a G4 and contains the binding site for a transcription factor. Destabilisation of the G4 structure by

point mutation led to a decrease of KRAS expression[331]. Altogether, this suggests that depending on G4s location the transcription can be amplified or decreased[332].

Furthermore, G4s might have a more profound impact on transcription and translation as they were found highly enriched in 5'- and 3'-UTR of messenger ribonucleic acid (mRNA)[264,333], regulatory elements that can adopt complex secondary structures[245,334]. A study conducted on the 5'-UTR of the BCL-2 gene, involved in cellular death[335], revealed that the formation of stable RNA G4s occurs *in vitro* in this region and correlates with translation repression[336]. Furthermore, recent evidence support that G4s are involved in the epigenetic regulation of the genome by sequestrating the DNA methyltransferase 1 enzyme, thus altering DNA methylation[337]. G4s also appeared to be enriched in DNA replication origins[338] and in viral RNA[339] where they seem to have regulatory roles.

Despite compelling evidence of G4s implication in many biological processes, the precise *in vivo* environment prone to induce G4s formation remains unclear. Indeed, the chromatin structure, epigenetic modifications and DNA-associated proteins could repress or promote G4s folding. For instance, telomeres are capped by a complex of six proteins, named the shelterin complex, in order to prevent degradation and aberrant chromosomal rearrangements[340]. A protein of this complex, POT1, binds to the overhanging ssDNA and contributes to the end protection of telomeres[341], likely reducing the availability of nucleotides prone to

fold into G4s structures. Indeed, POT1 has been identified as repressing telomeric G4s[342]. Interestingly, POT1 did not appear to act catalytically in this study, suggesting a competition between POT1 binding to telomere ends and G4s folding. This hypothesis is reinforced by the findings that stabilisation of G4s can cause telomere uncapping as shown with the G4 ligand RHSP4 in uterus carcinoma cells[343]. The opportunity for G4s formation seems more favourable when the DNA is transiently single-stranded and unprotected, such as during replication, transcription and DNA repair. This was reinforced by work using the specific G4s antibody BG4, showing that G4s propensity was cell-cycle dependent and peaked during S-phase[268]. Additionally, the WRN helicase is able to unwind G4s and is recruited to telomere ends during S phase[344]. Furthermore, this hypothesis is supported by the findings that G4 ligands-induced DNA damage is largely suppressed when both replication and transcription are inhibited[271,273]. However, whether the damage and its signalling arise due to G4s stabilisation during or prior to these events remains unclear.

Unresolved G4s can act as replication fork barriers or lead to replication-transcription collisions[345]. Both events induce fork stalling[346], eventually leading to DNA damage, if the replication fork collapses[155,271]. The impairment of the replication forks progression by G4s has been shown to further affect the transmission of histone epigenetics[345,346]. G4s might have a role as well during the

initiation of DNA replication as PQS were found enriched near frequently used origins in four different human cell lines[347].

The presence of PQS and the consequences of G4s formation has been described in biological processes essential to maintain genome integrity such as DNA replication, telomere maintenance, histone recycling, oncogene expression and more broadly gene expression. Alteration in these processes can cause genomic instability, a hallmark for tumourigenesis onset and fuel cancer cells. Therefore, approaches to target G4s have been considered as promising against tumour growth. For instance, the G4 ligand BRACO-19 decreased hTERT expression in the human uterus carcinoma cell line and inhibited tumour growth in a xenograft mouse model[348]. Alternatively, G4 ligands can be used as anticancer agent against tumours sensitive to replication stress and / or DNA damage.

Indeed, HR-like processes are critical to overcome replication barriers and promote the fork restart. Previous published work from our group revealed that in BRCA1/2-deficient cells, where HR is impaired, the stabilisation of G4s with PDS leads to DSBs accumulation and genomic instability[155]. The efficiency of PDS was further extended to an olaparib resistant mouse tumour-derived cell line, suggesting that PDS might induce a different type of toxicity compared to olaparib. Surprisingly, it has been observed in our laboratory that DSBs induced by PDS could be resolved in BRCA2-deficient cells. It has been shown that the human

DNA-PKcs-deficient MO59J cells were more sensitive to PDS than DNA-PKcs-proficient MO59K cells[271] and that a derivative of PDS (PDSI) had an increased toxicity when combined with a DNA-PKcs inhibitor in HCT116 cells[349]. However, the exact nature of breaks caused by G4s stabilisation and the repair mechanisms recruited upon DNA damage remain to be fully elucidated in the BRCA1/2-deficient background. In this study we will investigate whether cNHEJ is implicated in the repair of G4s ligand-induced DSBs in BRCA1/2-deficient cells, including those that have acquired olaparib resistance through the loss of 53BP1.

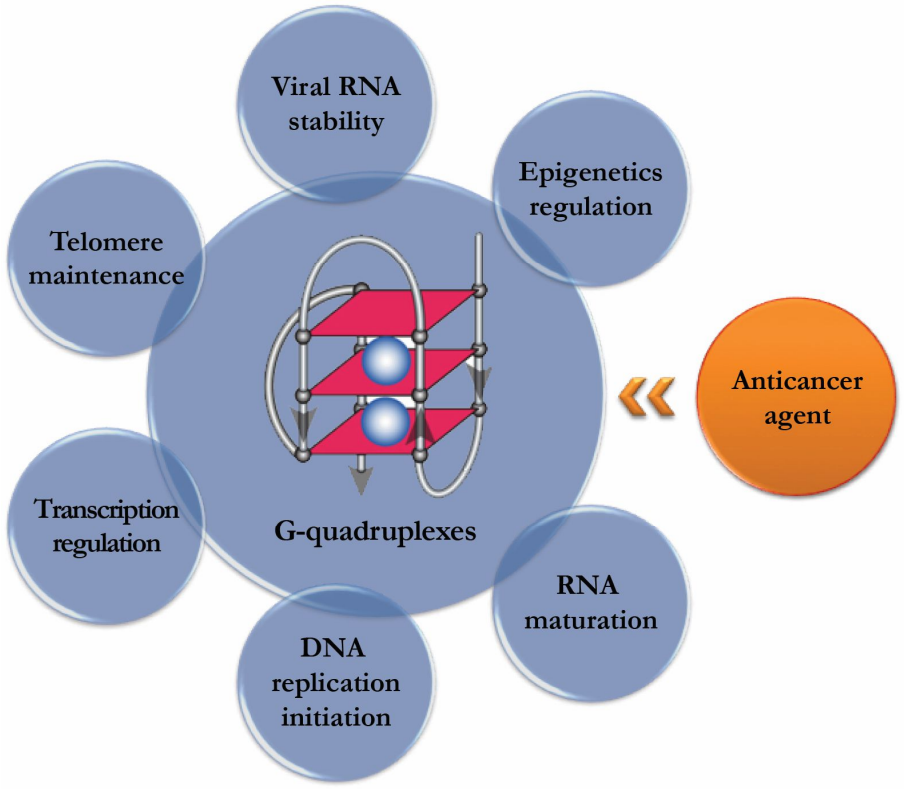


Figure 6: G-quadruplexes biological roles and potential application

In conclusion, G4s are versatile biological features involved in several biological processes, that could be exploited to target specific tumours and inhibit their growth (**Figure 6**). G4 ligands represent a useful tool for the study of G4s functions *in vivo* but their poor pharmacokinetics limit their use in clinical trial. Therefore, there is a need to improve our understanding of the mechanisms through which G4s stabilisation induces DNA damage and the repair mechanisms involved. Such findings could be further exploited to find synergistic combinations and / or synthetic lethality. Ultimately, this approach could be beneficial towards improving the therapeutic window of G4s ligands in clinical trials.

2 Results

2.1 Characterisation of the novel DNA-PKcs inhibitor, MSC

The activity and expression of DNA-PKcs, a central component of the cNHEJ machinery, was initially found to be elevated in different tumours type, including chemotherapy and radiotherapy resistant cancers[350-353]. For this reason, the inhibition of DNA-PKcs was proposed as a promising approach for sensitising tumours to irradiation and other DNA damaging agents[354,355]. However, designing potent and specific DNA-PKcs inhibitors can be challenging. Indeed, DNA-PKcs is a member of the PIKK family which shares a high homology with other proteins of this family. This includes ATR and ATM, both key proteins of the DDR[132] and the mammalian target of rapamycin (mTOR), a protein involved in many biological processes[356]. Therefore, an inhibitor's specificity for DNA-PKcs over other kinases is crucial to avoid biased results, especially when combined with DNA damaging approaches. Nevertheless, several small molecules have been reported to inhibit DNA-PKcs activity through interaction with the ATP binding site of the kinase domain[354]. Wortmannin is an early characterised DNA-PKcs inhibitor, initially derived from *Penicillium wortmannii* and identified as a PI3K inhibitor[357]. Despite its low selectivity for DNA-PKcs over other kinases, it successfully increased the cytotoxicity of IR in Chinese hamster ovary cells[358]. LY294002 is another reported

inhibitor of PI3K with a stronger activity against DNA-PKcs over ATR or ATM[359,360]. LY294002 was successfully used to decrease tumour growth in DLD1 and OVCAR-3 xenograft mouse models[361,362]. Unfortunately, this compound exhibits a high toxicity and has a rapid clearance *in vivo*. Subsequently, more potent DNA-PKcs inhibitors have been designed such as NU7441 (AstraZeneca) and MSC2490484A (also designated as M3814, Merck KGaA), both used in this study. NU7441 has been widely adopted in the literature and is reported to be a potent DNA-PKcs inhibitor with a low off target effect on other kinases. Moreover, NU7441 induced chemo-sensitisation and radio-sensitisation both *in vitro* and *in vivo*[363]. However, NU7441 has a poor water solubility, a common issue in drug development which can lead to a low bioavailability and therefore a poor drug delivery to the target[364]. This could explain, at least in part, why NU7441 has shown some limitations *in vivo*[354]. In contrast, MSC has a high solubility and is described as highly potent and selective, inducing a radio-sensitisation in various mouse models of human cancer[354,365]. Due to these promising results, MSC is currently being tested in phase I clinical trial in combination with radiotherapy against advanced solid tumours (NCT02516813). To date, only three DNA-PKcs inhibitors have moved forward to clinical trials[366], stressing the need to robustly characterise new inhibitors and their potential applications.

Initially, we characterised the cytotoxicity and specificity of both NU7441 and MSC in our cell models. At that time, very scarce published data were available on MSC. The cytotoxicity of MSC and NU7441 was assessed in three different human cellular models (**Figure 7)**. The two human colorectal carcinoma DLD1 and HCT116 cells are used as terminally adapted models to the loss of BRCA2. Conversely, human non-small cell lung carcinoma H1299 cells carrying a doxycycline (DOX) inducible short-hairpin RNA (shRNA) cassette was used to model the acute loss of BRCA2. Upon addition of doxycycline to the growth medium, shRNAs targeting *BRCA2* mRNA are expressed, depleting protein level over time. The decrease of BRCA2 protein level after 48 hours in DOX supplemented medium and the knockout of BRCA2-deficient cells were confirmed by western blot (**Figure 7C**). In all cell types, MSC had a lower toxicity than NU7441 over the used range of concentrations. The observed toxicities were independent of *BRCA2* status in both adapted and naïve models. In order to assess the efficiency of NU7441 and MSC in DLD1 cells, we monitored the phosphorylation level of DNA-PKcs at serine 2056. This auto-phosphorylation, part of the PQR phosphorylation cluster, is required for DNA-PKcs change in conformation upon binding to DNA and is substantially increased upon treatment with the DNA damaging agent bleomycin or the topoisomerase I (TOP1) inhibitor camptothecin (CPT). The phosphorylation of DNA-PKcs at serine 2056 is believed to be required for normal cNHEJ activity[92,93,367].

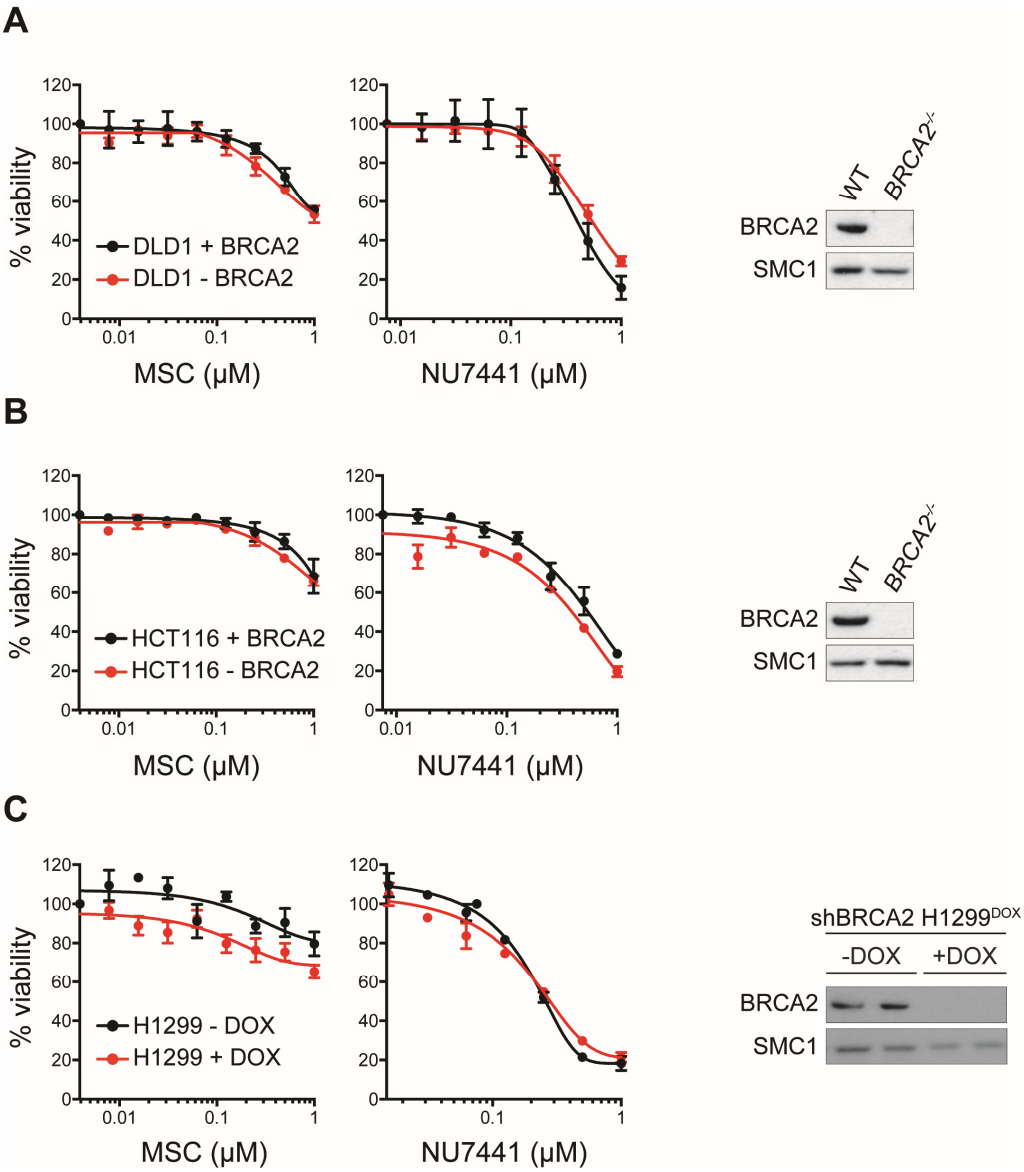


Figure 7: Toxicity of DNA-PKcs inhibitors on BRCA2-deficient human cells

(A-C) DLD1, HCT116 or H1299+shBRCA2^{DOX} human cells, BRCA2-proficient (+BRCA2) or -deficient (-BRCA2), were incubated with the indicated concentrations of NU7441 or MSC2490484A (MSC) for 6 days before processing for resazurin-based cell viability assays. (A, B) To confirm *BRCA2* knockout or (C) BRCA2 protein depletion upon DOX treatment, whole-cell extracts were prepared and immunoblotted as indicated. SMC1 was used as loading control. Graphs are representative of three (A), two (B) or one (C) independent experiment(s), each performed in technical triplicate. Error bars represent SEM values obtained from three (A), two (B) or one (C) independent experiment(s).

Both NU7441 and MSC appeared to significantly impair the S2056 auto-phosphorylation of DNA-PKcs in DLD1 cells upon CPT treatment (**Figure 8**).

To assess MSC specificity compared to NU7441, we monitored their effect on ATM and ATR activity upon DNA damage. The activity of ATM was extrapolated from the phosphorylation at serine 824 of the KRAB [Krüppel-associated box domain]-associated protein 1 (KAP1), a heterochromatin protein and substrate of ATM upon DNA damage[368]. ATR activity was measured based on CHK1 phosphorylation at serine 345[136], a checkpoint kinase involved in cell cycle control and DDR. We aimed to induce the phosphorylation of KAP1 by treatment with 1 M CPT and phosphorylation of CHK1 with 500 M HU.

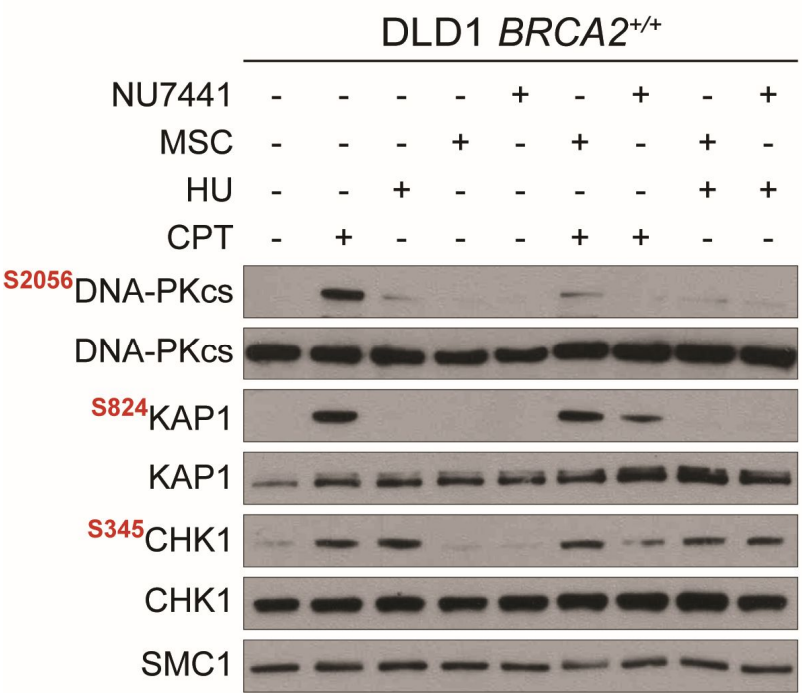


Figure 8: Efficiency and specificity of DNA-PKcs inhibitors in DLD1 cells

Human DLD1 BRCA2-proficient ($BRCA2^{+/+}$) cells, were incubated for 1 hour with CPT (1 M) or HU (500 M), alone or in combination with NU7441 (5 M) or MSC2490484A (5 M). Whole-cell extracts were prepared after treatment and immunoblotted as indicated. The structural maintenance of chromosomes 1 (SMC1) was used as loading control.

Treatment with 5 M MSC over 1 hour did not seem to affect ATM or ATR activity while inhibiting a large fraction of DNA-PKcs (S2056). Regarding MSC toxicity and specificity compared to NU7441, this new inhibitor seemed suitable, at the used concentrations, for further experiments in our cell models.

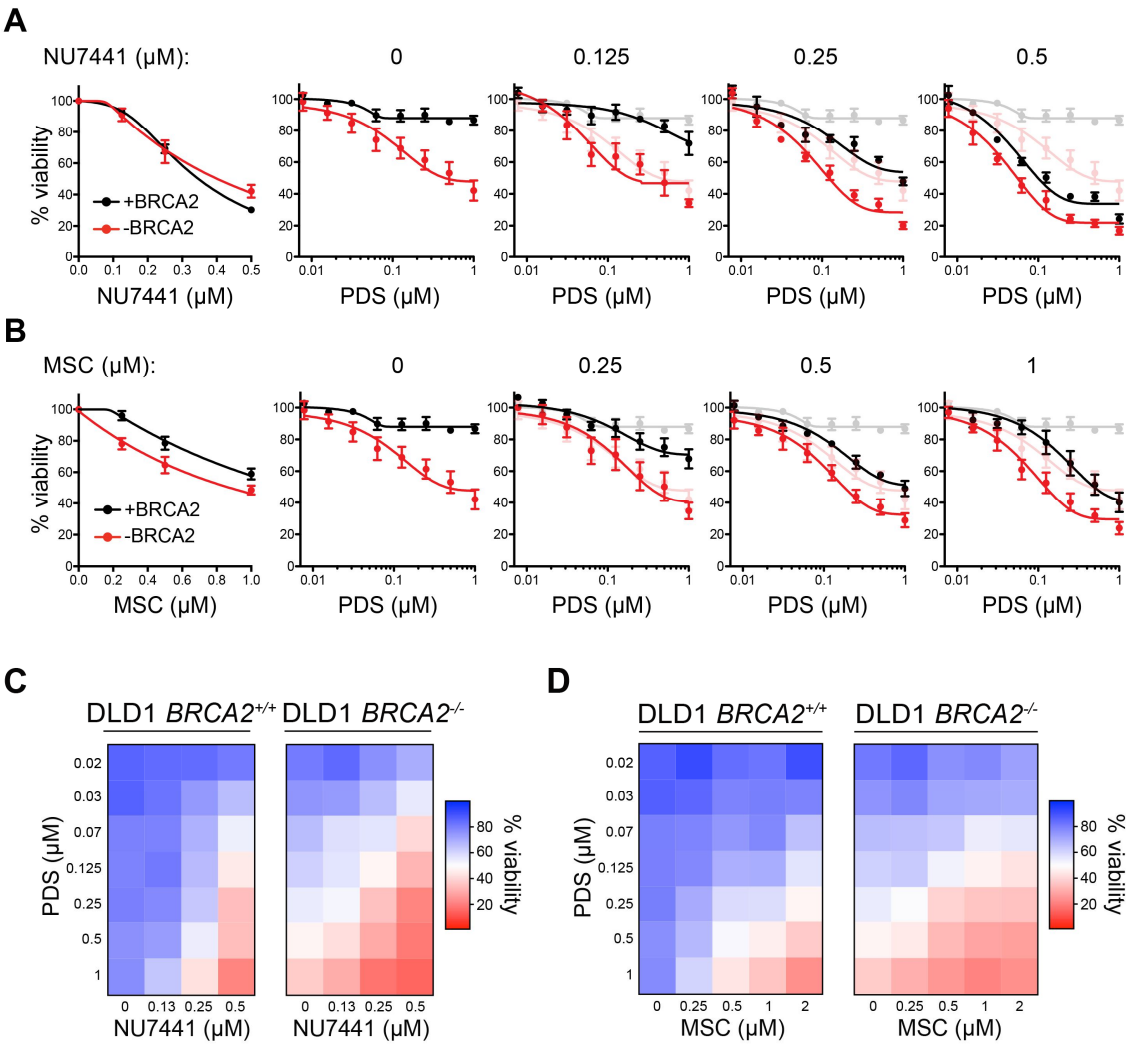
2.2 G4s ligands or olaparib in combination with DNA-PKcs inhibitors

Conventional approaches aiming to induce DNA damage in tumour cells, such as radiotherapy or chemotherapy, can have substantial side effects on patients, compromising the efficiency of therapies[369,370]. One way to overcome this challenge is to seek for synergistic effects between different treatments and / or drugs. A reaction is considered synergistic when the overall effect exceeds the addition of the individual effects. Such an approach can lead to an intensity and / or concentration decrease of the treatment inducing detrimental side effects while still achieving similar or greater efficacy. Here, we tested whether there are synergistic effects between G4 ligands and DNA-PKcs inhibitors in our cellular models.

PDS is a well-characterised small molecule able to stabilise G4s *in vitro*[371,372]. It impairs cell proliferation by inducing G2 arrest and triggers DDR activation. Furthermore, ChIP-seq analysis of the DSBs marker H2AX upon PDS treatment correlates with regions containing G4s forming sequences[271] suggesting that PDS causes DNA damage at G4s sites in human cells. PDS toxicity is strongly potentiated in BRCA-deficient cells due to their acute sensitivity to replication stress and DNA damage[155]. However, no study has been conducted so far with PDS in a mouse model due to the reported toxicity of PDS analogues in various cell lines[373], implying that the drug would be detrimental for animals' health. We reasoned that impairing further DNA repair mechanisms could increase BRCA-deficient cell sensitivity to PDS through synergistic effects. Such synergy could alleviate the toxicity of PDS, benefiting its use in animal models.

Consistent with previously published work, BRCA-deficient cells were more sensitive to PDS than BRCA-proficient cells[155] in the cell viability experiments conducted (**Figure 9**). Here, combination treatments were performed in a way that control cells were treated with the corresponding concentration of DNA-PKcs inhibitors. By doing so, the inherent toxicity of DNA-PKcs inhibitors was normalised and the cell viability difference between single and combined treatments should be resulting from synergistic effects. Indeed, synergistic effects were observed between PDS and both DNA-PKcs inhibitors (**Figure 9A**, **B**). Co-treatments with

either NU7441 or MSC increased the toxicity of PDS in a dose-dependent manner as illustrated in heat map representations (**Figure 9C, D**). The decrease in cell viability upon combined treatment occurred in both BRCA2-proficent and -deficient cells. Similar results were obtained using a second HR-deficient cell line (**Figure 9E**). Interestingly, PDS was far more potent in human retinal pigmented epithelium RPE1 BRCA1-deficient cells than in DLD1 BRCA2-deficient cells alone and in combination with MSC. The knockout of BRCA1-deficient RPE1 cells was previously confirmed in our lab (data not shown).



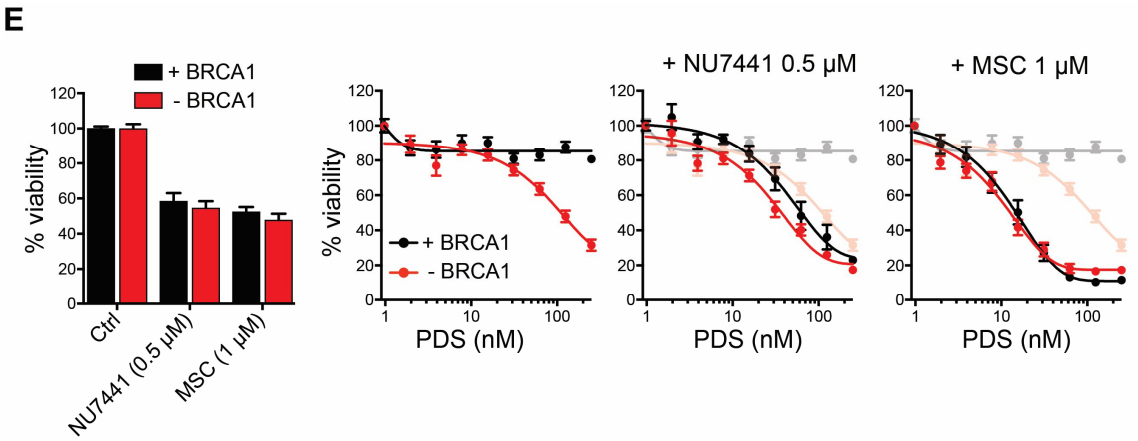


Figure 9: Effect of DNA-PKcs inhibitors in combination with PDS on BRCA-deficient human cell viability

(A, B) Human DLD1 cells, BRCA2-proficient (+BRCA2) or -deficient (-BRCA2), were incubated with the indicated concentrations of NU7441 (A) or MSC2490484A (B) for 24 hours, followed by 6-day incubation with NU7441 or MSC2 plus PDS. (C, D) Heat map representations of (A) and (B). (E) Human RPE1 cells, BRCA1-proficient (+BRCA1) or -deficient (-BRCA1), were incubated with the indicated concentrations of NU7441 or MSC plus PDS for 6 days. (A, B, E) At the end of the above treatments, cells were processed for resazurin-based cell viability assays. Graphs are representative of three independent experiments, each performed in technical triplicate. Light black and light red curves represent BRCA-proficient (+BRCA) and -deficient (-BRCA) cells respectively, treated only with PDS. Error bars represent SEM values obtained from three independent experiments.

Regarding that PDS induces fork stalling that leads to DNA damage in BRCA-deficient cells and synergises with DNA-PKcs inhibitors, we wondered if drugs targeting similar mechanisms would display the same phenotype. Among them, PARP inhibitors can trap PARP on DNA and induce fork stalling[374]. Moreover, PARP inhibitors are highly potent against BRCA-deficient cells and tumours. However, despite being selectively toxic to BRCA2-deficient cells, olaparib did not

exhibit any synergy with either NU7441 or MSC in the range of concentration used (**Figure 10**). It is worth noting that we observed a significant drop of cell viability in DLD1 BRCA2-proficient cells treated with olaparib and 0.5 M NU7441.

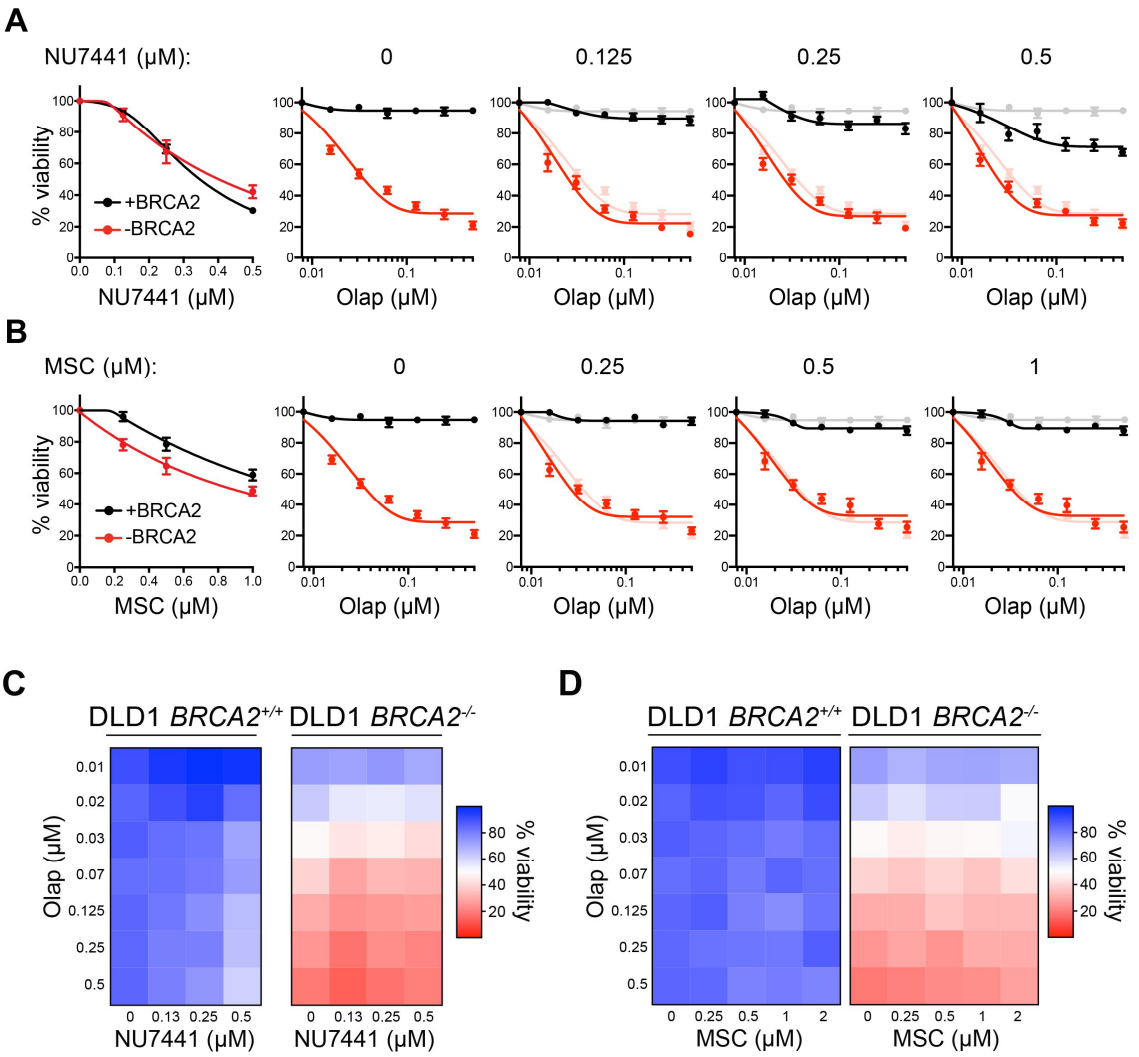


Figure 10: Effect of DNA-PKcs inhibitors in combination with olaparib on BRCA-deficient human cell viability

(A, B) Human DLD1 cells, BRCA2-proficient (+BRCA2) or -deficient (-BRCA2), were incubated with the indicated concentrations of NU7441 (A) or MSC (B) for 24 hours, followed by 6-day incubation with NU7441 or MSC2 plus olaparib. At the end of the above treatment, cells were

processed for resazurin-based cell viability assays. (C, D) Heat map representations of (A) and (B). Graphs are representative of three independent experiments, each performed in technical triplicate. Light black and light red curves represent BRCA2-proficient (+BRCA2) and -deficient (-BRCA2) cells respectively, treated only with olaparib. Error bars represent SEM values obtained from three independent experiments.

In order to address whether the synergies observed are solely due to DNA-PKcs activity or the result of unspecific side effects, we used the near-haploid human chronic myeloid leukaemia-derived HAP1 cells, WT or mutated *PRKDC* (gene encoding DNA-PKcs). We confirmed the knockout of DNA-PKcs-deficient cells by WB (**Figure 11A**). Cell viability experiments conducted with these cells showed that lack of DNA-PKcs sensitised cells to PDS and synergistic effects were observed in DNA-PKcs-proficient cells treated with PDS and DNA-PKcs inhibitors. In contrast, the synergies were more discreet in DNA-PKcs-deficient cells but still present (**Figure 11B, C**). These results obtained in HAP1 cells suggest that PDS induces a stronger synergy with MSC than with NU7441 while relying less on DNA-PKcs-independent effects.

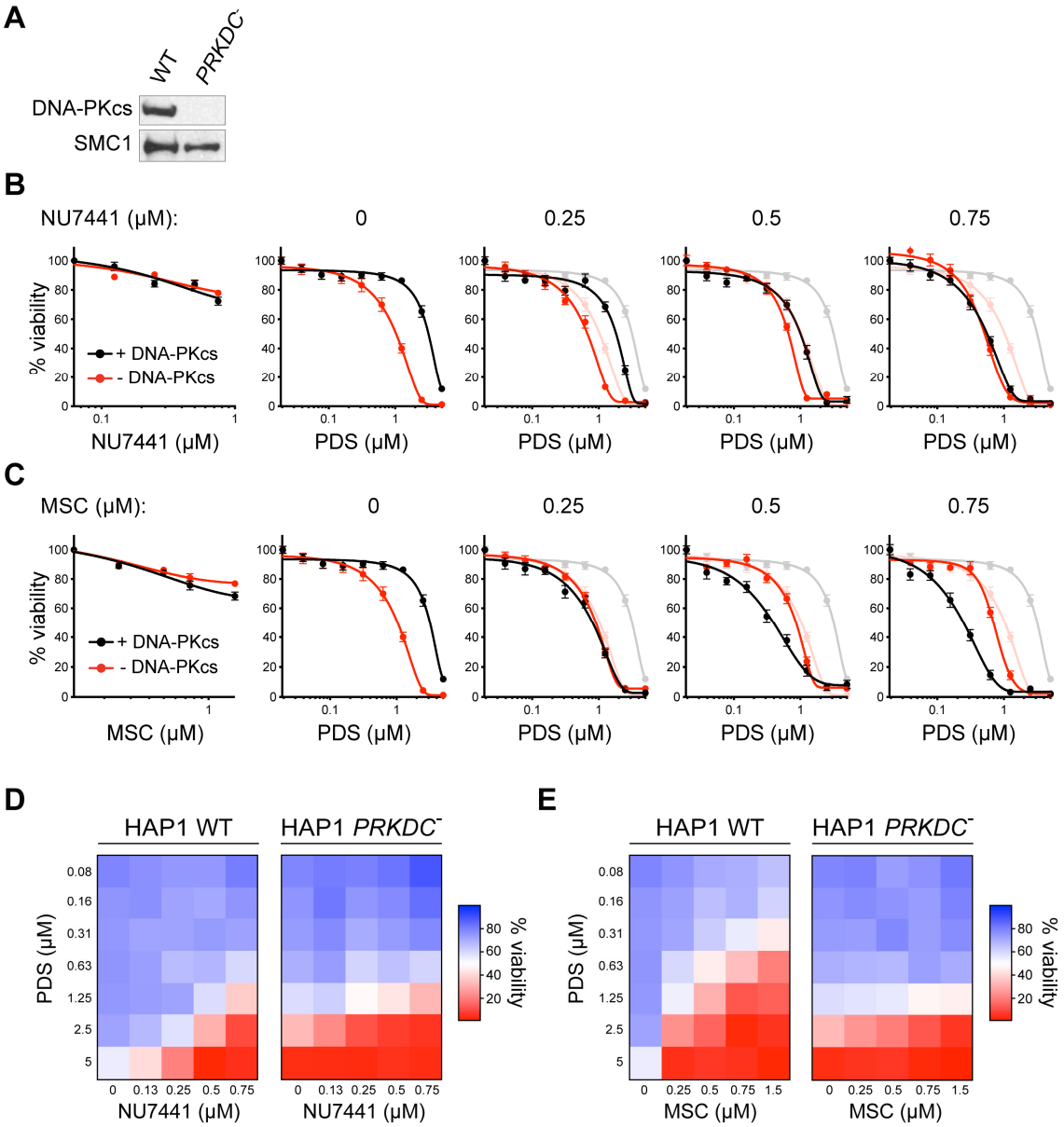


Figure 11: PDS synergy with NU7441 or MSC relies mainly on DNA-PKcs activity

(A) To confirm *PRKDC* knockout, whole-cell extracts of human HAP1 cells were prepared and immunoblotted as indicated. SMC1 was used as loading control. (B, C) Human HAP1 cells, DNA-PKcs-proficient (+DNA-PKcs) or -deficient (-DNA-PKcs), were incubated with the indicated concentrations of NU7441 and PDS for 6 days. At the end of the above treatment, cells were processed for resazurin-based cell viability assays. (D, E) Heat map representations of (B) and (C). Graphs are representative of three independent experiments, each performed in technical triplicate. Light black and light red curves represent DNA-PKcs-proficient (+DNA-PKcs) or -deficient (-DNA-PKcs) cells

respectively, treated only with PDS. Error bars represent SEM values obtained from three independent experiments.

Moreover, it is the only G4 ligand currently being tested in clinical trial phase I, against solid tumours harbouring *BRCA* status (**NCT02719977**). Consistent with published results, BRCA-deficient cells were more sensitive to CX5461 than BRCA-proficient cells in cell viability experiments.

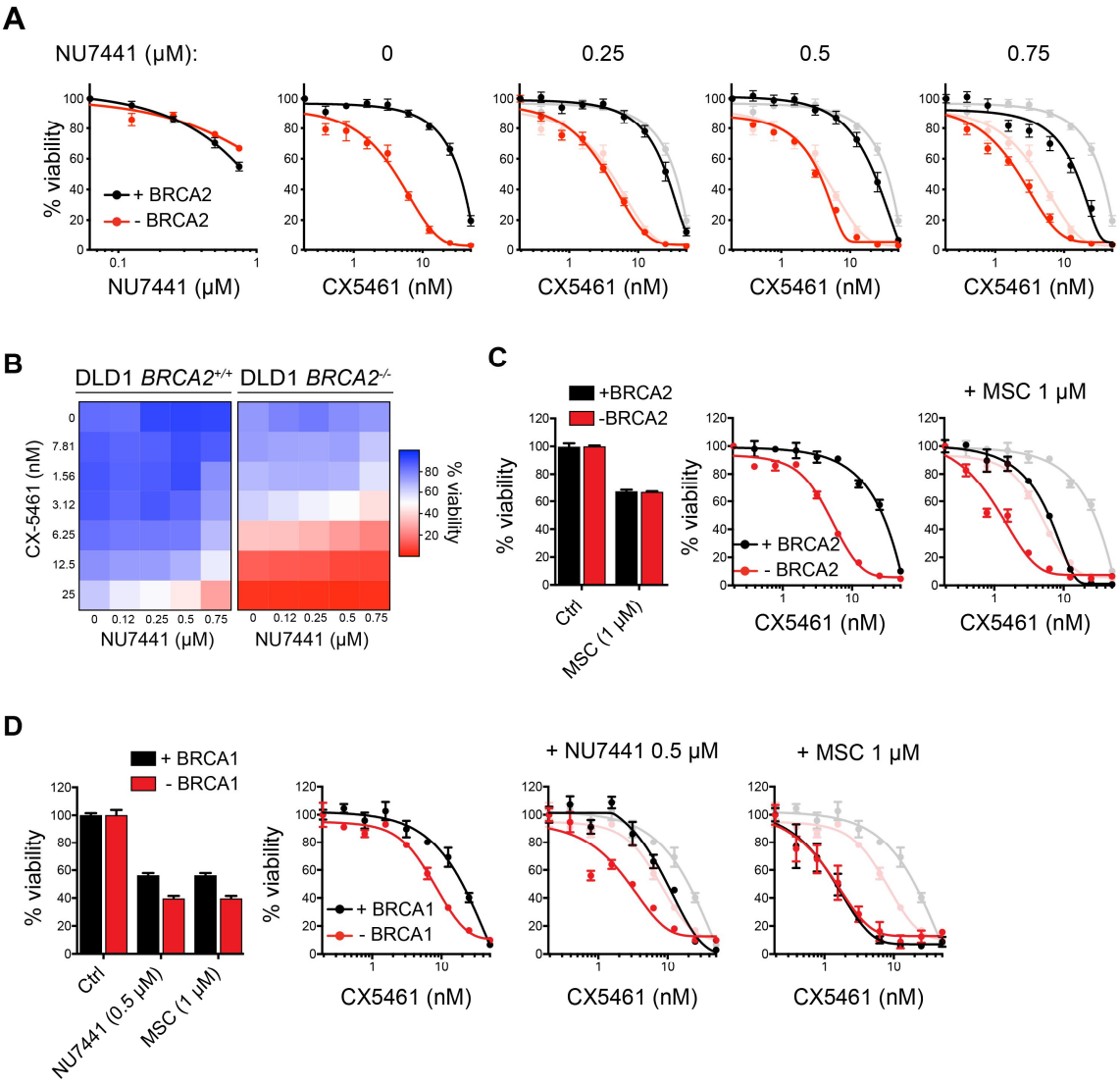


Figure 12: Effect of DNA-PKcs inhibitors in combination with CX5461 on BRCA-deficient human cell viability

(A, C) Human DLD1 cells, BRCA2-proficient (+BRCA2) or -deficient (-BRCA2), or (D) human RPE1 cells, BRCA1-proficient (+BRCA1) or -deficient (-BRCA1) were incubated with the indicated concentrations of CX5461 alone or in combination with NU7441 or MSC. (B) Heat map representations of (A). (A, C, D) At the end of the above treatments, cells were processed for resazurin-based cell viability assays. Graphs are representative of three independent experiments, each performed in technical triplicate. Light black and light red curves represent BRCA-proficient (+BRCA) and -deficient (-BRCA) cells respectively, treated only with CX5461. Error bars represent SEM values obtained from three independent experiments.

Furthermore, CX5461 exhibited, in both cell lines, a mild synergy with NU7441 and a more pronounced one with MSC (**Figure 12**). However, the toxicity of DNA-PKcs inhibitors alone, especially at high concentration (up to 40% cell viability for 0.5 M NU7441), might account for a part of the synergies observed when combined with G4 ligands. This could explain as well as the unexpected cell viability drop in DLD1 BRCA2-proficient treated with both olaparib and 0.5 M NU7441 (**Figure 10A**). To clarify such possibility, we used an assay with a greater sensitivity than cell viability assay, called clonogenic assay (or colony formation assay). This method relies on single cell proliferation and ability to form substantial colonies (approximately 50 cells) while cell viability assays measure the remaining metabolic activity by the end of the treatment. It means that cells undergoing critical cellular stress are unlikely to form solid colonies, even if they maintain some metabolic activity, and will not be considered 'alive' during the read-out. The results are represented as the survival fraction (%). We conducted clonogenic assays using

DLD1 and RPE1 BRCA-deficient and -proficient cells treated with PDS alone or in combination with DNA-PKcs inhibitors. RPE1 cells were able to form colonies after NU7441 (1 M) or MSC (2 M) treatments for 24 hours, while PDS strongly impaired the formation of BRCA1-deficient cell colonies (**Figure 13B**).

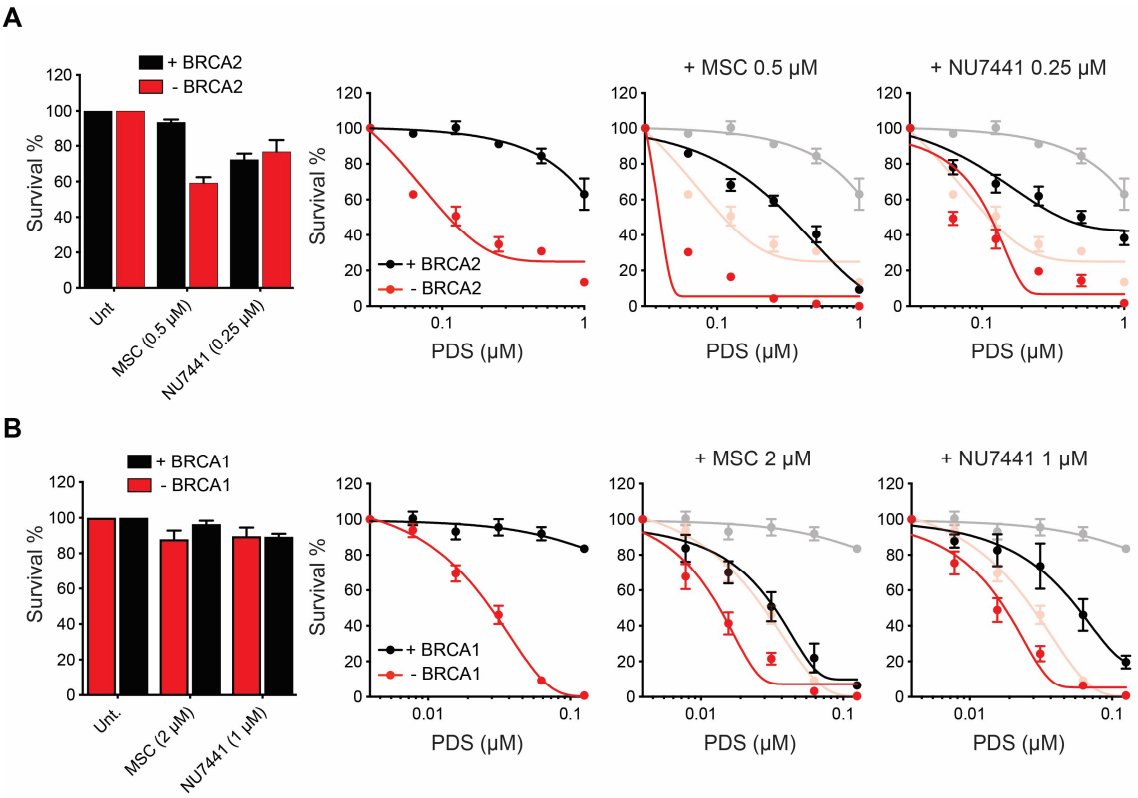


Figure 13: Effect of PDS in combination with NU7441 or MSC on BRCA-deficient human cell survival

(A) Human DLD1 cells, BRCA2-proficient (+BRCA2) or -deficient (-BRCA2) were incubated with the indicated concentration of PDS alone or in combination with NU7441 or MSC for 6 days. (B) human RPE1 cells, BRCA1-proficient (+BRCA1) or -deficient (-BRCA1) were incubated 24 hours with the indicated concentration of PDS, alone or in combination with NU7441 or MSC then released into fresh growth medium. Light black and light red curves represent BRCA-proficient (+BRCA) and -deficient (-BRCA) cells respectively, treated only with PDS. When colonies of roughly 50 cells were formed (7-15 days), cells

were stained with a crystal violet solution and colonies were counted manually. Graphs are representative of three independent experiments, performed in technical triplicate. Error bars represent SEM of values obtained from three independent experiments.

Conversely, DLD1 BRCA2-deficient cells were mildly affected by 24 hours PDS treatment compared to BRCA2-proficient (data no shown), therefore drugs were maintained in the growth medium until colonies were stained (**Figure 13A**). In both cell lines, PDS-induced toxicity was accentuated by the addition of NU7441 or MSC, in BRCA-proficient and -deficient cells.

Altogether, these results show that NU7441 and MSC are specific DNA-PKcs inhibitors that synergise with the G4 ligands PDS and CX5461 in BRCA1/2-proficient and -deficient cells.

2.3 PDS- and olaparib-induced DNA damage recovery in BRCA-deficient cells

Immunofluorescence (IF) experiments conducted in DLD1 BRCA2-deficient cells by Dr Jutta Zimmer, a former DPhil student in our laboratory, revealed that, following a short PDS treatment, there is a strong increase of cells displaying multiple yH2AX and 53BP1 foci, both markers of DNA damage[375]. Interestingly, 3 days after the removal of PDS, the percentage of cells with yH2AX or 53BP1 foci was significantly lower in comparison to a few hours following the overnight

treatment. These preliminary experiments suggested that DNA damage induced by PDS were resolved over time even in HR-compromised cells. In order to consolidate such findings, we further assessed the integrity of DLD1 BRCA2-deficient cells following 24 hours PDS treatment using various techniques. We first monitored the DDR signalling by western blot following the phosphorylation of KAP1 at serine 824 and the phosphorylation of RPA at Serine 4/8 (**Figure 14A**). The treatment with 2 M PDS for 24 hours did not induce a significant phosphorylation of neither KAP1 nor RPA in DLD1 BRCA2-proficient cells while inducing a strong response after PDS treatment in BRCA2-deficient cells. The phosphorylation of KAP1 and RPA returned to similar levels as untreated 3 days after the removal of PDS from the growth medium. The cell cycle distribution upon the same PDS treatment was assessed using flow cytometry (**Figure 14B-D**). Treatment with 2 M PDS for 24 hours induced a significant arrest in G2/M specifically in BRCA2-deficient cells. At the end of the recovery period of 3 days, the cell cycle of BRCA2-deficient cells was back to a similar profile as untreated, implying that normal cell cycle was restored. Replication stress and DNA damage can induce chromosome instability, manifested in the formation of breaks or abnormal rearrangements. These events can be visualised and quantified using the metaphase spread and Giemsa staining method. BRCA2-deficient cells displayed an increase of chromosome aberrations per metaphase after treatment with 2 M PDS for 24 hours. The number of

chromosome aberrations was reduced to a similar level as untreated after 3 days of PDS removal (**Figure 14E, F**).

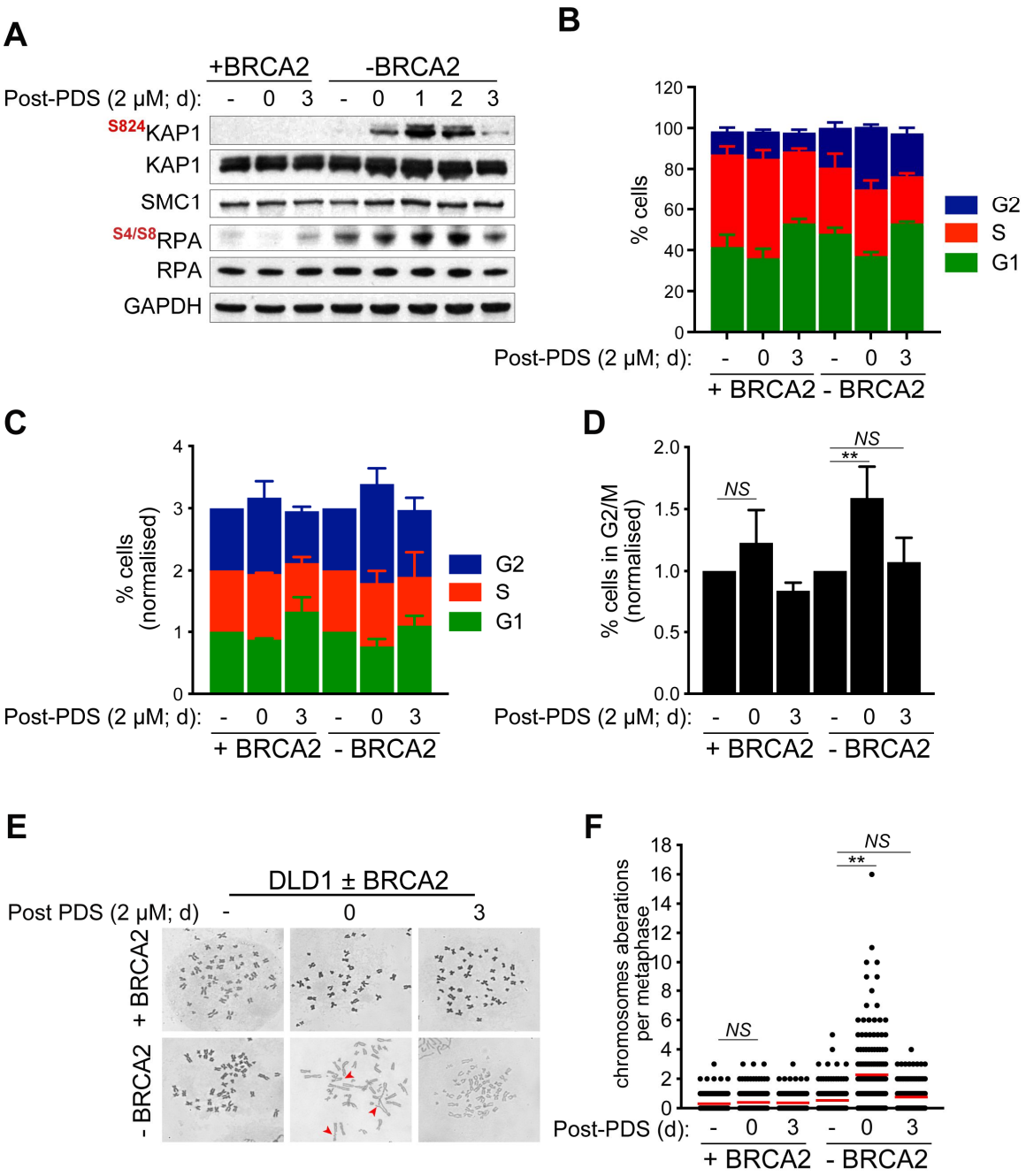


Figure 14: PDS-induced DNA damage can be partly repaired in a BRCA2-independent manner

(A, B, E) Human DLD1 cells, BRCA2-proficient (+BRCA2) and -deficient (–BRCA2) were treated with 2 μM PDS for 24 hours and released into fresh growth medium for indicated times. (A) Whole-cell extracts were prepared after treatment and immunoblotted as indicated. SMC1 and GAPDH were used as loading controls. (B-D) Cells were fixed in PFA and the whole cell cycle profile (B, C) or G2/M (D) phases were analysed by flow cytometry. (C, D) Values were normalised per cell cycle phase and relative to untreated. At least 25,000 cells were analysed per condition and experiment. (E) Representative images of cells processed for metaphase spread and stained with Giemsa staining. (F) Quantitative graph of (E), at least 50 cells were analysed per condition and experiment. (B-D, F) Error bars represent SEM values of three (F) or four independent experiments.

These results showed that BRCA2-deficient cells treated with PDS for 24 hours were able to largely restore genomic stability 3 days after the removal of the drug.

Regarding that BRCA-deficient cells lack functional HR we wondered which repair pathways could be involved to repair PDS-induced lesions. In order to assess whether cNHEJ was involved in the recovery of BRCA2-deficient cells following PDS treatment, we monitored the phosphorylation of KAP1 at serine 824 during the recovery period with or without the DNA-PKcs inhibitor NU7441. Consistent with **Figure 14**, the phosphorylation of KAP1 was largely reduced at the end of the recovery period compared to after 24 hours treatment with PDS. As expected, the recovery was partly impaired by daily addition of NU7441 (**Figure 15**).

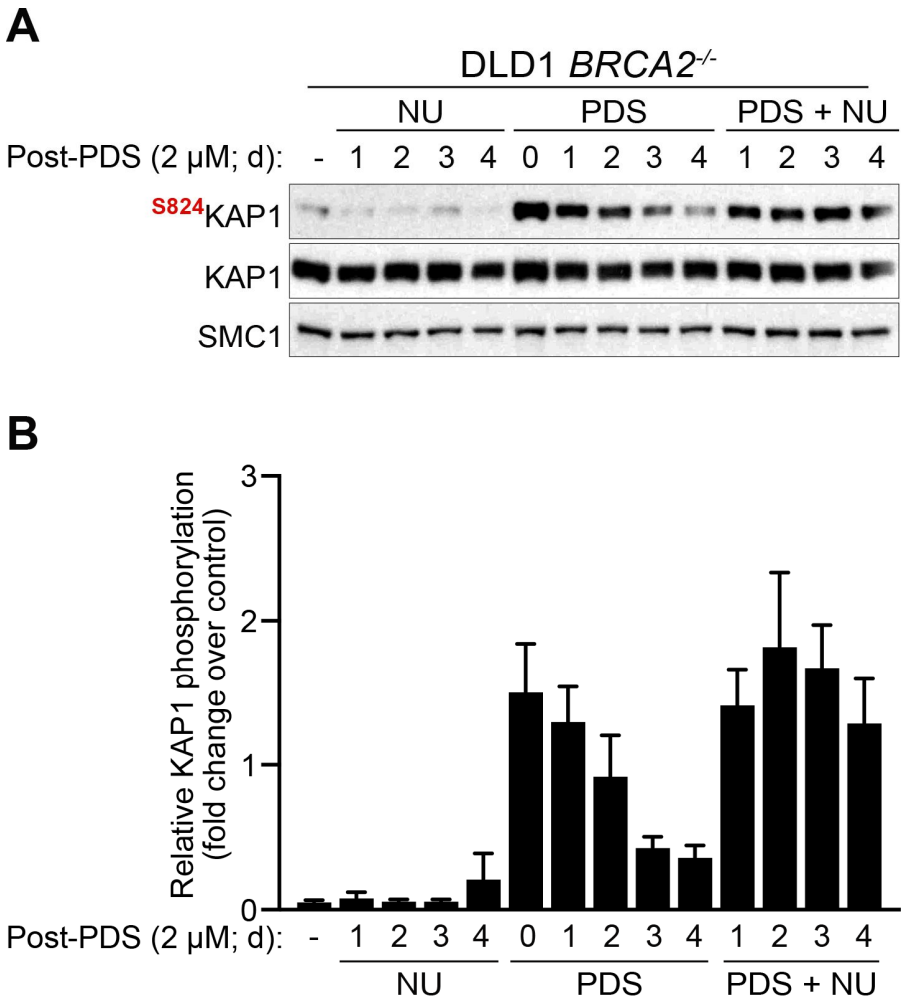


Figure 15: DNA-PKcs inhibitor NU7441 impairs the recovery of BRCA2-deficient cells upon PDS treatment

(A) Human DLD1 cells BRCA2-deficient were incubated with 2 μM PDS for 24 hours and released into growth medium with 0.25 M NU7441 or fresh growth medium. Cells were then treated daily with 0.25 M NU7441 or supplemented with fresh growth medium for indicated time. Whole-cell extracts were prepared after treatment and immunoblotted as indicated. SMC1 was used as loading control. (B) Quantitative graph of (A). Error bars represent SEM values of two (NU) or three (PDS and PDS + NU) independent experiments.

Interestingly, BRCA2-deficient cells treated with olaparib 0.5 M for 24 hours showed an increased phosphorylated KAP1 level during the recovery period, which was unaffected by the addition of NU7441 (**Figure 16**). Contrary to PDS

treatments, BRCA2-deficient cells treated with either 5 nM or 20 nM CX5461 exhibited an increasing level of phosphorylated KAP1 during the recovery period (**Supplementary Figure 1**). However, the addition of NU7441 during the recovery period might have induced a slight increase of phosphorylated KAP1 level 3 days after the removal of CX5461 (**Supplementary Figure 1B, D**).

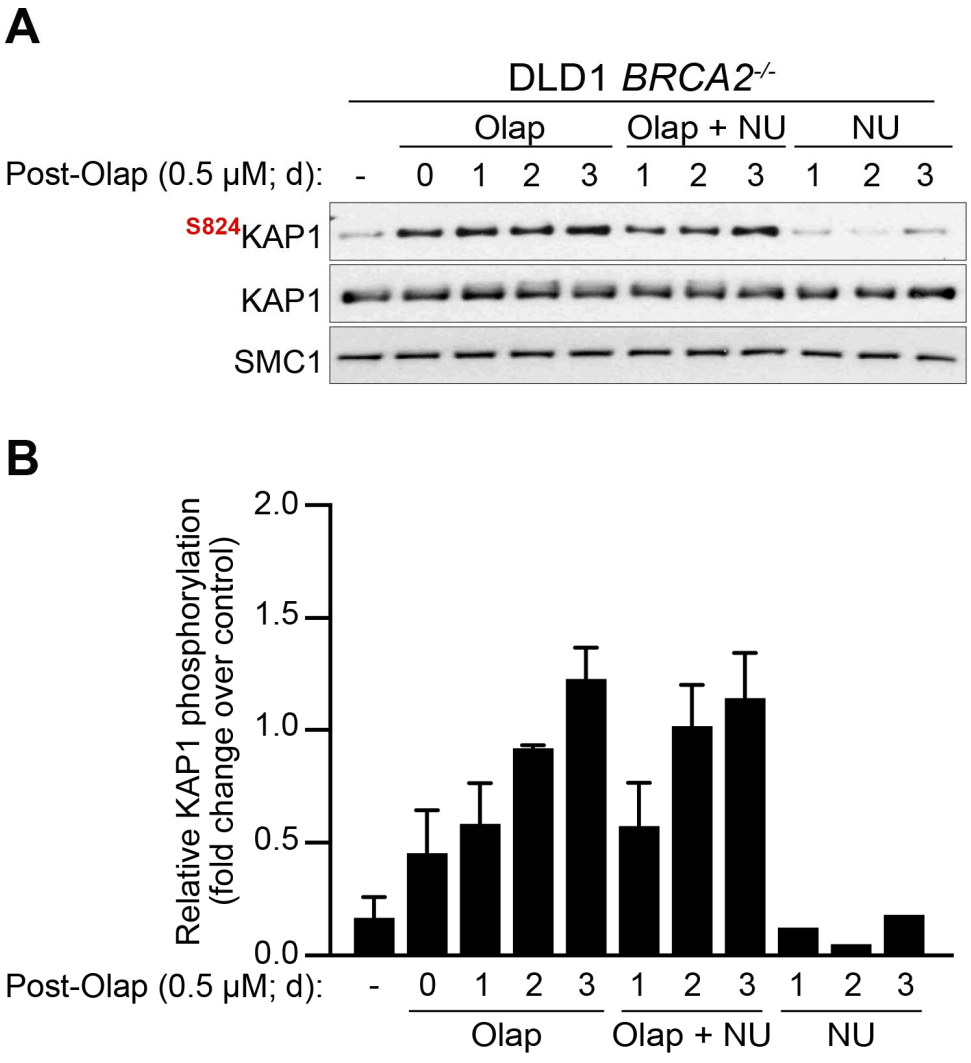
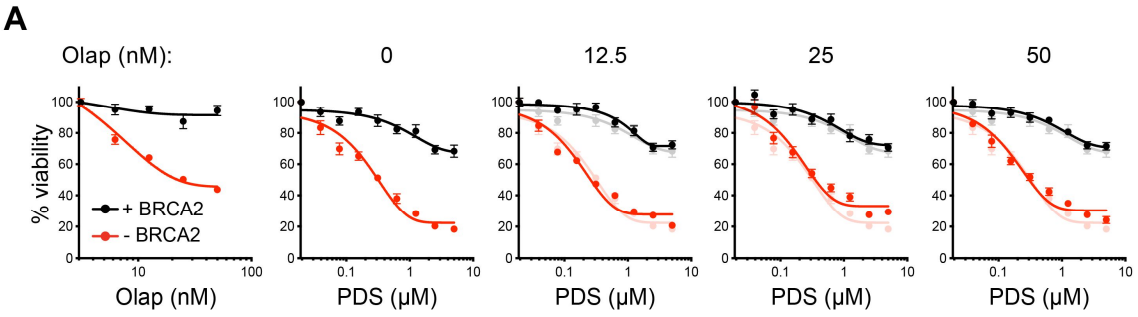


Figure 16: Effect of DNA-PKcs inhibitor NU7441 on BRCA2-deficient cells upon olaparib treatment

(A) Human DLD1 cells BRCA2-deficient were incubated with 0.5 M olaparib for 24 hours and released into growth medium with 0.25 M NU7441 or fresh growth medium. Cells were then treated daily with 0.25 M NU7441 or supplemented with fresh growth medium for indicated time. Whole-cell extracts were prepared after treatment and immunoblotted as indicated. SMC1 was used as loading control. (B) Quantitative graph of (A). Error bars represent SEM values of one (NU) or three (Olap and Olap + NU) independent experiments.

These results suggest that the DNA damage induced by olaparib or PDS treatments are repaired differently in BRCA2-deficient cells. We thought that the combination of PDS and olaparib was an appealing idea that could lead to genome instability overload in BRCA-deficient cells. Indeed, with DNA damage and replication stress from different origins one can expect a dramatic increase in cell death. Thus, we tested whether olaparib and PDS have synergistic effects when combined. Surprisingly, the cell viability experiments we conducted in DLD1 BRCA2-deficient cells revealed no synergistic effects between the two drugs (**Figure 17**).



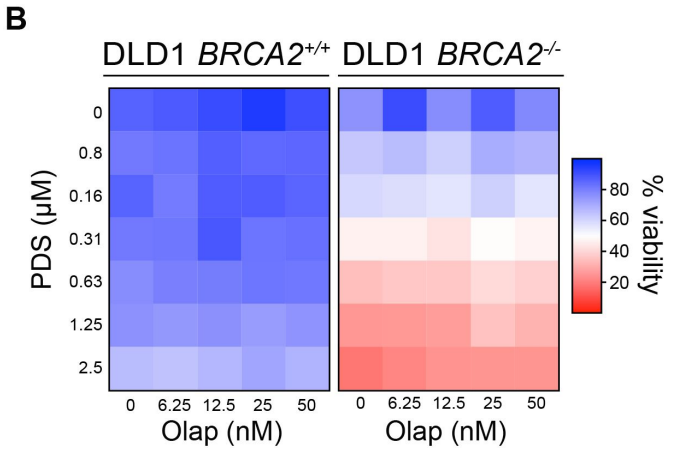


Figure 17: Effect of PDS in combination with olaparib on BRCA2-deficient human cell viability

(A) Human DLD1 cells, BRCA2-proficient (+BRCA2) or -deficient (-BRCA2), were incubated with the indicated concentrations of olaparib and PDS for 6 days. At the end of the above treatment, cells were processed for resazurin-based cell viability assays. (B) Heat map representations of (A). Graphs are representative of three independent experiments, each performed in technical triplicate. Light black and light red curves represent BRCA2-proficient (+BRCA2) and -deficient (-BRCA2) cells respectively, treated only with PDS. Error bars represent SEM values obtained from three independent experiments.

Taken together these results showed that DLD1 BRCA2-deficient cells were mostly able to recover cell viability, 3 days after PDS treatment, in a DNA-PKcs-dependent manner. In contrast, the DDR response after olaparib treatment increased over the 3 days recovery period, independently of DNA-PKcs activity.

2.4 PDS treatment on cells with various cNHEJ defects

We have previously shown that DNA-PKcs activity is partially required for the repair of PDS-induced DNA damage. We therefore wondered whether this observation can be extended to cells with other cNHEJ defects. Indeed, cNHEJ can be considered as a flexible pathway as the depletion of one component does not always result in the complete abrogation of the repair[42]. The most critical proteins being XRCC4, LIG4 and XLF, the components of the ligation complex, as they are required for the last step of the repair. DNA-PKcs is a central element of cNHEJ and DDR with multiple functions. Indeed, it stabilises KU70/80 on chromatin, induces DNA end processing in association with Artemis and enhances the recruitment of the ligation complex. However, breaks with short complementary overhangs can be directly repaired by ligases without DNA-PKcs activity[376] and its absence leads to KU70/80 destabilisation[377]. Despite 53BP1 being a positive regulator of cNHEJ by inhibiting DNA end resection, its implication in the repair itself is unclear.

In order to investigate the role of components involved at different stages of the cNHEJ machinery, we used HAP1 cells, WT, 53BP1-deficient, DNA-PKcs-deficient or XRCC4-deficient and treated them with PDS, CX5461 or olaparib in cell viability experiments (**Figure 18**). Whilst we validated the knockout of XRCC4-deficient cells by WB (**Figure 18A**), 53BP1-deficient cells were validated by Dr Joanna Loizu (who kindly gifted us the cells). Only HAP1 XRCC4-deficient cells

exhibited a mild sensitivity to olaparib while DNA-PKcs-, XRCC4-, and 53BP1-deficient cells were more sensitive to PDS than WT. Interestingly, DNA-PKcs- and XRCC4-deficient cells had a similar sensitivity to PDS although they exhibited different cell viability curves when treated with CX5461 (**Figure 18B**). Whilst 53BP1-deficient cells were more sensitive to PDS than WT they did not show any sensitivity to CX5461. Surprisingly, only XRCC4-deficient cells displayed a higher sensitivity to Olaparib compared to WT.

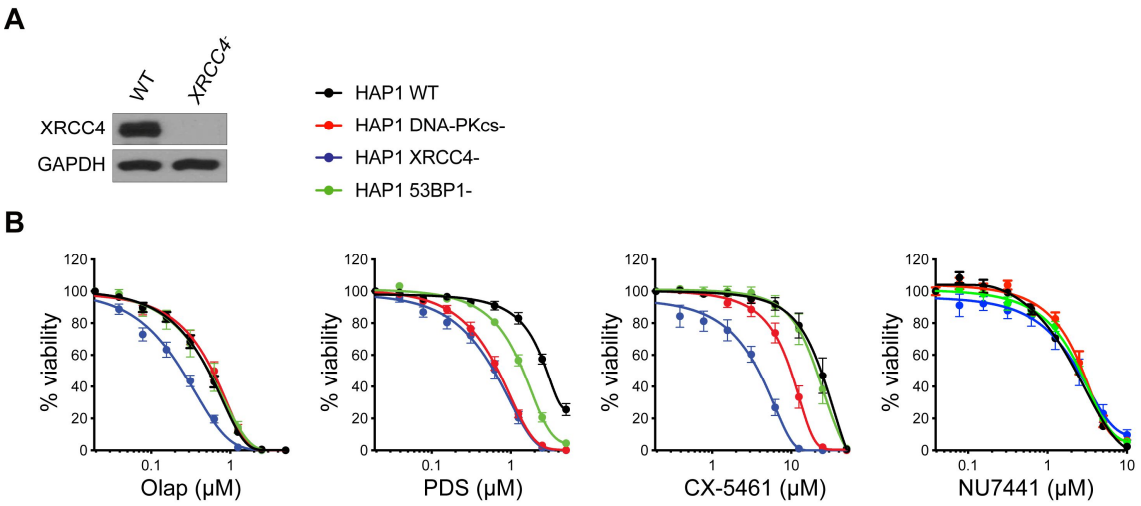


Figure 18: Effect of G4 ligands, olaparib and NU7441 on cNHEJ-deficient human cell

(A) To confirm *XRCC4* knockout, whole-cell extracts of human HAP1 cells were prepared and immunoblotted as indicated. SMC1 was used as loading control. (B) Human HAP1 cells were incubated with the indicated concentrations of olaparib, PDS, CX5461 or NU7441 for 6 days. At the end of the above treatment, cells were processed for resazurin-based cell viability assays. Error bars represent SEM values obtained from three independent experiments.

These results suggest that cells harbouring cNHEJ defects are likely to be sensitive to G4 ligands. However, the relative sensitivities seem to vary depending on the G4 ligand used.

2.5 PDS- and olaparib-induced DNA damage recovery in BRCA1-deficient and olaparib resistant cells.

BRCA1-deficient mouse cells become resistant to olaparib upon depletion of 53BP1[207], or associated proteins, by partially restoring DNA end resection. This allows the loading of RPA on ssDNA and subsequently the displacement of RPA by RAD51, an essential step for HR[378,379]. However, such resistant cells remain sensitive to several DNA damaging agents, including IR[380], chlorambucil[381], cisplatin[208,382] and G4 ligands[155,383]. In some occasion, olaparib resistant cells are even more sensitive to treatment than BRCA1-deficient cells[155,381]. To address the impact of 53BP1 loss on the repair of PDS-induced DNA damage, we used three murine mammary tumour-derived cell lines[207], BRCA1-proficient, BRCA1-deficient and the double BRCA1-/ 53BP1-deficient cells. These cells were originally generated as K14cre; Brca1 F/F; p53 F/F and the loss of 53BP1 arose *in vivo* due to sustained olaparib treatment[207,384].

We initially treated these three cell lines with similar concentrations as previously used with DLD1 BRCA2-deficient cells (i.e. 2 M PDS or 2 M olaparib for 24 hours) (**Supplementary Figure 2**). While such concentrations did not induce

detectable phosphorylation of KAP1 in BRCA1-proficient cells, it induced a strong response in BRCA1-deficient cells immediately after treatment by either olaparib or PDS, which largely decreased during the recovery period of 4 days. Consistently with these cells being resistant to olaparib, BRCA1-/ 53BP1-deficient cells exhibited a reduced response to olaparib treatment when compared to BRCA1-deficient cells (**supplementary Figure 2D**). Importantly, BRCA1-/ 53BP1-deficient cells did not seem to fully recover from PDS treatment regarding that the level of phosphorylated KAP1 was maintained during the recovery period. Despite revealing very interesting phenotypes, we noticed a robust cellular death while conducting the experiments in BRCA1-deficient cells treated with olaparib or PDS and in BRCA1-/ 53BP1-deficient cells treated with PDS. We therefore decided to reduce the drugs concentrations to 0.5 M PDS and 0.5 M olaparib. Regarding that treatment with 2 M PDS or olaparib appeared to be non-toxic to BRCA1-proficient cells we focused on BRCA1-deficient and BRCA1-/ 53BP1-deficient cells only (**Supplementary Figure 3**). We observed similar trends as in **Supplementary Figure 2** regarding KAP1 phosphorylation patterns. Unfortunately, we still noticed a substantial cell death while conducting the experiments and decided to decrease the concentrations of treatments once again to 0.2 M PDS or olaparib. In both **Supplementary Figures 2** and **3,** we detected small, if any, variations between the samples after 3 days and 4 days recovery, in almost all conditions. For this reason, we decided to focus on the recovery up to 3

days only. From these two initial experiments we saw a substantial recovery of PDS- and olaparib-induced DNA damage in BRCA1-deficient cells during the recovery period. We wondered whether such recovery was due to DNA-PKcs activity as we showed in DLD1 cells (**Figure 15**). In BRCA1-deficient cells, phosphorylated KAP1 seemed to peak after 24 hours treatment and then decreased during the recovery period. However, this decrease was strongly impaired when cells were supplemented with NU7441 during the recovery period (**Figure 19**). Importantly, the concentration of NU7441 used did not induce noticeable phosphorylation of KAP1. It is worth noting that the phosphorylation level of KAP1 seemed to be rather increased than just maintained upon the addition of NU7441 (**Figure 19B**). We conducted a similar experiment in BRCA1-deficient cells with olaparib instead of PDS. BRCA1-deficient cells were able to partly recover from olaparib-induced DNA damage, in a seemingly DNA-PKcs-independent way (**Figure 20**). Regarding the endogenous level of KAP1 phosphorylation in the untreated conditions it seemed that the damage induced by olaparib was less severe compared to PDS (**Figure 19**).

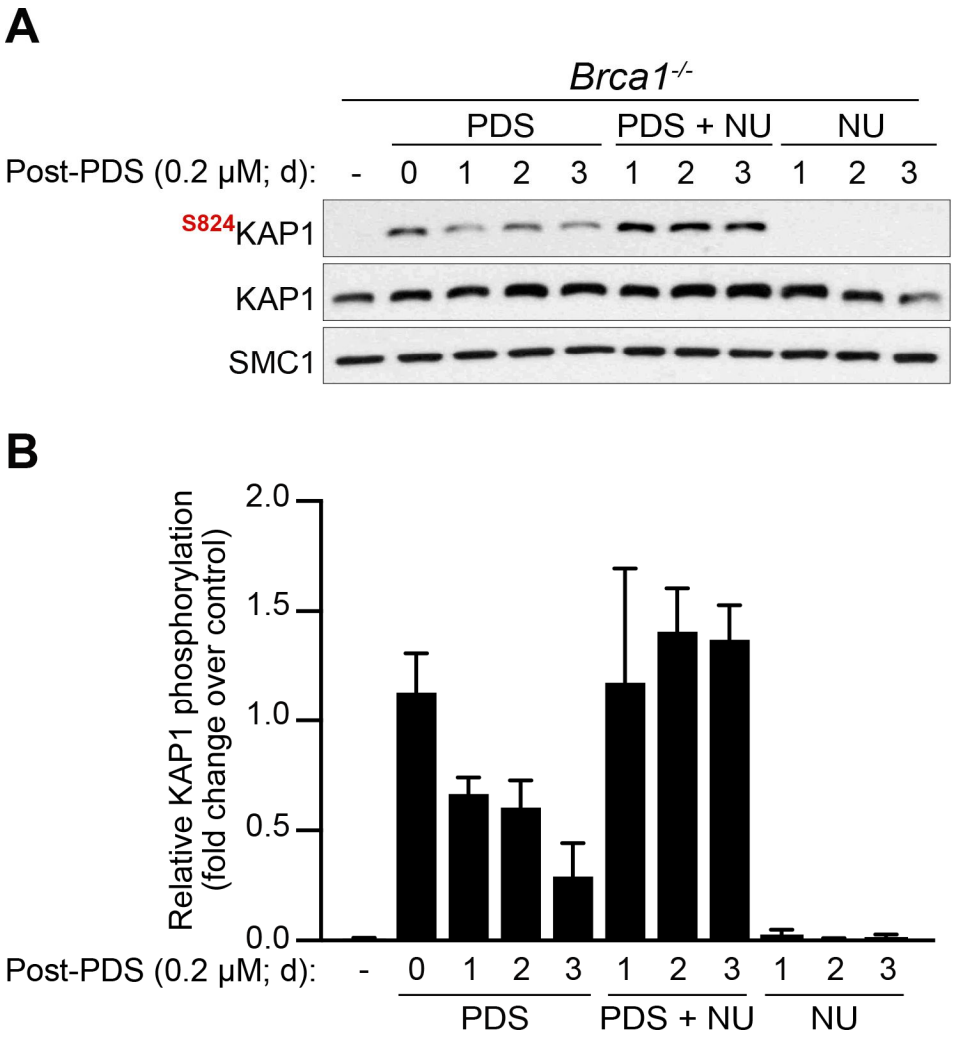


Figure 19: Recovery of BRCA1-deficient mouse cells upon PDS treatment is impaired by NU7441

(A) Mouse BRCA1-deficient (*Brca1*$^{-/-}$) cells were incubated with 0.2 µM PDS for 24 hours then released into growth medium with 2 M NU7441 or fresh growth medium. Cells were then treated daily with 2 M NU7441 or supplemented with fresh growth medium for indicated time. Whole-cell extracts were prepared after treatment and immunoblotted as indicated. SMC1 was used as loading control. (B) Quantitative graph of (A). Error bars represent SEM values of two (NU and PDS + NU) or five (PDS) independent experiments.

Finally, we assessed again the DNA damage recovery upon PDS and olaparib treatments in the olaparib resistant BRCA1-/ 53BP1-deficient cell line, using

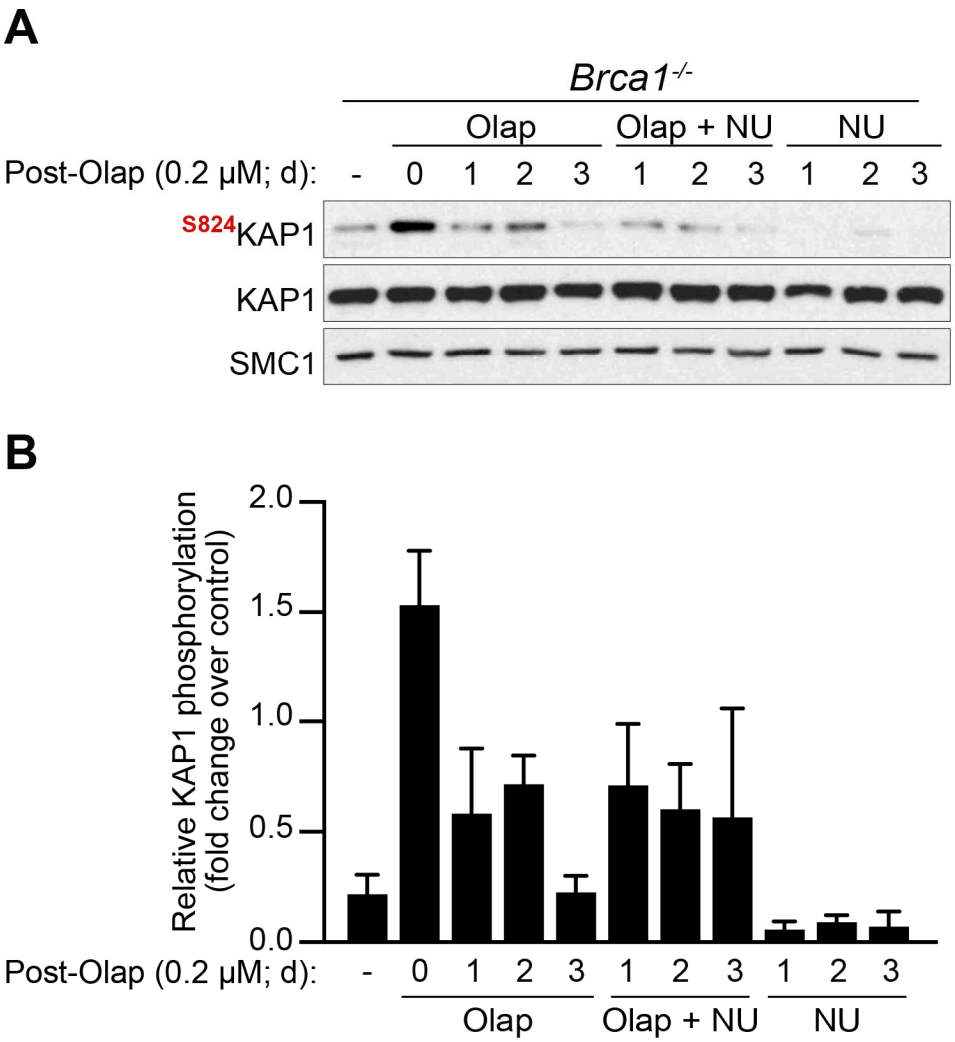


Figure 20: Recovery of BRCA-deficient mouse cells upon olaparib treatment

(A) Mouse BRCA1-deficient (*Brca1*$^{-/-}$) cells were incubated with 0.2 μM olaparib for 24 hours then released into growth medium with 0.25 M NU7441 or fresh growth medium. Cells were then treated daily with 0.25 M NU7441 or supplemented with fresh growth medium for indicated time. Whole-cell extracts were prepared after treatment and immunoblotted as indicated. SMC1 was used as loading control. (B) Quantitative graph of (A). Error bars represent SEM values of two (NU and Olap + NU) or three (Olap) independent experiments.

concentrations that induced low apparent cellular death (0.2 M). Whilst we validated the knockout of 53BP1-deficient cells by WB (**Figure 21A**), BRCA1 knockout was validated by Dr. Sven Rottenberg (who kindly gifted us the cells).

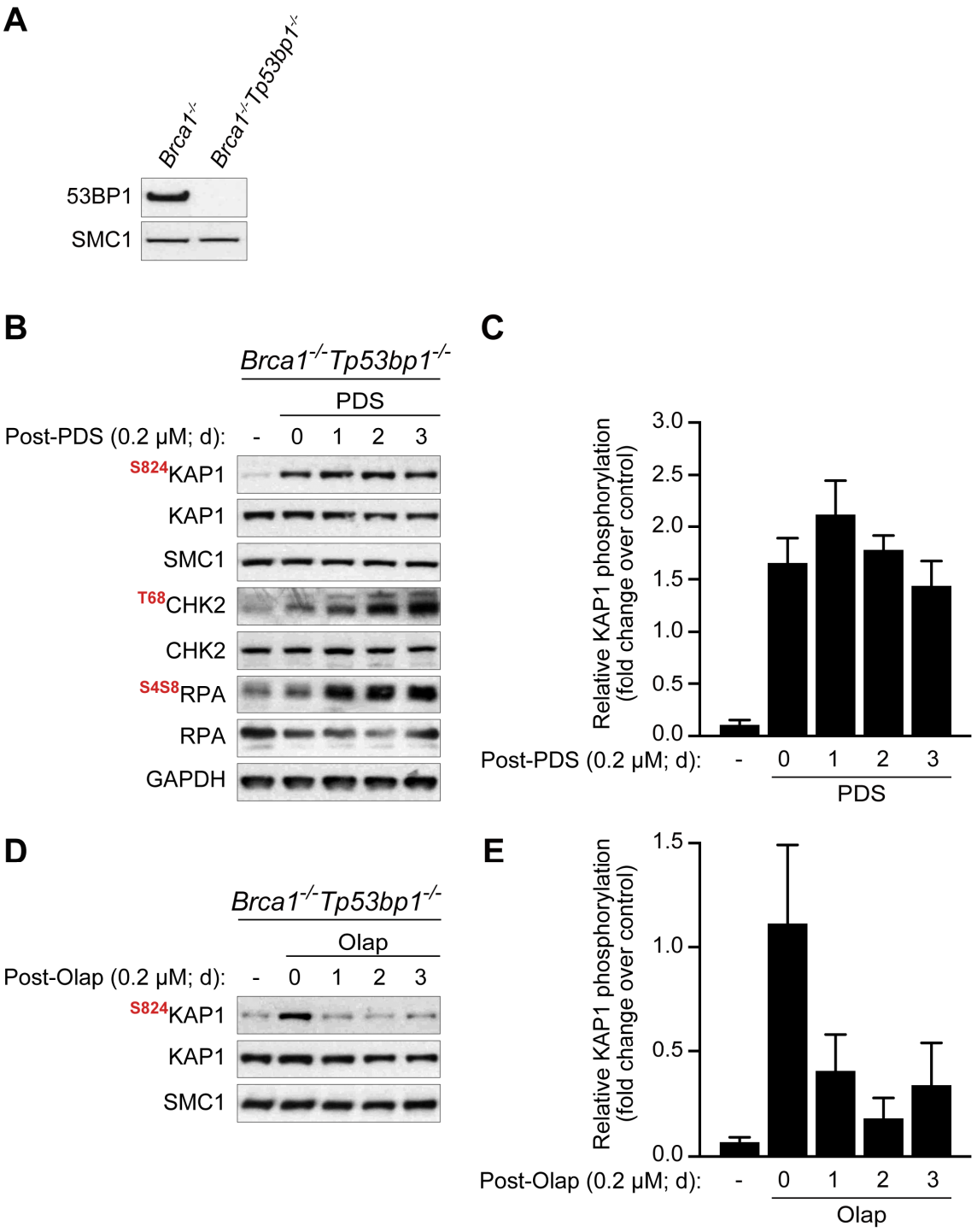


Figure 21: Recovery of olaparib resistant BRCA-deficient mouse cells upon PDS or olaparib treatment

(A) Confirmation of *Tp53BP1* knockout. (B) Mouse BRCA1-/ 53BP1-deficient (*Brca1*$^{-/-}$ *Tp53bp1*$^{-/-}$) cells were incubated with 0.2 μM PDS (B, C) or 0.2 M olaparib (D, E) for 24 hours and released into fresh growth medium for indicated time. (A, B, D) Whole-cell extracts were prepared after treatment and immunoblotted as indicated. SMC1 was used as loading control. (C, E) Quantitative graph of (B) and (D) respectively. Error bars represent SEM values of three independent experiments.

Furthermore, the phosphorylation level of CHK2 (another substrate for ATM that becomes phosphorylated at Threonine 68 upon DNA damage[385]) and the phosphorylation level of RPA at Serine 4/8 increased after treatment and even during the recovery period. Conversely, BRCA1-/ 53BP1-deficient cells treated with olaparib almost fully recovered from the initial damage during the recovery period (**Figure 21D, E**). In order to assess whether the inability of BRCA1-/ 53BP1-deficient cells to fully recover from PDS-induced DNA damage depends on resection mechanisms, we used two different small interfering RNAs (siRNAs) against CtIP and treated cells with PDS. Interestingly, CtIP depletion in combination with PDS treatment impaired recovery and dramatically increased the phosphorylation level of KAP1, CHK2 and RPA over the 3 days recovery period compared to cells treated with PDS and control siRNA (siCTRL) (**Supplementary Figure 4**).

Taken together these results showed similar phenotypes between BRCA1-/ 53BP1-deficient cells treated with PDS and BRCA1-deficient cells treated with PDS in combination with NU7441. Conversely, olaparib treatment in BRCA1-deficient and

BRCA1-/ 53BP1-deficient cells increased KAP1 phosphorylation level which strongly decreased during the recovery period independently of DNA-PKcs inhibitor addition.

3 Discussion

3.1 MSC seems more potent than NU7441

Interestingly, neither NU7441 nor MSC displayed a specific toxicity towards BRCA-deficient cells in both the acute (H1299 shBRCA2 cells) or the terminally adapted (DLD1 BRCA2-deficient, HCT116 BRCA2-deficient and RPE1 BRCA1-deficient cells) loss of BRCA models. This initial observation suggests that endogenous DNA damage is repaired in a DNA-PKcs-independent manner even in HR-compromised cells, supporting the idea that back-up DNA repair pathways, such as a-EJ, are primarily involved to compensate HR defects[125,126]. In our cell model, MSC and NU7441 effectively impaired the phosphorylation of DNA-PKcs at serine 2056 and they both exhibited similar specificity for DNA-PKcs over ATM or ATR. However, to robustly characterise the specificity and selectivity of such inhibitors, extensive biochemical assays monitoring the enzymatic activities of DNA-PKcs and related kinases against a gradient of inhibitors concentrations would be required. Fortunately, the *in vitro* characterisation of MSC has been recently published, revealing its high potency and selectivity over a panel of 276 kinases from the same family. For instance, MSC had an IC50 more than 10,000-fold smaller for DNA-PKcs than for ATM or mTOR[386]. As a comparison NU7441 showed an IC50 for DNA-PKcs only 100-fold smaller compared to ATM, ATR or mTOR[387]. Overall, MSC has a better water solubility, a lower toxicity and a better

selectivity and specificity compared to NU7441. These features suggest that MSC is a better DNA-PKcs inhibitor than NU7441.

3.2 G4s ligands synergise with DNA-PKcs inhibitors

PDS treatments displayed significant synergistic effects when combined with both NU7441 and MSC in DLD1 and RPE1 BRCA-proficient and -deficient cells. These results suggest that although PDS sensitivity is higher in BRCA-deficient cells, the cell viability of BRCA-proficient cells upon G4s stabilisation depends, to a certain extent, on DNA-PKcs activity as well. Some damage induced by PDS might arise independently of HR failure (for instance during transcription[271] or due to collision between the replication fork and the transcription machinery). Another hypothesis would be that only a certain amount of stalled replication forks can be fixed by HR-like processes simultaneously before the exhaustion of protein pools. It is likely that when the system is overloaded with DNA damage, multiple repair mechanisms become involved. The synergies between PDS and DNA-PKcs inhibitors were observed in both *BRCA1*- and *BRCA2*-mutated cell lines, implying that proteins that can disrupt HR (such as PALB2 or BARD1) are likely to exhibit the same phenotypes. Interestingly, CX5461 and DNA-PKcs inhibitors displayed more discrete synergies compared to PDS. This suggests that different G4 ligands induce different types of DNA damage that recruit different repair mechanisms.

Cell viability experiments conducted with HAP1 DNA-PKcs-deficient cells showed that lack of DNA-PKcs sensitises cells to PDS (**Figure 11**), consistent with results obtained in other studies using the DNA-PKcs-deficient MO59J cells[271]. Moreover, these findings demonstrate that NU7441 and MSC synergise with PDS mainly due to DNA-PKcs activity, as its absence largely reduced the synergistic effects. However, some residual synergies were observed even in DNA-PKcs-deficient cells (**Figure 11D, E**), likely due to side effects of the inhibitors. It is important to bear in mind that regarding the low toxicity of DNA-PKcs inhibitors treatments alone in **Figure 11** (approximately 80% cell viability at the highest concentrations), the mild synergies observed in DNA-PKcs-deficient cells likely indicate DNA-PKcs-independent effects (possibly via inhibition of other PIKK members). Curiously, treatment with PDS in combination with MSC (at concentrations between 0.5 and 1.5 M) sensitised more DNA-PKcs-proficient cells compared to DNA-PKcs-deficient cells (**Figure 11C, E**). It means that, in this context, the presence of DNA-PKcs was more detrimental to cell viability than its absence. However, these cells might have adapted to the loss of DNA-PKcs. Alternatively, live cell imaging experiments showed that the DNA-PKcs mutant S2056A (the serine at residue 2056 was replaced by an alanine) was retained longer on chromatin than the WT protein[93]. When trapped on chromatin, DNA-PKcs might block the access of DNA ends to other repair mechanisms, therefore impairing any form of DNA ligation and decreasing cell viability upon DNA damage. It would be interesting to investigate

whether DNA-PKcs inhibitors can trap DNA-PKcs on chromatin. This could be addressed by monitoring over time the amount of DNA-PKcs present in the chromatin fraction after inducing DNA damage. Regarding MSC efficiency compared to NU7441, it is appealing to hypothesise that MSC has a higher trapping potential than NU7441.

Overall, MSC was less toxic, induced stronger synergies and showed less DNA-PKcs-independent effects than NU7441, over the range of concentrations used, reinforcing the hypothesis that MSC is a better DNA-PKcs inhibitor than NU7441.

3.3 PDS-induced DNA damage can be partly repaired in BRCA-deficient cells

The DNA damage induced by acute PDS treatment largely decreased over time in DLD1 BRCA2-deficient cells after the drug removal (**Figure 14A**), suggesting that part of the damage can be repaired in an HR-independent manner. Such recovery was largely impaired by the addition of NU7441 during the recovery period. This indicates that the activity of DNA-PKcs is required to restore cell viability in HR-deficient cells upon PDS treatment. Moreover, RPA was highly phosphorylated at Serine 4 and Serine 8 upon PDS treatment (**Figure 14A**) and evidence showed that this phosphorylation site is activated by DNA-PKcs during replication stress[388,389]. However, the role of DNA-PKcs during replication stress is poorly

understood. It would be interesting to address the potential role of DNA-PKcs at stalled replication fork in HR-deficient background using DNA fiber analysis.

In order to induce DNA damage first and in a second time impair DNA-PKcs activity, NU7441 was added to the growth medium only after the removal of PDS or CX5461. These experiments could be further improved by determining the half-life of NU7441 in our cell models. Knowing this parameter would allow us to optimally time the delivery of the drugs and likely increase the synergies efficacies. However, it is possible that instead of recovering and repairing DNA damage, cells undergoing cellular death accounts for a large part of the population exhibiting aberrations and DDR signalling. Regarding that 1 M PDS treatment for 6 days induced a 50% decrease of cell viability in DLD1 BRCA-deficient cells (**Figure 9A)**, we estimated that 2 M PDS for 24 hours was a reasonable concentration to induce DNA damage while sparing most of the cells. In order to robustly confirm this estimation, DLD1 BRCA2-deficient cells could be treated with 2 M for 24 hours then monitored in cell viability experiments and population doubling assays until the end of the recovery time. The fraction of cells undergoing apoptosis could also be measured by WB using antibodies against cleaved-PARP (PARP cleavage by caspase-3 is a marker of early stages of apoptosis[390,391]).

In contrast to PDS, the amount of DNA damage induced by olaparib increased during the recovery period despite the removal of the drug. This observation might indicate that whilst PDS treatments induce an acute increase of DNA damage

during a short period of time, olaparib treatment might induce DNA damage that is amplified during the cell cycle. Therefore, PDS and olaparib treatments seem to induce different types of DNA damage that require different mechanisms for their repair. Surprisingly, PDS and olaparib combination did not show synergistic effect in either DLD1 BRCA2-proficient nor -deficient cells. It indicates that even in BRCA2-deficient cells the presence of PDS-induced DNA damage does not worsen the cellular management of olaparib-induced DNA damage and vice versa. An appealing hypothesis would be that olaparib-induced lesions are repaired via a-EJ while PDS-induced damage is repaired via cNHEJ. However, in the PARP inhibitors family, olaparib has a moderate ability to trap PARP on DNA[392] and may have other mechanisms to induce DNA damage. It would be interesting to address DNA-PKcs combination with PARP inhibitors of different trapping potency such as talazoparib or niraparib[392,393]. Indeed, CX5461 has been recently reported to display synergistic effects in combination with talazoparib in HR-deficient high grade serous ovarian cancer-patient-derived xenograft[394]. This suggests that the right combination of G4 ligands with PARP inhibitors remain a promising approach to treat HR-compromised cells and tumours.

We demonstrated the ability of BRCA2-deficient cells to recover from the G4 ligand PDS and to restore cell integrity over the course of 3 days post treatment. However, whether the recovery is due to drug dissociation from G4s or the actual repair of induced DSBs must be specified. G4 ligands dissociation in cells and eventual

metabolites could be addressed using mass spectrometry analysis at different time points after drugs addition to the medium.

3.4 Cells with cNHEJ defects have an increased sensitivity to PDS

In order to assess whether the observed phenotypes were due to DNA-PKcs roles in replication stress[388,389] or cNHEJ, the G4 ligands sensitivity of other cNHEJ-deficient cells were investigated by cell viability assays. HAP1 XRCC4-deficient cells displayed the most sensitive phenotypes to G4 ligands. This could be explained by the fact that alteration of the ligation complex does not prevent the initiation of cNHEJ[42], likely resulting in incomplete repair and trapped proteins on DNA ends, eventually blocking the access to other repair pathways. Intriguingly, HAP1 DNA-PKcs-deficient cells exhibited the same sensitivity as XRCC4-deficeint cells upon PDS treatment (**Figure 18B**), which contrasts with phenotypes obtained upon CX546 treatment. It could imply that the lack of DNA-PKcs is not as dramatic as a complete loss of cNHEJ (represented here by XRCC4 deficiency) upon CX5461 treatment. The end processing activity of DNA-PKcs in complex with Artemis[89,98-101] might be more important for DNA damage induced by PDS than CX5461. Whilst 53BP1-deficient cells were more sensitive to PDS than WT it showed no further sensitivity when treated with CX5461. This could suggest that the type of breaks (or their availability) induced by PDS and CX5461 might be

different. The stability of the interaction between the G4 ligands and the G4s structures could also account for these phenotypes. Whether the G4 ligands remain attached to G4s during the repair or whether the repair is initiated after dissociation remains unknown.

These results suggest that cells with cNHEJ defects are likely to be sensitive to G4 ligands. However, the implication of 53BP1 in cNHEJ upon G4 ligands treatment remains to be elucidated.

3.5 PDS-induced DNA damage is retained in olaparib resistant cells

We showed that olaparib resistant cells were not able to fully recover from DNA damage induced by PDS, even 3 days after the removal of the drug **(Figure 21)**. This phenotype closely resembles BRCA1-deficient cells treated with PDS in combination with NU7441, making the correlation between 53BP1 and DNA-PKcs activity appealing. This suggests that the loss of 53BP1 could be a double-edge sword, allowing end resection processing at the likely cost of cNHEJ efficiency. However, the increased phosphorylation of RPA S4/S8 upon PDS treatment in olaparib resistant cells challenge this hypothesis. Indeed, a fraction of DNA-PKcs activity seems to be maintained even in the absence of 53BP1. Whether this activity is completely independent of cNHEJ or not remains to be determined. It would be interesting to assess whether the addition of DNA-PKcs inhibitors could further

worsen the phenotype of BRCA1-/ 53BP1-deficient cells treated with PDS. Such results could clarify whether 53BP1 and DNA-PKcs have redundant roles in this context. Regarding that PDS treatment combined with depletion of CtIP induced an increase of DNA damage (**Supplementary figure 4**), the loss of 53BP1 could actually retain DNA damage over time due to its role in DNA end resection. Indeed, 53BP1 depletion has been linked to DNA end resection increase in Brca1-deficient cells[111] and CtIP promotes the MRN complex endonuclease activity[44,47]. This result suggests that PDS might induce DNA damage that require some DNA end processing to be repaired. This hypothesis is supported by findings showing that, in G1, CtIP-dependent resection can prime DSBs towards cNHEJ repair[395]. Alternatively, CtIP was also described to protect stalled replication fork against DNA2 extensive resection independently of MRE11[154]. This could also explain why we observed an increase of DNA damage since a stalled replication fork, due to G4s stabilisation, would be depleted of a protecting factor. In order to address which function of CtIP is linked to the phenotypes we observed, DNA2, MRE11 or Artemis could be depleted in cells treated with PDS and the DNA damage recovery followed after the drug removal. Moreover, it would be of interest to monitor DNA end resection upon drug treatment using a flow cytometry-based method coupled with RPA foci detection[396]. Such an approach could shed light on whether DNA end resection plays a role upon PDS treatment and in which phase of the cell cycle it occurs. In contrast with DLD1 BRCA2-deficient cells, BRCA1-deficient and

olaparib resistant cells both recovered from DNA damage induced by olaparib (**Figures 20-21**). Additionally, the DNA damage induced by olaparib did not require DNA-PKcs activity to be repaired in BRCA1-deficient cells. These results raise the need for interrogations on the exact type of DNA damage that is induced by olaparib, which seem different from most of other DNA damaging agents.

4 Conclusion and outlook

In this study, we characterised MSC regarding its cytotoxicity, its effect on the activity of DNA-PKcs and potential side effects comparatively with NU7441. We demonstrated that MSC was specific for the inhibition of phosphorylated DNA-PKcs (S2056) and displayed a small noticeable effect on cell viability in DNA-PKcs absence. However, the ability of MSC to impair DSBs repair via cNHEJ remains unclear. Despite DNA-PKcs being a major effector of cNHEJ, DNA ligases can still achieve DNA ligation in the absence of DNA-PKcs[42]. Many functional systems have been engineered to investigate the repair mechanism pathways involved upon induced DNA damage[397], including the DSB-inducing sequence-specific endonuclease I-SceI[398] system or based on CRISPR/Cas9 fluorescent reporters[399]. Experiments conducted with such tools could shed light on the effect of DNA-PKcs inhibitors on the effectiveness of the repair through cNHEJ machinery and the eventual back up repair pathways.

In two different *BRCA* WT and *BRCA*-mutated cell lines, NU7441 and MSC both synergised in a dose-dependent manner with PDS. This observation was further strengthened with the use of a second G4 ligand, CX5461. However, G4 ligands are versatile and can bind to different types of G4s structures with various specificity. Efforts to better understand the binding preference of G4 ligands has been recently made via a high throughput model using DNA microarrays covered with PQS[400].

It would be of interest to address this synergy in a larger panel of G4 ligands with different molecular structures and binding affinities. Synergistic effects from drug combinations could also be quantified using the so-called Chou-Talalay method, resulting in combination index values[401]. This type of experiments could shed light on whether small molecules targeting G4s induce the same type of DNA damage, ultimately leading to a better classification of their genotoxic effects in cells.

We demonstrated that PDS-induced DNA damage can be partly repaired in an HR-deficient background, depending on DNA-PKcs normal activity. However, we mainly monitored the DDR signalling via the phosphorylation of KAP1 or RPA in human and mouse cells. Regarding the intricate activity of ATM, ATR and DNA-PKcs during the DDR[132], phosphorylated KAP1 might not fully represent DNA damage variations and further markers of DNA damage should be monitored in this context such as 53BP1, yH2AX or the phosphorylation of RPA at Serine 33 (substrate of ATR upon replication stress[402]). Such markers could be investigated using WB or IF, regarding that most of the DDR markers form foci.

In order to better understand the dynamics of DNA damage onset upon G4 ligands treatment, it would be insightful to monitor the type of DNA damage induced by PDS during treatment and after drug removal via neutral and alkaline comet assay[273]. This could reveal the dynamic of DNA damage and DSBs formation upon PDS treatment. For instance, CX5461 has been shown to induce mainly SSB lesions

30 minutes after treatment[273]. Following the damage over a longer period would allow to time and quantify SSBs conversion into DSBs. The impact of the cell cycle would also be of interest to better understand the mechanisms involved in the transition of SSB into DSB.

Furthermore, a recent study has shown that PDS might induce DNA lesions by trapping topoisomerase II (TOP2) on DNA[403]. This observation was validated with CX5461 as well[404]. This could explain why we obtained different phenotypes between olaparib and PDS treatments. It would be interesting to test whether TOP2 inhibitors display synergistic effects when combined with DNA-PKcs inhibitors or G4 ligands. Recently, a class of TOP1 inhibitor have been shown to interact as G4 ligands with the c-MYC promoter G4[323]. This suggest that some G4 ligands might induce DNA damage due to DNA supercoiling issues rather than G4s stabilization[404]. This is consistent with our observation that PDS induces DNA damage depending on CtIP, which has been showed to be required for TOP2-induced DNA damage repair in G1 by cNHEJ as well[405]. It is worth noting that DNA-PKcs has been shown to be activated by ATM upon DNA damage induced by the TOP1 inhibitor CPT[406]. Altogether, these findings suggest another hypothesis to explain the synergistic effects we observed when G4 ligands are combined with DNA-PKcs inhibitors.

A recent CRISPR screen has identified genomic ribonucleotides incorporation as a source of olaparib-induced DNA lesions in Hela, RPE1 and SUM149PT (*BRCA1*-mutated) cells[213]. In fact, DLD1 cells lack MutL homolog 1 (MLH1), a critical component of the mismatch repair (MMR) pathway[407]. Considering that MMR has been shown to interact with ribonucleotide excision repair (RER)[408,409], it might explain the different phenotypes we observed during the recovery period upon olaparib treatments in DLD1 *BRCA2*-mutated compared to *Brca1*-mutated mouse cells.

Recently, DNA damage caused by stalled replication fork has been linked to an increase in inflammation and interferon (IFN) stimulated genes (ISG) via the cGAS-STING pathway[410]. Such findings were observed as well in *BRCA*-mutated cells upon treatment with DNA damaging agents, such as olaparib[411]. Regarding that, PDS induces replication fork stalling in *BRCA*-mutated cells, it would be interesting to investigate whether it triggers cGAS-STING activation as well. Moreover, our *in vivo* collaborators have observed a highly potent synergistic effect between PDS and paclitaxel (PTX, also known as Taxol), a taxane which targets tubulin and induces defects in mitotic spindle assembly[412]. Interestingly, PTX is linked to cGAS and has been shown to induce mitotic arrest, pushing towards cGAS-dependent mitotic cell death[413].

Our *in vitro* results provide valuable tools for further *in vivo* experiments, that are currently being conducted, with the aim to reproduce the synergy between PDS

and NU7441 in xenograft mouse models. Regarding that, no study has been conducted so far to assess PDS effects *in vivo*, our data could be useful resources for further animal studies. While RPE1 cells do not form tumours *in vivo*, DLD1 cells can be used to generate xenografts in nude mice[155] and survival assays can be useful to estimate the range of concentrations to be used *in vivo*. We believe that addressing PDS efficacy in *Brca*-mutated mouse models alone or in combination with DNA-PKcs inhibitors would be very valuable preclinical knowledge.

Whilst PDS and CX5461 have shown promising results against BRCA1-deficient cells and tumours that have acquired resistance to olaparib[155,404], it is likely that tumours will eventually become resistant to G4 ligands as well if treatments are sustained. Targeting resistant tumours with new drugs hoping that resistance does not arise once again can appear as an endless mildly promising approach. However, the characterisation of new drugs mechanisms in specific types of cancer lead to highly valuable therapeutic knowledge. Indeed, regarding tumour heterogenicity, single drug treatments usually have a limited potency whilst the appropriate drugs combinations can induce powerful synergistic effects and synthetic lethality[414-416], ultimately killing a larger fraction of tumours cells. Fortuitously, herculean efforts driven by the personalised medicine model are leading to a better characterisation of patient tumours types and vulnerabilities, paving the way for the use of personalised anticancer cocktails as the first line of treatment. I believe that such

ambitious approach has the potential to substantially improve cancer patient survival.

5 Material and methods

5.1 Cell lines and growth conditions

Cells were cultivated in monolayers at 37C in 5% CO2 incubators unless specified. Human colorectal adenocarcinoma DLD1 cells, parental and *BRCA2*-mutated (Horizon Discovery[155]), were grown in Dulbecco's Modified Eagle's Medium (DMEM, D5796, Sigma Aldrich) supplemented with 10% foetal bovine serum (FBS, F7524, Sigma Aldrich). Human non-small cell lung carcinoma H1299 cells were cultivated in DMEM supplemented with tetracycline-free FBS (631106, Clonetech). The expression of shRNA against BRCA2 was induced via growth medium containing 2 g /mL doxycycline (D9881, Sigma Aldrich). Human colorectal carcinoma HCT116 cells, parental and *BRCA2*-mutated (153531, Ximbio), were grown in McCoy's 5a media (16600082, Thermo Fisher Scientific) supplemented with 10% foetal bovine serum (F7524, Sigma Aldrich) and 1% penicillin-streptomycin (15140148, Thermo Fisher Scientific). Human retinal pigmented epithelium RPE1 cells, parental and *BRCA1*-mutated, were grown in DMEM supplemented with 10% FBS (F7524, Sigma Aldrich) and 5 g /mL blasticidin (A11139-03, Thermo Fisher Scientific). Human HAP1 cells, parental, *XRCC4*-mutated (kind gift from Dr Andrew Blackford), *DNA-PKcs*-mutated (kind gift from Dr Anderson Ryan) and *TP53BP1*-mutated (kind gift from Dr Joanna Loizu), were cultivated in Iscove's Modified Eagle's Medium (IMDM, 12440061, Thermo Fisher

Scientific) supplemented with 10% FBS (16000-044, Thermo Fisher Scientific). The following mouse mammary tumour-derived cell lines were used: *Brca1*$^{+/+}$, *Brca1*$^{-/-}$ and *Brca1-/ Tp53bp1*-mutated[207]. These cell lines were cultured at 37°C, 5% CO_2 and 3% O_2 in complete DMEM/F-12 growth medium (11320033, Thermo Fisher Scientific) supplemented with 10% FBS (26140079, Thermo Fisher Scientific), 5 µg/mL insulin (I0516, Sigma Aldrich), 5 ng/mL epidermal growth factor (PHG0315, Thermo Fisher Scientific), and 5 ng/mL cholera toxin (100B-9100B, List Biological Laboratories). Cells were treated with PDS (SML0678, Sigma Aldrich), olaparib (S1060, Selleck Chemicals), NU7441 (S2638, Selleck Chemicals), CX5461 (A11065, AdooQ Bioscience) and HU (127-07-1, Sigma Aldrich) as indicated.

5.2 Immunoblotting

To prepare whole cell extracts, cells were washed in phosphate buffer saline (PBS, BR0014G, Thermo Fisher Scientific), harvested using trypsin (T3924, Sigma Aldrich), washed in PBS again and re-suspended in sodium dodecyl sulfate-polyacrylamide gel electrophoresis (SDS-PAGE) loading buffer. SDS-PAGE was made of 0.16 M Tris pH 8 (BPE1762-1, Thermo Fisher Scientific), 100 mM dithiothreitol (DTT, 441494N, VWR), 20% glycerol (02193996, MP Biomedical), 4% SDS (BP1311-200, Thermo Fisher Scientific), 0.01% bromophenol blue (B392-

5, Thermo Fisher Scientific) and further supplemented with phosphatase and protease inhibitor cocktails (respectively 04906845 and 04693159001, Roche). Samples were sonicated for 5 seconds using the Ultrasonic Homogeniser 300 V/T (Biologics Inc.) and heated at 70 C for 10 minutes. Protein concentration was determined using the Spectrophotometer ND-1000 (NanoDrop technologies Inc.). Equal amounts of protein (between 50 and 100 g) were loaded onto NuPAGE-Novex 3-8% Tris-Acetate gels (Thermo Fisher Scientific) or NuPAGE-Novex 4-12% Bis-Tris (Thermo Fisher Scientific) depending on the molecular weight of proteins of interest, according to manufacturer's instructions. Gels were fixed in XCell SureLock Mini-Cell (EI0001, Thermo Fisher Scientific) and immersed with Tris-Acetate SDS running buffer (LA0041, Thermo Fisher Scientific) for Tris-Acetate gels or MOPS buffer (N0001, Thermo Fisher Scientific) for Bis-Tris gels. A voltage of 180 V was applied to the system for approximately one hour, depending on the pre-stained protein ladder progression (HiMark™ for Tris-Acetate gels (LC5699, Thermo Fisher Scientific) and PageRuler™ for Bis-Tris gels (26616, Thermo Fisher Scientific)). Proteins were then transferred onto a nitrocellulose membrane (10600001, GE Healthcare Life Sciences) by applying 30 V for 100 minutes in transfer buffer (NP0006-1, Thermo Fisher Scientific) with 10% methanol (32213M, Merck Millipore). Membranes were blocked in PBS (BR0014G, Thermo Fisher Scientific) supplemented with 5% dried skimmed milk (Tesco) and 0.05% Tween 20 (P7949, Sigma Aldrich) for approximately 1 hour at room temperature (RT).

Membranes were then incubated overnight at 4 C with primary antibodies diluted in PBS supplemented with 2% bovine serum albumin (BSA, A7906, Sigma Aldrich), 0.05% azide and 0.05 % Tween 20. The following day, membranes were washed three times 10 minutes with PBS Tween-20 (PBST) at RT, then incubated with secondary antibodies for 1 hour at RT and washed again three times 7 minutes with PBST. Bands were revealed using chemiluminescent WB reagents (RPN2235, GE Healthcare; WBKLS0100, Merck Millipore; 32106, Thermo Fisher Scientific), based on protein abundance. Band intensities were captured using X-ray films (34089, Thermo Fisher Scientific) and processed by the X-ray film processor Protec Ecomax (1186-3-4000, American Laboratory Trading).

5.3 Antibodies

The following antibodies were used for immunoblotting: mouse monoclonal antibodies raised against BRCA2 (OP95, Merck Millipore), GAPDH (6C5, Novus Biologicals); rabbit polyclonal antibodies raised against phosphorylated KAP1 S824 (A300-767A, Bethyl Laboratories), KAP1 (A300-274A, Bethyl Laboratories), phosphorylated RPA32 Ser4&Ser8 (A300-245A, Bethyl Laboratories), RPA32/2 (ab2175, Abcam), SMC1 (A300-055A, Bethyl Laboratories), phosphorylated CHK2 T68 (2661, Cell Signaling Technology), CHK2 (2662, Cell Signaling Technology), CHK1 (A300-274A, Bethyl Laboratories), CtIP (kind gift from Richard Baer),

phosphorylated DNA-PKcs S2053 (ab18192, Abcam), DNA-PKcs (a300-519a, Bethyl Laboratories), XRCC4 (611506, BD Bioscience); rabbit monoclonal antibody raised against phosphorylated CHK1 S345 (2348, Cell Signaling Technology). Anti GAPDH or SMC1 antibodies were used as loading controls.

5.4 Western blot quantification

Band intensities were measured using the analysis software ImageJ according to a recently proposed method for background subtraction[417]. Briefly, X-ray films were scanned using a TASKAlfa 8052ci printer (Kyocera Document Solutions) at a resolution of 600 pixels per inch (ppi). Images were converted to 8-bit format, then a background image was created using the "Subtract background" function. In order to take into consideration non-uniform background, the newly created background image was subtracted to the initial 8-bit one using the function "Image calculator". The obtained images were inverted, then bands were selected and analysed using the "Gels" function. The peak areas of obtained histograms were measured manually using the "Wand tool" and then plotted as indicated.

5.5 FACS analysis

To label replicated DNA, cells were incubated with 10 M 5-ethynyl-2'-deoxyuridine (EdU) for 1 hour. Samples were then harvested by trypsinization and

processed for EdU staining using the Click-iT™ Plus Alexa Fluor™ 647 Flow Cytometry Assay Kit (C10634, Thermo Fisher Scientific) according to manufacturer's instructions. Cells were incubated with 20 g /mL propidium iodide (P4864, Sigma Aldrich) and 10 g /mL RNase A (12091, Thermo Fisher Scientific) in PBS. At least 25,000 cells were analysed per condition using the flow cytometer FACSCalibur™ (342975, BD Biosciences). Obtained data were processed using FlowJo software (BD Biosciences).

5.6 Cell viability assays and combinations

Cells were seeded in 96-well plates at density previously estimated to reach 70 - 80% confluence after 6 days in the absence of treatment. 24 hours following seeding, drugs were added to the growth medium. Cell viability was determined using resazurin-based assays 6 days after treatment. Cells were incubated with 10 µg/mL resazurin (R7017, Sigma-Aldrich) diluted in growth medium at 37 C for 2 hours. Fluorescence was measured at 544 nm excitation and 590 nm emission using POLARstar Omega plate reader (BMG Labtech).

5.7 Clonogenic assays

Cell survival was measured using a colony formation-based assay. To allow single cell proliferation, only 200 BRCA-proficient or 400 BRCA-deficient cells were

seeded per well in 6-well plates. Human colorectal adenocarcinoma DLD1 cells, parental and BRCA2-deficient, were grown in 20% O2 while human retinal pigmented epithelium RPE1 cells, parental and *BRCA1*-muated, were grown in 3% O2 incubators in order to obtain denser colonies. When colonies of approximately 50 cells appeared in control wells the colonies were stained with a crystal violet straining solution (0.5% crystal violet (548-62-9, Merck Millipore), 50% methanol (32213M, Merck Millipore), 20% ethanol (E/0665/DF/17, Thermo Fisher Scientific) and 30% double distilled water (ddH_2O)) for 15 minutes then abundantly washed with water and allowed to dry at RT. Colonies were then counted manually and plotted as indicated.

5.8 Preparation of metaphase chromosome spreads

Cells were synchronised in mitosis via overnight incubation with 0.1 mg/mL KaryoMAX™ Colcemid™ (15212012, Thermo Fisher Scientific) and were collected by mitotic shake-off and swollen in hypotonic buffer (0.03 M sodium citrate (6132, Sigma Aldrich) at 37°C for 25 minutes. Cells were fixed in freshly prepared 3:1 mix of methanol (32213M, Merck Millipore) : glacial acetic acid (20103-330, VWR Chemicals), and nuclear preparations were dropped onto SuperFrost Plus microscope slides (J1800AMNZ, Thermo Fisher Scientific), pre-soaked in 45% acetic acid (20103-330, VWR Chemicals) prior to being allowed to dry overnight.

The following day, slides were incubated with 0.025 trypsin in 0.1 M phosphate buffer (pH 6.8) for 2 minutes then mitotic chromosomes were stained using Giemsa's stain improved solution R66, Gurr™ (350864X, VWR Chemicals) for 15 minutes and viewed with a Leica DMI6000B inverted microscope (Leica Microsystems) equipped with an HCX PL APO 100Å~/1.4–0.7 oil objective (Leica Microsystems). Chromosomal aberrations were quantified manually.

5.9 Transfection with siRNA

siRNAs against CtIP1 (CTM-488777-HR1ZN006090, sense sequence: CGU CUC UAU GUA CAA AUG AAU UAU U, Horizon Discovery) and against CtIP2 (CTM-488778-HR1ZN006092, sense sequence: AAA CAU ACC UGC UGA UAA AUU, Horizon Discovery) were resuspended in siRNA buffer (B-003000-WB-100, Horizon Discovery) at a concentration of 40 M. For transfection, DharmaFECT1 transfection solution (11591731, Thermo Fisher Scientific) was mixed with Opti-MEM™ medium (31985062, Thermo Fisher Scientific) to a 1:100 ratio and incubated 5 minutes at RT. Resuspended siRNAs were mixed with Opti-MEM™ to a 1:100 ratio. Both solutions were mixed to a 1:1 ratio, incubated at RT for 20 minutes and added to cells suspension before seeding. Growth medium containing transfection reagent was washed the following day and replaced with fresh growth

medium. All Star Negative Control siRNA (1027281, Qiagen) was used as control (siCTRL).

6 References

1 J.D. Watson and F.H. Crick, **(1953)** *Molecular structure of nucleic acids; a structure for deoxyribose nucleic acid.* Nature, 171(4356): p. 737-8.

2 J. Monod, *Chance and Necessity.* **(1971)**, New York: Vintage Books.

3 E. Bianconi, A. Piovesan, F. Facchin, A. Beraudi, R. Casadei, F. Frabetti, L. Vitale, M.C. Pelleri, S. Tassani, F. Piva, S. Perez-Amodio, P. Strippoli and S. Canaider, **(2013)** *An estimation of the number of cells in the human body.* Ann Hum Biol, 40(6): p. 463-71.

4 T. Lindahl and D.E. Barnes, **(2000)** *Repair of endogenous DNA damage.* Cold Spring Harb Symp Quant Biol, 65: p. 127-33.

5 E.C. Friedberg, **(2008)** *A brief history of the DNA repair field.* Cell Res, 18(1): p. 3-7.

6 D.J. Betteridge, **(2000)** *What is oxidative stress?* Metabolism, 49(2 Suppl 1): p. 3-8.

7 D.E. Barnes and T. Lindahl, **(2004)** *Repair and genetic consequences of endogenous DNA base damage in mammalian cells.* Annu Rev Genet, 38: p. 445-76.

8 A. Tubbs and A. Nussenzweig, **(2017)** *Endogenous DNA Damage as a Source of Genomic Instability in Cancer.* Cell, 168(4): p. 644-656.

9 T. Rich, R.L. Allen and A.H. Wyllie, **(2000)** *Defying death after DNA damage.* Nature, 407(6805): p. 777-83.

10 C. Hoege, B. Pfander, G.L. Moldovan, G. Pyrowolakis and S. Jentsch, **(2002)** *RAD6-dependent DNA repair is linked to modification of PCNA by ubiquitin and SUMO.* Nature, 419(6903): p. 135-41.

11 M.K. Zeman and K.A. Cimprich, **(2014)** *Causes and consequences of replication stress.* Nat Cell Biol, 16(1): p. 2-9.

12 T. Varga and P.D. Aplan, **(2005)** *Chromosomal aberrations induced by double strand DNA breaks.* DNA Repair (Amst), 4(9): p. 1038-46.

13 A.G. Tsai and M.R. Lieber, **(2010)** *Mechanisms of chromosomal rearrangement in the human genome.* BMC Genomics, 11 Suppl 1: p. S1.

14 K.K. Khanna and S.P. Jackson, **(2001)** *DNA double-strand breaks: signaling, repair and the cancer connection.* Nat Genet, 27(3): p. 247-54.

15 R. Buisson. **(2020)**; Available from: https://buissonlab.com/research/.

16 S. Nowsheen and E.S. Yang, **(2012)** *The intersection between DNA damage response and cell death pathways.* Exp Oncol, 34(3): p. 243-54.

17 K. Rodgers and M. McVey, **(2016)** *Error-Prone Repair of DNA Double-Strand Breaks.* J Cell Physiol, 231(1): p. 15-24.

18 S.A. Shabalina and N.A. Spiridonov, **(2004)** *The mammalian transcriptome and the function of non-coding DNA sequences.* Genome Biol, 5(4): p. 105.

19 D.P. Lane, **(1992)** *Cancer. p53, guardian of the genome.* Nature, 358(6381): p. 15-6.

20 S. Jancik, J. Drabek, D. Radzioch and M. Hajduch, **(2010)** *Clinical relevance of KRAS in human cancers.* J Biomed Biotechnol, 2010: p. 150960.

21 M.R. Stratton, P.J. Campbell and P.A. Futreal, **(2009)** *The cancer genome.* Nature, 458(7239): p. 719-24.

22 S.P. Jackson and J. Bartek, **(2009)** *The DNA-damage response in human biology and disease.* Nature, 461(7267): p. 1071-8.

23 K. Savitsky, A. Bar-Shira, S. Gilad, G. Rotman, Y. Ziv, L. Vanagaite, D.A. Tagle, S. Smith, T. Uziel, S. Sfez, M. Ashkenazi, I. Pecker, M. Frydman, R. Harnik, S.R. Patanjali, A. Simmons, G.A. Clines, A. Sartiel, R.A. Gatti, L. Chessa, O. Sanal, M.F. Lavin, N.G. Jaspers, A.M. Taylor, C.F. Arlett, T. Miki, S.M. Weissman, M. Lovett, F.S. Collins and Y. Shiloh, **(1995)** *A single ataxia telangiectasia gene with a product similar to PI-3 kinase.* Science, 268(5218): p. 1749-53.

24 S.P. Gotoff, E. Amirmokri and E.J. Liebner, **(1967)** *Ataxia telangiectasia. Neoplasia, untoward response to x-irradiation, and tuberous sclerosis.* Am J Dis Child, 114(6): p. 617-25.

25 A.M. Taylor, D.G. Harnden, C.F. Arlett, S.A. Harcourt, A.R. Lehmann, S. Stevens and B.A. Bridges, **(1975)** *Ataxia telangiectasia: a human mutation with abnormal radiation sensitivity.* Nature, 258(5534): p. 427-9.

26 A.M. Taylor, J.A. Metcalfe, J.M. Oxford and D.G. Harnden, **(1976)** *Is chromatid-type damage in ataxia telangiectasia after irradiation at G0 a consequence of defective repair?* Nature, 260(5550): p. 441-3.

27 S. Matsuoka, B.A. Ballif, A. Smogorzewska, E.R. McDonald, 3rd, K.E. Hurov, J. Luo, C.E. Bakalarski, Z. Zhao, N. Solimini, Y. Lerenthal, Y. Shiloh, S.P. Gygi and S.J. Elledge, **(2007)** *ATM and ATR substrate analysis reveals extensive protein networks responsive to DNA damage.* Science, 316(5828): p. 1160-6.

28 Y. Shiloh and Y. Ziv, **(2013)** *The ATM protein kinase: regulating the cellular response to genotoxic stress, and more.* Nat Rev Mol Cell Biol, 14(4): p. 197-210.

29 J.D. Siliciano, C.E. Canman, Y. Taya, K. Sakaguchi, E. Appella and M.B. Kastan, **(1997)** *DNA damage induces phosphorylation of the amino terminus of p53.* Genes Dev, 11(24): p. 3471-81.

30 S. Banin, L. Moyal, S. Shieh, Y. Taya, C.W. Anderson, L. Chessa, N.I. Smorodinsky, C. Prives, Y. Reiss, Y. Shiloh and Y. Ziv, **(1998)** *Enhanced phosphorylation of p53 by ATM in response to DNA damage.* Science, 281(5383): p. 1674-7.

31 C. Kandoth, M.D. McLellan, F. Vandin, K. Ye, B. Niu, C. Lu, M. Xie, Q. Zhang, J.F. McMichael, M.A. Wyczalkowski, M.D.M. Leiserson, C.A. Miller, J.S. Welch, M.J. Walter, M.C. Wendl, T.J. Ley, R.K. Wilson, B.J. Raphael and L. Ding, **(2013)** *Mutational landscape and significance across 12 major cancer types.* Nature, 502(7471): p. 333-339.

32 J. Falck, J. Coates and S.P. Jackson, **(2005)** *Conserved modes of recruitment of ATM, ATR and DNA-PKcs to sites of DNA damage.* Nature, 434(7033): p. 605-11.

33 R. Scully and A. Xie, **(2013)** *Double strand break repair functions of histone H2AX.* Mutat Res, 750(1-2): p. 5-14.

34 P. Caron, J. Choudjaye, T. Clouaire, B. Bugler, V. Daburon, M. Aguirrebengoa, T. Mangeat, J.S. Iacovoni, A. Alvarez-Quilon, F. Cortes-Ledesma and G. Legube, **(2015)** *Non-redundant Functions of ATM and DNA-PKcs in Response to DNA Double-Strand Breaks.* Cell Rep, 13(8): p. 1598-609.

35 E.P. Rogakou, D.R. Pilch, A.H. Orr, V.S. Ivanova and W.M. Bonner, **(1998)** *DNA double-stranded breaks induce histone H2AX phosphorylation on serine 139.* J Biol Chem, 273(10): p. 5858-68.

36 M. Stucki, J.A. Clapperton, D. Mohammad, M.B. Yaffe, S.J. Smerdon and S.P. Jackson, **(2005)** *MDC1 directly binds phosphorylated histone H2AX to regulate cellular responses to DNA double-strand breaks.* Cell, 123(7): p. 1213-26.

37 S. Jungmichel, J.A. Clapperton, J. Lloyd, F.J. Hari, C. Spycher, L. Pavic, J. Li, L.F. Haire, M. Bonalli, D.H. Larsen, C. Lukas, J. Lukas, D. MacMillan, M.L. Nielsen, M. Stucki and S.J. Smerdon, **(2012)** *The molecular basis of ATM-dependent dimerization of the Mdc1 DNA damage checkpoint mediator.* Nucleic Acids Res, 40(9): p. 3913-28.

38 S. Bekker-Jensen, C. Lukas, F. Melander, J. Bartek and J. Lukas, **(2005)** *Dynamic assembly and sustained retention of 53BP1 at the sites of DNA damage are controlled by Mdc1/NFBD1.* J Cell Biol, 170(2): p. 201-11.

39 L. Krejci, V. Altmannova, M. Spirek and X. Zhao, **(2012)** *Homologous recombination and its regulation.* Nucleic Acids Res, 40(13): p. 5795-818.

40 R. Prakash, Y. Zhang, W. Feng and M. Jasin, **(2015)** *Homologous recombination and human health: the roles of BRCA1, BRCA2, and associated proteins.* Cold Spring Harb Perspect Biol, 7(4): p. a016600.

41 L. Deriano and D.B. Roth, **(2013)** *Modernizing the nonhomologous end-joining repertoire: alternative and classical NHEJ share the stage.* Annu Rev Genet, 47: p. 433-55.

42 M.R. Lieber, **(2010)** *The mechanism of double-strand DNA break repair by the nonhomologous DNA end-joining pathway.* Annu Rev Biochem, 79: p. 181-211.

43 R.D. Johnson and M. Jasin, **(2000)** *Sister chromatid gene conversion is a prominent double-strand break repair pathway in mammalian cells.* EMBO J, 19(13): p. 3398-407.

44 A.A. Sartori, C. Lukas, J. Coates, M. Mistrik, S. Fu, J. Bartek, R. Baer, J. Lukas and S.P. Jackson, **(2007)** *Human CtIP promotes DNA end resection.* Nature, 450(7169): p. 509-14.

45 H. Wang, L.Z. Shi, C.C. Wong, X. Han, P.Y. Hwang, L.N. Truong, Q. Zhu, Z. Shao, D.J. Chen, M.W. Berns, J.R. Yates, 3rd, L. Chen and X. Wu, **(2013)** *The interaction of CtIP and Nbs1 connects CDK and ATM to regulate HR-mediated double-strand break repair.* PLoS Genet, 9(2): p. e1003277.

46 A.V. Nimonkar, J. Genschel, E. Kinoshita, P. Polaczek, J.L. Campbell, C. Wyman, P. Modrich and S.C. Kowalczykowski, **(2011)** *BLM-DNA2-RPA-MRN and EXO1-BLM-RPA-MRN constitute two DNA end resection machineries for human DNA break repair.* Genes Dev, 25(4): p. 350-62.

47 R. Anand, L. Ranjha, E. Cannavo and P. Cejka, **(2016)** *Phosphorylated CtIP Functions as a Co-factor of the MRE11-RAD50-NBS1 Endonuclease in DNA End Resection.* Mol Cell, 64(5): p. 940-950.

48 S. Gravel, J.R. Chapman, C. Magill and S.P. Jackson, **(2008)** *DNA helicases Sgs1 and BLM promote DNA double-strand break resection.* Genes Dev, 22(20): p. 2767-72.

49 E.P. Mimitou and L.S. Symington, **(2008)** *Sae2, Exo1 and Sgs1 collaborate in DNA double-strand break processing.* Nature, 455(7214): p. 770-4.

50 Z. Zhu, W.H. Chung, E.Y. Shim, S.E. Lee and G. Ira, **(2008)** *Sgs1 helicase and two nucleases Dna2 and Exo1 resect DNA double-strand break ends.* Cell, 134(6): p. 981-94.

51 C. Pinto, K. Kasaciunaite, R. Seidel and P. Cejka, **(2016)** *Human DNA2 possesses a cryptic DNA unwinding activity that functionally integrates with BLM or WRN helicases.* Elife, 5: p.

52 A. Sturzenegger, K. Burdova, R. Kanagaraj, M. Levikova, C. Pinto, P. Cejka and P. Janscak, **(2014)** *DNA2 cooperates with the WRN and BLM RecQ helicases to mediate long-range DNA end resection in human cells.* J Biol Chem, 289(39): p. 27314-26.

53 A. Shibata, S. Conrad, J. Birraux, V. Geuting, O. Barton, A. Ismail, A. Kakarougkas, K. Meek, G. Taucher-Scholz, M. Lobrich and P.A. Jeggo, **(2011)** *Factors determining DNA double-strand break repair pathway choice in G2 phase.* EMBO J, 30(6): p. 1079-92.

54 Q. Zhong, C.F. Chen, S. Li, Y. Chen, C.C. Wang, J. Xiao, P.L. Chen, Z.D. Sharp and W.H. Lee, **(1999)** *Association of BRCA1 with the hRad50-hMre11-p95 complex and the DNA damage response.* Science, 285(5428): p. 747-50.

55 A.K. Wong, P.A. Ormonde, R. Pero, Y. Chen, L. Lian, G. Salada, S. Berry, Q. Lawrence, P. Dayananth, P. Ha, S.V. Tavtigian, D.H. Teng and P.L. Bartel, **(1998)** *Characterization of a carboxy-terminal BRCA1 interacting protein.* Oncogene, 17(18): p. 2279-85.

56 X. Yu and J. Chen, **(2004)** *DNA damage-induced cell cycle checkpoint control requires CtIP, a phosphorylation-dependent binding partner of BRCA1 C-terminal domains.* Mol Cell Biol, 24(21): p. 9478-86.

57 X. Yu, S. Fu, M. Lai, R. Baer and J. Chen, **(2006)** *BRCA1 ubiquitinates its phosphorylation-dependent binding partner CtIP.* Genes Dev, 20(13): p. 1721-6.

58 L. Chen, C.J. Nievera, A.Y. Lee and X. Wu, **(2008)** *Cell cycle-dependent complex formation of BRCA1.CtIP.MRN is important for DNA double-strand break repair.* J Biol Chem, 283(12): p. 7713-20.

59 A. Cruz-Garcia, A. Lopez-Saavedra and P. Huertas, **(2014)** *BRCA1 accelerates CtIP-mediated DNA-end resection.* Cell Rep, 9(2): p. 451-9.

60 C.R. Reczek, M. Szabolcs, J.M. Stark, T. Ludwig and R. Baer, **(2013)** *The interaction between CtIP and BRCA1 is not essential for resection-mediated DNA repair or tumor suppression.* J Cell Biol, 201(5): p. 693-707.

61 F. Polato, E. Callen, N. Wong, R. Faryabi, S. Bunting, H.T. Chen, M. Kozak, M.J. Kruhlak, C.R. Reczek, W.H. Lee, T. Ludwig, R. Baer, L. Feigenbaum,

S. Jackson and A. Nussenzweig, **(2014)** *CtIP-mediated resection is essential for viability and can operate independently of BRCA1.* J Exp Med, 211(6): p. 1027-36.

62 W. Zhao, J.B. Steinfeld, F. Liang, X. Chen, D.G. Maranon, C. Jian Ma, Y. Kwon, T. Rao, W. Wang, C. Sheng, X. Song, Y. Deng, J. Jimenez-Sainz, L. Lu, R.B. Jensen, Y. Xiong, G.M. Kupfer, C. Wiese, E.C. Greene and P. Sung, **(2017)** *BRCA1-BARD1 promotes RAD51-mediated homologous DNA pairing.* Nature, 550(7676): p. 360-365.

63 M. Tarsounas and P. Sung, **(2020)** *The antitumorigenic roles of BRCA1-BARD1 in DNA repair and replication.* Nat Rev Mol Cell Biol, 21(5): p. 284-299.

64 R.M. Densham, A.J. Garvin, H.R. Stone, J. Strachan, R.A. Baldock, M. Daza-Martin, A. Fletcher, S. Blair-Reid, J. Beesley, B. Johal, L.H. Pearl, R. Neely, N.H. Keep, F.Z. Watts and J.R. Morris, **(2016)** *Human BRCA1-BARD1 ubiquitin ligase activity counteracts chromatin barriers to DNA resection.* Nat Struct Mol Biol, 23(7): p. 647-55.

65 E. Bochkareva, S. Korolev, S.P. Lees-Miller and A. Bochkarev, **(2002)** *Structure of the RPA trimerization core and its role in the multistep DNA-binding mechanism of RPA.* EMBO J, 21(7): p. 1855-63.

66 B. Xia, Q. Sheng, K. Nakanishi, A. Ohashi, J. Wu, N. Christ, X. Liu, M. Jasin, F.J. Couch and D.M. Livingston, **(2006)** *Control of BRCA2 cellular and clinical functions by a nuclear partner, PALB2.* Mol Cell, 22(6): p. 719-29.

67 S.M. Sy, M.S. Huen and J. Chen, **(2009)** *PALB2 is an integral component of the BRCA complex required for homologous recombination repair.* Proc Natl Acad Sci U S A, 106(17): p. 7155-60.

68 M.E. Moynahan, A.J. Pierce and M. Jasin, **(2001)** *BRCA2 is required for homology-directed repair of chromosomal breaks.* Mol Cell, 7(2): p. 263-72.

69 R.B. Jensen, A. Carreira and S.C. Kowalczykowski, **(2010)** *Purified human BRCA2 stimulates RAD51-mediated recombination.* Nature, 467(7316): p. 678-83.

70 J. Liu, T. Doty, B. Gibson and W.D. Heyer, **(2010)** *Human BRCA2 protein promotes RAD51 filament formation on RPA-covered single-stranded DNA.* Nat Struct Mol Biol, 17(10): p. 1260-2.

71 T. Allers and M. Lichten, **(2001)** *Differential timing and control of noncrossover and crossover recombination during meiosis.* Cell, 106(1): p. 47-57.

72 Y. Liu, J.Y. Masson, R. Shah, P. O'Regan and S.C. West, **(2004)** *RAD51C is required for Holliday junction processing in mammalian cells.* Science, 303(5655): p. 243-6.

73 M.N. Boddy, P.H. Gaillard, W.H. McDonald, P. Shanahan, J.R. Yates, 3rd and P. Russell, **(2001)** *Mus81-Eme1 are essential components of a Holliday junction resolvase.* Cell, 107(4): p. 537-48.

74 H.D. Wyatt, S. Sarbajna, J. Matos and S.C. West, **(2013)** *Coordinated actions of SLX1-SLX4 and MUS81-EME1 for Holliday junction resolution in human cells.* Mol Cell, 52(2): p. 234-47.

75 S. Fekairi, S. Scaglione, C. Chahwan, E.R. Taylor, A. Tissier, S. Coulon, M.Q. Dong, C. Ruse, J.R. Yates, 3rd, P. Russell, R.P. Fuchs, C.H. McGowan and P.H. Gaillard, **(2009)** *Human SLX4 is a Holliday junction resolvase subunit that binds multiple DNA repair/recombination endonucleases.* Cell, 138(1): p. 78-89.

76 H.D. Wyatt, R.C. Laister, S.R. Martin, C.H. Arrowsmith and S.C. West, **(2017)** *The SMX DNA Repair Tri-nuclease.* Mol Cell, 65(5): p. 848-860 e11.

77 S.C. Ip, U. Rass, M.G. Blanco, H.R. Flynn, J.M. Skehel and S.C. West, **(2008)** *Identification of Holliday junction resolvases from humans and yeast.* Nature, 456(7220): p. 357-61.

78 J. San Filippo, P. Sung and H. Klein, **(2008)** *Mechanism of eukaryotic homologous recombination.* Annu Rev Biochem, 77: p. 229-57.

79 M. Bzymek, N.H. Thayer, S.D. Oh, N. Kleckner and N. Hunter, **(2010)** *Double Holliday junctions are intermediates of DNA break repair.* Nature, 464(7290): p. 937-41.

80 W. Zhao, C. Wiese, Y. Kwon, R. Hromas and P. Sung, **(2019)** *The BRCA Tumor Suppressor Network in Chromosome Damage Repair by Homologous Recombination.* Annu Rev Biochem, 88: p. 221-245.

81 K. Karanam, R. Kafri, A. Loewer and G. Lahav, **(2012)** *Quantitative live cell imaging reveals a gradual shift between DNA repair mechanisms and a maximal use of HR in mid S phase.* Mol Cell, 47(2): p. 320-9.

82 R. Ceccaldi, B. Rondinelli and A.D. D'Andrea, **(2016)** *Repair Pathway Choices and Consequences at the Double-Strand Break.* Trends Cell Biol, 26(1): p. 52-64.

83 C.H. Bassing, W. Swat and F.W. Alt, **(2002)** *The mechanism and regulation of chromosomal V(D)J recombination.* Cell, 109 Suppl: p. S45-55.

84 F.W. Alt, Y. Zhang, F.L. Meng, C. Guo and B. Schwer, **(2013)** *Mechanisms of programmed DNA lesions and genomic instability in the immune system.* Cell, 152(3): p. 417-29.

85 J. Stavnezer, J.E. Guikema and C.E. Schrader, **(2008)** *Mechanism and regulation of class switch recombination.* Annu Rev Immunol, 26: p. 261-92.

86 L. Woodbine, A.R. Gennery and P.A. Jeggo, **(2014)** *The clinical impact of deficiency in DNA non-homologous end-joining.* DNA Repair (Amst), 16: p. 84-96.

87 G. Balmus, A.C. Barros, P.W. Wijnhoven, C. Lescale, H.L. Hasse, K. Boroviak, C. le Sage, B. Doe, A.O. Speak, A. Galli, M. Jacobsen, L. Deriano, D.J. Adams, A.N. Blackford and S.P. Jackson, **(2016)** *Synthetic lethality between PAXX and XLF in mammalian development.* Genes Dev, 30(19): p. 2152-2157.

88 X. Liu, Z. Shao, W. Jiang, B.J. Lee and S. Zha, **(2017)** *PAXX promotes KU accumulation at DNA breaks and is essential for end-joining in XLF-deficient mice.* Nat Commun, 8: p. 13816.

89 D. Moshous, I. Callebaut, R. de Chasseval, B. Corneo, M. Cavazzana-Calvo, F. Le Deist, I. Tezcan, O. Sanal, Y. Bertrand, N. Philippe, A. Fischer and J.P. de Villartay, **(2001)** *Artemis, a novel DNA double-strand break*

repair/V(D)J recombination protein, is mutated in human severe combined immune deficiency. Cell, 105(2): p. 177-86.

90 B.K. Singleton, M.I. Torres-Arzayus, S.T. Rottinghaus, G.E. Taccioli and P.A. Jeggo, **(1999)** *The C terminus of Ku80 activates the DNA-dependent protein kinase catalytic subunit.* Mol Cell Biol, 19(5): p. 3267-77.

91 T. Ochi, A.N. Blackford, J. Coates, S. Jhujh, S. Mehmood, N. Tamura, J. Travers, Q. Wu, V.M. Draviam, C.V. Robinson, T.L. Blundell and S.P. Jackson, **(2015)** *DNA repair. PAXX, a paralog of XRCC4 and XLF, interacts with Ku to promote DNA double-strand break repair.* Science, 347(6218): p. 185-188.

92 D.W. Chan, B.P. Chen, S. Prithivirajsingh, A. Kurimasa, M.D. Story, J. Qin and D.J. Chen, **(2002)** *Autophosphorylation of the DNA-dependent protein kinase catalytic subunit is required for rejoining of DNA double-strand breaks.* Genes Dev, 16(18): p. 2333-8.

93 N. Uematsu, E. Weterings, K. Yano, K. Morotomi-Yano, B. Jakob, G. Taucher-Scholz, P.O. Mari, D.C. van Gent, B.P. Chen and D.J. Chen, **(2007)** *Autophosphorylation of DNA-PKCS regulates its dynamics at DNA double-strand breaks.* J Cell Biol, 177(2): p. 219-29.

94 S.H. Teo and S.P. Jackson, **(1997)** *Identification of Saccharomyces cerevisiae DNA ligase IV: involvement in DNA double-strand break repair.* EMBO J, 16(15): p. 4788-95.

95 S.E. Critchlow, R.P. Bowater and S.P. Jackson, **(1997)** *Mammalian DNA double-strand break repair protein XRCC4 interacts with DNA ligase IV.* Curr Biol, 7(8): p. 588-98.

96 U. Grawunder, M. Wilm, X. Wu, P. Kulesza, T.E. Wilson, M. Mann and M.R. Lieber, **(1997)** *Activity of DNA ligase IV stimulated by complex formation with XRCC4 protein in mammalian cells.* Nature, 388(6641): p. 492-5.

97 P. Ahnesorg, P. Smith and S.P. Jackson, **(2006)** *XLF interacts with the XRCC4-DNA ligase IV complex to promote DNA nonhomologous end-joining.* Cell, 124(2): p. 301-13.

98 Y. Ma, U. Pannicke, K. Schwarz and M.R. Lieber, **(2002)** *Hairpin opening and overhang processing by an Artemis/DNA-dependent protein kinase complex in nonhomologous end joining and V(D)J recombination.* Cell, 108(6): p. 781-94.

99 E. Riballo, M. Kuhne, N. Rief, A. Doherty, G.C. Smith, M.J. Recio, C. Reis, K. Dahm, A. Fricke, A. Krempler, A.R. Parker, S.P. Jackson, A. Gennery, P.A. Jeggo and M. Lobrich, **(2004)** *A pathway of double-strand break rejoining dependent upon ATM, Artemis, and proteins locating to gamma-H2AX foci.* Mol Cell, 16(5): p. 715-24.

100 S. Malu, P. De Ioannes, M. Kozlov, M. Greene, D. Francis, M. Hanna, J. Pena, C.R. Escalante, A. Kurosawa, H. Erdjument-Bromage, P. Tempst, N. Adachi, P. Vezzoni, A. Villa, A.K. Aggarwal and P. Cortes, **(2012)** *Artemis C-terminal region facilitates V(D)J recombination through its interactions with DNA Ligase IV and DNA-PKcs.* J Exp Med, 209(5): p. 955-63.

101 W. Jiang, J.L. Crowe, X. Liu, S. Nakajima, Y. Wang, C. Li, B.J. Lee, R.L. Dubois, C. Liu, X. Yu, L. Lan and S. Zha, **(2015)** *Differential phosphorylation of DNA-PKcs regulates the interplay between end-processing and end-ligation during nonhomologous end-joining.* Mol Cell, 58(1): p. 172-85.

102 E. Heidenreich, R. Novotny, B. Kneidinger, V. Holzmann and U. Wintersberger, **(2003)** *Non-homologous end joining as an important mutagenic process in cell cycle-arrested cells.* EMBO J, 22(9): p. 2274-83.

103 M. Betermier, P. Bertrand and B.S. Lopez, **(2014)** *Is non-homologous end-joining really an inherently error-prone process?* PLoS Genet, 10(1): p. e1004086.

104 B.M. Stinson, A.T. Moreno, J.C. Walter and J.J. Loparo, **(2020)** *A Mechanism to Minimize Errors during Non-homologous End Joining.* Mol Cell, 77(5): p. 1080-1091 e8.

105 J.R. Becker, R. Cuella-Martin, M. Barazas, R. Liu, C. Oliveira, A.W. Oliver, K. Bilham, A.B. Holt, A.N. Blackford, J. Heierhorst, J. Jonkers, S. Rottenberg and J.R. Chapman, **(2018)** *The ASCIZ-DYNLL1 axis promotes 53BP1-dependent non-homologous end joining and PARP inhibitor sensitivity.* Nat Commun, 9(1): p. 5406.

106 S. Kuhfittig-Kulle, E. Feldmann, A. Odersky, A. Kuliczkowska, W. Goedecke, A. Eggert and P. Pfeiffer, **(2007)** *The mutagenic potential of non-homologous end joining in the absence of the NHEJ core factors Ku70/80, DNA-PKcs and XRCC4-LigIV.* Mutagenesis, 22(3): p. 217-33.

107 G. Balmus, D. Pilger, J. Coates, M. Demir, M. Sczaniecka-Clift, A.C. Barros, M. Woods, B. Fu, F. Yang, E. Chen, M. Ostermaier, T. Stankovic, H. Ponstingl, M. Herzog, K. Yusa, F.M. Martinez, S.T. Durant, Y. Galanty, P. Beli, D.J. Adams, A. Bradley, E. Metzakopian, J.V. Forment and S.P. Jackson, **(2019)** *ATM orchestrates the DNA-damage response to counter toxic non-homologous end-joining at broken replication forks.* Nat Commun, 10(1): p. 87.

108 J.R. Chapman, M.R. Taylor and S.J. Boulton, **(2012)** *Playing the end game: DNA double-strand break repair pathway choice.* Mol Cell, 47(4): p. 497-510.

109 A. Guenole and G. Legube, **(2017)** *A meeting at risk: Unrepaired DSBs go for broke.* Nucleus, 8(6): p. 589-599.

110 N. Hustedt and D. Durocher, **(2016)** *The control of DNA repair by the cell cycle.* Nat Cell Biol, 19(1): p. 1-9.

111 S.F. Bunting, E. Callen, N. Wong, H.T. Chen, F. Polato, A. Gunn, A. Bothmer, N. Feldhahn, O. Fernandez-Capetillo, L. Cao, X. Xu, C.X. Deng, T. Finkel, M. Nussenzweig, J.M. Stark and A. Nussenzweig, **(2010)** *53BP1 inhibits homologous recombination in Brca1-deficient cells by blocking resection of DNA breaks.* Cell, 141(2): p. 243-54.

112 C. Escribano-Diaz, A. Orthwein, A. Fradet-Turcotte, M. Xing, J.T. Young, J. Tkac, M.A. Cook, A.P. Rosebrock, M. Munro, M.D. Canny, D. Xu and D. Durocher, **(2013)** *A cell cycle-dependent regulatory circuit composed of 53BP1-RIF1 and BRCA1-CtIP controls DNA repair pathway choice.* Mol Cell, 49(5): p. 872-83.

113 J.R. Chapman, P. Barral, J.B. Vannier, V. Borel, M. Steger, A. Tomas-Loba, A.A. Sartori, I.R. Adams, F.D. Batista and S.J. Boulton, **(2013)** *RIF1 is essential for 53BP1-dependent nonhomologous end joining and suppression of DNA double-strand break resection.* Mol Cell, 49(5): p. 858-71.

114 P. Bouwman, A. Aly, J.M. Escandell, M. Pieterse, J. Bartkova, H. van der Gulden, S. Hiddingh, M. Thanasoula, A. Kulkarni, Q. Yang, B.G. Haffty, J. Tommiska, C. Blomqvist, R. Drapkin, D.J. Adams, H. Nevanlinna, J. Bartek, M. Tarsounas, S. Ganesan and J. Jonkers, **(2010)** *53BP1 loss rescues BRCA1 deficiency and is associated with triple-negative and BRCA-mutated breast cancers.* Nat Struct Mol Biol, 17(6): p. 688-95.

115 J.R. Chapman, A.J. Sossick, S.J. Boulton and S.P. Jackson, **(2012)** *BRCA1-associated exclusion of 53BP1 from DNA damage sites underlies temporal control of DNA repair.* J Cell Sci, 125(Pt 15): p. 3529-34.

116 M.H. Yun and K. Hiom, **(2009)** *CtIP-BRCA1 modulates the choice of DNA double-strand-break repair pathway throughout the cell cycle.* Nature, 459(7245): p. 460-3.

117 R. Bhargava, D.O. Onyango and J.M. Stark, **(2016)** *Regulation of Single-Strand Annealing and its Role in Genome Maintenance.* Trends Genet, 32(9): p. 566-575.

118 H.H.Y. Chang, N.R. Pannunzio, N. Adachi and M.R. Lieber, **(2017)** *Non-homologous DNA end joining and alternative pathways to double-strand break repair.* Nat Rev Mol Cell Biol, 18(8): p. 495-506.

119 N. Bennardo, A. Cheng, N. Huang and J.M. Stark, **(2008)** *Alternative-NHEJ is a mechanistically distinct pathway of mammalian chromosome break repair.* PLoS Genet, 4(6): p. e1000110.

120 A. Sallmyr and A.E. Tomkinson, **(2018)** *Repair of DNA double-strand breaks by mammalian alternative end-joining pathways.* J Biol Chem, 293(27): p. 10536-10546.

121 Y. Zhang and M. Jasin, **(2011)** *An essential role for CtIP in chromosomal translocation formation through an alternative end-joining pathway.* Nat Struct Mol Biol, 18(1): p. 80-4.

122 E. Rothenberg, J.M. Grimme, M. Spies and T. Ha, **(2008)** *Human Rad52-mediated homology search and annealing occurs by continuous interactions between overlapping nucleoprotein complexes.* Proc Natl Acad Sci U S A, 105(51): p. 20274-9.

123 T.A. Motycka, T. Bessho, S.M. Post, P. Sung and A.E. Tomkinson, **(2004)** *Physical and functional interaction between the XPF/ERCC1 endonuclease and hRad52.* J Biol Chem, 279(14): p. 13634-9.

124 A.A. Kelso, F.W. Lopezcolorado, R. Bhargava and J.M. Stark, **(2019)** *Distinct roles of RAD52 and POLQ in chromosomal break repair and replication stress response.* PLoS Genet, 15(8): p. e1008319.

125 R. Ceccaldi, J.C. Liu, R. Amunugama, I. Hajdu, B. Primack, M.I. Petalcorin, K.W. O'Connor, P.A. Konstantinopoulos, S.J. Elledge, S.J. Boulton, T. Yusufzai and A.D. D'Andrea, **(2015)** *Homologous-recombination-deficient tumours are dependent on Poltheta-mediated repair.* Nature, 518(7538): p. 258-62.

126 P.A. Mateos-Gomez, F. Gong, N. Nair, K.M. Miller, E. Lazzerini-Denchi and A. Sfeir, **(2015)** *Mammalian polymerase theta promotes alternative NHEJ and suppresses recombination.* Nature, 518(7538): p. 254-7.

127 H. Gaillard, T. Garcia-Muse and A. Aguilera, **(2015)** *Replication stress and cancer.* Nat Rev Cancer, 15(5): p. 276-89.

128 E. Petermann, M.L. Orta, N. Issaeva, N. Schultz and T. Helleday, **(2010)** *Hydroxyurea-stalled replication forks become progressively inactivated and require two different RAD51-mediated pathways for restart and repair.* Mol Cell, 37(4): p. 492-502.

129 Y. Hashimoto, F. Puddu and V. Costanzo, **(2011)** *RAD51- and MRE11-dependent reassembly of uncoupled CMG helicase complex at collapsed replication forks.* Nat Struct Mol Biol, 19(1): p. 17-24.

130 T. Wilhelm, I. Magdalou, A. Barascu, H. Techer, M. Debatisse and B.S. Lopez, **(2014)** *Spontaneous slow replication fork progression elicits mitosis alterations in homologous recombination-deficient mammalian cells.* Proc Natl Acad Sci U S A, 111(2): p. 763-8.

131 H. Liao, F. Ji, T. Helleday and S. Ying, **(2018)** *Mechanisms for stalled replication fork stabilization: new targets for synthetic lethality strategies in cancer treatments.* EMBO Rep, 19(9): p.

132 A.N. Blackford and S.P. Jackson, **(2017)** *ATM, ATR, and DNA-PK: The Trinity at the Heart of the DNA Damage Response.* Mol Cell, 66(6): p. 801-817.

133 L. Zou and S.J. Elledge, **(2003)** *Sensing DNA damage through ATRIP recognition of RPA-ssDNA complexes.* Science, 300(5625): p. 1542-8.

134 A. Kumagai, J. Lee, H.Y. Yoo and W.G. Dunphy, **(2006)** *TopBP1 activates the ATR-ATRIP complex.* Cell, 124(5): p. 943-55.

135 D.A. Mordes, G.G. Glick, R. Zhao and D. Cortez, **(2008)** *TopBP1 activates ATR through ATRIP and a PIKK regulatory domain.* Genes Dev, 22(11): p. 1478-89.

136 Q. Liu, S. Guntuku, X.S. Cui, S. Matsuoka, D. Cortez, K. Tamai, G. Luo, S. Carattini-Rivera, F. DeMayo, A. Bradley, L.A. Donehower and S.J. Elledge, **(2000)** *Chk1 is an essential kinase that is regulated by Atr and required for the G(2)/M DNA damage checkpoint.* Genes Dev, 14(12): p. 1448-59.

137 H. Zhao and H. Piwnica-Worms, **(2001)** *ATR-mediated checkpoint pathways regulate phosphorylation and activation of human Chk1.* Mol Cell Biol, 21(13): p. 4129-39.

138 J. Bartek, C. Lukas and J. Lukas, **(2004)** *Checking on DNA damage in S phase.* Nat Rev Mol Cell Biol, 5(10): p. 792-804.

139 T. Shen and S. Huang, **(2012)** *The role of Cdc25A in the regulation of cell proliferation and apoptosis.* Anticancer Agents Med Chem, 12(6): p. 631-9.

140 J. Falck, N. Mailand, R.G. Syljuasen, J. Bartek and J. Lukas, **(2001)** *The ATM-Chk2-Cdc25A checkpoint pathway guards against radioresistant DNA synthesis.* Nature, 410(6830): p. 842-7.

141 F.B. Couch, C.E. Bansbach, R. Driscoll, J.W. Luzwick, G.G. Glick, R. Betous, C.M. Carroll, S.Y. Jung, J. Qin, K.A. Cimprich and D. Cortez, **(2013)** *ATR phosphorylates SMARCAL1 to prevent replication fork collapse.* Genes Dev, 27(14): p. 1610-23.

142 H. Techer, S. Koundrioukoff, A. Nicolas and M. Debatisse, **(2017)** *The impact of replication stress on replication dynamics and DNA damage in vertebrate cells.* Nat Rev Genet, 18(9): p. 535-550.

143 R. Scully, J. Chen, R.L. Ochs, K. Keegan, M. Hoekstra, J. Feunteun and D.M. Livingston, **(1997)** *Dynamic changes of BRCA1 subnuclear location and phosphorylation state are initiated by DNA damage.* Cell, 90(3): p. 425-35.

144 G. Maga and U. Hubscher, **(2003)** *Proliferating cell nuclear antigen (PCNA): a dancer with many partners.* J Cell Sci, 116(Pt 15): p. 3051-60.

145 G.L. Moldovan, B. Pfander and S. Jentsch, **(2007)** *PCNA, the maestro of the replication fork.* Cell, 129(4): p. 665-79.

146 K. Schlacher, N. Christ, N. Siaud, A. Egashira, H. Wu and M. Jasin, **(2011)** *Double-strand break repair-independent role for BRCA2 in blocking stalled replication fork degradation by MRE11.* Cell, 145(4): p. 529-42.

147 K. Schlacher, H. Wu and M. Jasin, **(2012)** *A distinct replication fork protection pathway connects Fanconi anemia tumor suppressors to RAD51-BRCA1/2.* Cancer Cell, 22(1): p. 106-16.

148 S. Ying, F.C. Hamdy and T. Helleday, **(2012)** *Mre11-dependent degradation of stalled DNA replication forks is prevented by BRCA2 and PARP1.* Cancer Res, 72(11): p. 2814-21.

149 W. Feng and M. Jasin, **(2017)** *Homologous Recombination and Replication Fork Protection: BRCA2 and More!* Cold Spring Harb Symp Quant Biol, 82: p. 329-338.

150 K.J. Neelsen and M. Lopes, **(2015)** *Replication fork reversal in eukaryotes: from dead end to dynamic response.* Nat Rev Mol Cell Biol, 16(4): p. 207-20.

151 A.M. Kolinjivadi, V. Sannino, A. De Antoni, K. Zadorozhny, M. Kilkenny, H. Techer, G. Baldi, R. Shen, A. Ciccia, L. Pellegrini, L. Krejci and V. Costanzo, **(2017)** *Smarcal1-Mediated Fork Reversal Triggers Mre11-Dependent Degradation of Nascent DNA in the Absence of Brca2 and Stable Rad51 Nucleofilaments.* Mol Cell, 67(5): p. 867-881 e7.

152 S. Mijic, R. Zellweger, N. Chappidi, M. Berti, K. Jacobs, K. Mutreja, S. Ursich, A. Ray Chaudhuri, A. Nussenzweig, P. Janscak and M. Lopes, **(2017)** *Replication fork reversal triggers fork degradation in BRCA2-defective cells.* Nat Commun, 8(1): p. 859.

153 A. Taglialatela, S. Alvarez, G. Leuzzi, V. Sannino, L. Ranjha, J.W. Huang, C. Madubata, R. Anand, B. Levy, R. Rabadan, P. Cejka, V. Costanzo and A. Ciccia, **(2017)** *Restoration of Replication Fork Stability in BRCA1- and BRCA2-Deficient Cells by Inactivation of SNF2-Family Fork Remodelers.* Mol Cell, 68(2): p. 414-430 e8.

154 S. Przetocka, A. Porro, H.A. Bolck, C. Walker, A. Lezaja, A. Trenner, C. von Aesch, S.F. Himmels, A.D. D'Andrea, R. Ceccaldi, M. Altmeyer and A.A. Sartori, **(2018)** *CtIP-Mediated Fork Protection Synergizes with BRCA1 to Suppress Genomic Instability upon DNA Replication Stress.* Mol Cell, 72(3): p. 568-582 e6.

155 J. Zimmer, E.M.C. Tacconi, C. Folio, S. Badie, M. Porru, K. Klare, M. Tumiati, E. Markkanen, S. Halder, A. Ryan, S.P. Jackson, K. Ramadan, S.G. Kuznetsov, A. Biroccio, J.E. Sale and M. Tarsounas, **(2016)** *Targeting BRCA1 and BRCA2 Deficiencies with G-Quadruplex-Interacting Compounds.* Mol Cell, 61(3): p. 449-460.

156 J.M. Hall, M.K. Lee, B. Newman, J.E. Morrow, L.A. Anderson, B. Huey and M.C. King, **(1990)** *Linkage of early-onset familial breast cancer to chromosome 17q21.* Science, 250(4988): p. 1684-9.

157 S.A. Narod, J. Feunteun, H.T. Lynch, P. Watson, T. Conway, J. Lynch and G.M. Lenoir, **(1991)** *Familial breast-ovarian cancer locus on chromosome 17q12-q23.* Lancet, 338(8759): p. 82-3.

158 E. Steichen-Gersdorf, H.H. Gallion, D. Ford, C. Girodet, D.F. Easton, R.A. DiCioccio, G. Evans, M.A. Ponder, C. Pye, S. Mazoyer and et al., **(1994)** *Familial site-specific ovarian cancer is linked to BRCA1 on 17q12-21.* Am J Hum Genet, 55(5): p. 870-5.

159 L.H. Castilla, F.J. Couch, M.R. Erdos, K.F. Hoskins, K. Calzone, J.E. Garber, J. Boyd, M.B. Lubin, M.L. Deshano, L.C. Brody and et al., **(1994)** *Mutations in the BRCA1 gene in families with early-onset breast and ovarian cancer.* Nat Genet, 8(4): p. 387-91.

160 Y. Miki, J. Swensen, D. Shattuck-Eidens, P.A. Futreal, K. Harshman, S. Tavtigian, Q. Liu, C. Cochran, L.M. Bennett, W. Ding and et al., **(1994)** *A strong candidate for the breast and ovarian cancer susceptibility gene BRCA1.* Science, 266(5182): p. 66-71.

161 P.A. Futreal, Q. Liu, D. Shattuck-Eidens, C. Cochran, K. Harshman, S. Tavtigian, L.M. Bennett, A. Haugen-Strano, J. Swensen, Y. Miki and et al., **(1994)** *BRCA1 mutations in primary breast and ovarian carcinomas.* Science, 266(5182): p. 120-2.

162 M. Esteller, J.M. Silva, G. Dominguez, F. Bonilla, X. Matias-Guiu, E. Lerma, E. Bussaglia, J. Prat, I.C. Harkes, E.A. Repasky, E. Gabrielson, M. Schutte, S.B. Baylin and J.G. Herman, **(2000)** *Promoter hypermethylation and BRCA1 inactivation in sporadic breast and ovarian tumors.* J Natl Cancer Inst, 92(7): p. 564-9.

163 R. Wooster, S.L. Neuhausen, J. Mangion, Y. Quirk, D. Ford, N. Collins, K. Nguyen, S. Seal, T. Tran, D. Averill and et al., **(1994)** *Localization of a breast cancer susceptibility gene, BRCA2, to chromosome 13q12-13.* Science, 265(5181): p. 2088-90.

164 R. Wooster, G. Bignell, J. Lancaster, S. Swift, S. Seal, J. Mangion, N. Collins, S. Gregory, C. Gumbs and G. Micklem, **(1995)** *Identification of the breast cancer susceptibility gene BRCA2.* Nature, 378(6559): p. 789-92.

165 S.V. Tavtigian, J. Simard, J. Rommens, F. Couch, D. Shattuck-Eidens, S. Neuhausen, S. Merajver, S. Thorlacius, K. Offit, D. Stoppa-Lyonnet, C. Belanger, R. Bell, S. Berry, R. Bogden, Q. Chen, T. Davis, M. Dumont, C. Frye, T. Hattier, S. Jammulapati, T. Janecki, P. Jiang, R. Kehrer, J.F. Leblanc, J.T. Mitchell, J. McArthur-Morrison, K. Nguyen, Y. Peng, C. Samson, M. Schroeder, S.C. Snyder, L. Steele, M. Stringfellow, C. Stroup, B. Swedlund, J. Swense, D. Teng, A. Thomas, T. Tran, M. Tranchant, J. Weaver-Feldhaus, A.K. Wong, H. Shizuya, J.E. Eyfjord, L. Cannon-Albright, M. Tranchant, F. Labrie, M.H. Skolnick, B. Weber, A. Kamb and D.E. Goldgar, **(1996)** *The complete BRCA2 gene and mutations in chromosome 13q-linked kindreds.* Nat Genet, 12(3): p. 333-7.

166 T. Ludwig, D.L. Chapman, V.E. Papaioannou and A. Efstratiadis, **(1997)** *Targeted mutations of breast cancer susceptibility gene homologs in mice:*

lethal phenotypes of Brca1, Brca2, Brca1/Brca2, Brca1/p53, and Brca2/p53 nullizygous embryos. Genes Dev, 11(10): p. 1226-41.

167 L. Cao, X. Xu, S.F. Bunting, J. Liu, R.H. Wang, L.L. Cao, J.J. Wu, T.N. Peng, J. Chen, A. Nussenzweig, C.X. Deng and T. Finkel, **(2009)** *A selective requirement for 53BP1 in the biological response to genomic instability induced by Brca1 deficiency.* Mol Cell, 35(4): p. 534-41.

168 L. Cao, S. Kim, C. Xiao, R.H. Wang, X. Coumoul, X. Wang, W.M. Li, X.L. Xu, J.A. De Soto, H. Takai, S. Mai, S.J. Elledge, N. Motoyama and C.X. Deng, **(2006)** *ATM-Chk2-p53 activation prevents tumorigenesis at an expense of organ homeostasis upon Brca1 deficiency.* EMBO J, 25(10): p. 2167-77.

169 S.K. Sharan, M. Morimatsu, U. Albrecht, D.S. Lim, E. Regel, C. Dinh, A. Sands, G. Eichele, P. Hasty and A. Bradley, **(1997)** *Embryonic lethality and radiation hypersensitivity mediated by Rad51 in mice lacking Brca2.* Nature, 386(6627): p. 804-10.

170 A. Suzuki, J.L. de la Pompa, R. Hakem, A. Elia, R. Yoshida, R. Mo, H. Nishina, T. Chuang, A. Wakeham, A. Itie, W. Koo, P. Billia, A. Ho, M. Fukumoto, C.C. Hui and T.W. Mak, **(1997)** *Brca2 is required for embryonic cellular proliferation in the mouse.* Genes Dev, 11(10): p. 1242-52.

171 D. Ford, D.F. Easton, M. Stratton, S. Narod, D. Goldgar, P. Devilee, D.T. Bishop, B. Weber, G. Lenoir, J. Chang-Claude, H. Sobol, M.D. Teare, J. Struewing, A. Arason, S. Scherneck, J. Peto, T.R. Rebbeck, P. Tonin, S. Neuhausen, R. Barkardottir, J. Eyfjord, H. Lynch, B.A. Ponder, S.A. Gayther, M. Zelada-Hedman and et al., **(1998)** *Genetic heterogeneity and penetrance analysis of the BRCA1 and BRCA2 genes in breast cancer families. The Breast Cancer Linkage Consortium.* Am J Hum Genet, 62(3): p. 676-89.

172 S. Chen, E.S. Iversen, T. Friebel, D. Finkelstein, B.L. Weber, A. Eisen, L.E. Peterson, J.M. Schildkraut, C. Isaacs, B.N. Peshkin, C. Corio, L. Leondaridis, G. Tomlinson, D. Dutson, R. Kerber, C.I. Amos, L.C. Strong, D.A. Berry, D.M. Euhus and G. Parmigiani, **(2006)** *Characterization of BRCA1 and BRCA2 mutations in a large United States sample.* J Clin Oncol, 24(6): p. 863-71.

173 J.M. Noh, D.H. Choi, H. Baek, S.J. Nam, J.E. Lee, J.W. Kim, C.S. Ki, W. Park and S.J. Huh, **(2012)** *Associations between BRCA Mutations in High-Risk Breast Cancer Patients and Familial Cancers Other than Breast or Ovary.* J Breast Cancer, 15(3): p. 283-7.

174 H. Cavanagh and K.M. Rogers, **(2015)** *The role of BRCA1 and BRCA2 mutations in prostate, pancreatic and stomach cancers.* Hered Cancer Clin Pract, 13(1): p. 16.

175 J. Mersch, M.A. Jackson, M. Park, D. Nebgen, S.K. Peterson, C. Singletary, B.K. Arun and J.K. Litton, **(2015)** *Cancers associated with BRCA1 and BRCA2 mutations other than breast and ovarian.* Cancer, 121(2): p. 269-75.

176 P.A. Mateos-Gomez, T. Kent, S.K. Deng, S. McDevitt, E. Kashkina, T.M. Hoang, R.T. Pomerantz and A. Sfeir, **(2017)** *The helicase domain of Poltheta counteracts RPA to promote alt-NHEJ.* Nat Struct Mol Biol, 24(12): p. 1116-1123.

177 S. Pathania, S. Bade, M. Le Guillou, K. Burke, R. Reed, C. Bowman-Colin, Y. Su, D.T. Ting, K. Polyak, A.L. Richardson, J. Feunteun, J.E. Garber and D.M. Livingston, **(2014)** *BRCA1 haploinsufficiency for replication stress suppression in primary cells.* Nat Commun, 5: p. 5496.

178 M. Karaayvaz-Yildirim, R.E. Silberman, A. Langenbucher, S.V. Saladi, K.N. Ross, E. Zarcaro, A. Desmond, M. Yildirim, V. Vivekanandan, H. Ravichandran, R. Mylavagnanam, M.C. Specht, S. Ramaswamy, M. Lawrence, A. Amon and L.W. Ellisen, **(2020)** *Aneuploidy and a deregulated DNA damage response suggest haploinsufficiency in breast tissues of BRCA2 mutation carriers.* Sci Adv, 6(5): p. eaay2611.

179 A. Minchom, C. Aversa and J. Lopez, **(2018)** *Dancing with the DNA damage response: next-generation anti-cancer therapeutic strategies.* Ther Adv Med Oncol, 10: p. 1758835918786658.

180 M. Morimatsu, G. Donoho and P. Hasty, **(1998)** *Cells deleted for Brca2 COOH terminus exhibit hypersensitivity to gamma-radiation and premature senescence.* Cancer Res, 58(15): p. 3441-7.

181 S.X. Shen, Z. Weaver, X. Xu, C. Li, M. Weinstein, L. Chen, X.Y. Guan, T. Ried and C.X. Deng, **(1998)** *A targeted disruption of the murine Brca1 gene*

causes gamma-irradiation hypersensitivity and genetic instability. Oncogene, 17(24): p. 3115-24.

182 L.C. Gowen, A.V. Avrutskaya, A.M. Latour, B.H. Koller and S.A. Leadon, **(1998)** *BRCA1 required for transcription-coupled repair of oxidative DNA damage.* Science, 281(5379): p. 1009-12.

183 S.S. Yuan, S.Y. Lee, G. Chen, M. Song, G.E. Tomlinson and E.Y. Lee, **(1999)** *BRCA2 is required for ionizing radiation-induced assembly of Rad51 complex in vivo.* Cancer Res, 59(15): p. 3547-51.

184 A. Bhattacharyya, U.S. Ear, B.H. Koller, R.R. Weichselbaum and D.K. Bishop, **(2000)** *The breast cancer susceptibility gene BRCA1 is required for subnuclear assembly of Rad51 and survival following treatment with the DNA cross-linking agent cisplatin.* J Biol Chem, 275(31): p. 23899-903.

185 D.W. Abbott, M.L. Freeman and J.T. Holt, **(1998)** *Double-strand break repair deficiency and radiation sensitivity in BRCA2 mutant cancer cells.* J Natl Cancer Inst, 90(13): p. 978-85.

186 P.L. Chen, C.F. Chen, Y. Chen, J. Xiao, Z.D. Sharp and W.H. Lee, **(1998)** *The BRC repeats in BRCA2 are critical for RAD51 binding and resistance to methyl methanesulfonate treatment.* Proc Natl Acad Sci U S A, 95(9): p. 5287-92.

187 J. Boyd, Y. Sonoda, M.G. Federici, F. Bogomolniy, E. Rhei, D.L. Maresco, P.E. Saigo, L.A. Almadrones, R.R. Barakat, C.L. Brown, D.S. Chi, J.P. Curtin, E.A. Poynor and W.J. Hoskins, **(2000)** *Clinicopathologic features of BRCA-linked and sporadic ovarian cancer.* JAMA, 283(17): p. 2260-5.

188 R.D. Kennedy, J.E. Quinn, P.B. Mullan, P.G. Johnston and D.P. Harkin, **(2004)** *The role of BRCA1 in the cellular response to chemotherapy.* J Natl Cancer Inst, 96(22): p. 1659-68.

189 H.E. Bryant, N. Schultz, H.D. Thomas, K.M. Parker, D. Flower, E. Lopez, S. Kyle, M. Meuth, N.J. Curtin and T. Helleday, **(2005)** *Specific killing of BRCA2-deficient tumours with inhibitors of poly(ADP-ribose) polymerase.* Nature, 434(7035): p. 913-7.

190 H. Farmer, N. McCabe, C.J. Lord, A.N. Tutt, D.A. Johnson, T.B. Richardson, M. Santarosa, K.J. Dillon, I. Hickson, C. Knights, N.M. Martin, S.P. Jackson, G.C. Smith and A. Ashworth, **(2005)** *Targeting the DNA repair defect in BRCA mutant cells as a therapeutic strategy.* Nature, 434(7035): p. 917-21.

191 S. Rottenberg, J.E. Jaspers, A. Kersbergen, E. van der Burg, A.O. Nygren, S.A. Zander, P.W. Derksen, M. de Bruin, J. Zevenhoven, A. Lau, R. Boulter, A. Cranston, M.J. O'Connor, N.M. Martin, P. Borst and J. Jonkers, **(2008)** *High sensitivity of BRCA1-deficient mammary tumors to the PARP inhibitor AZD2281 alone and in combination with platinum drugs.* Proc Natl Acad Sci U S A, 105(44): p. 17079-84.

192 W. Sakai, E.M. Swisher, B.Y. Karlan, M.K. Agarwal, J. Higgins, C. Friedman, E. Villegas, C. Jacquemont, D.J. Farrugia, F.J. Couch, N. Urban and T. Taniguchi, **(2008)** *Secondary mutations as a mechanism of cisplatin resistance in BRCA2-mutated cancers.* Nature, 451(7182): p. 1116-20.

193 E.M. Swisher, W. Sakai, B.Y. Karlan, K. Wurz, N. Urban and T. Taniguchi, **(2008)** *Secondary BRCA1 mutations in BRCA1-mutated ovarian carcinomas with platinum resistance.* Cancer Res, 68(8): p. 2581-6.

194 B. Norquist, K.A. Wurz, C.C. Pennil, R. Garcia, J. Gross, W. Sakai, B.Y. Karlan, T. Taniguchi and E.M. Swisher, **(2011)** *Secondary somatic mutations restoring BRCA1/2 predict chemotherapy resistance in hereditary ovarian carcinomas.* J Clin Oncol, 29(22): p. 3008-15.

195 G. Kim, G. Ison, A.E. McKee, H. Zhang, S. Tang, T. Gwise, R. Sridhara, E. Lee, A. Tzou, R. Philip, H.J. Chiu, T.K. Ricks, T. Palmby, A.M. Russell, G. Ladouceur, E. Pfuma, H. Li, L. Zhao, Q. Liu, R. Venugopal, A. Ibrahim and R. Pazdur, **(2015)** *FDA Approval Summary: Olaparib Monotherapy in Patients with Deleterious Germline BRCA-Mutated Advanced Ovarian Cancer Treated with Three or More Lines of Chemotherapy.* Clin Cancer Res, 21(19): p. 4257-61.

196 M. Robson, S.A. Im, E. Senkus, B. Xu, S.M. Domchek, N. Masuda, S. Delaloge, W. Li, N. Tung, A. Armstrong, W. Wu, C. Goessl, S. Runswick and P. Conte, **(2017)** *Olaparib for Metastatic Breast Cancer in Patients with a Germline BRCA Mutation.* N Engl J Med, 377(6): p. 523-533.

197 M.R. Mirza, B.J. Monk, J. Herrstedt, A.M. Oza, S. Mahner, A. Redondo, M. Fabbro, J.A. Ledermann, D. Lorusso, I. Vergote, N.E. Ben-Baruch, C. Marth, R. Madry, R.D. Christensen, J.S. Berek, A. Dorum, A.V. Tinker, A. du Bois, A. Gonzalez-Martin, P. Follana, B. Benigno, P. Rosenberg, L. Gilbert, B.J. Rimel, J. Buscema, J.P. Balser, S. Agarwal, U.A. Matulonis and E.-O.N. Investigators, **(2016)** *Niraparib Maintenance Therapy in Platinum-Sensitive, Recurrent Ovarian Cancer.* N Engl J Med, 375(22): p. 2154-2164.

198 E.M. Swisher, K.K. Lin, A.M. Oza, C.L. Scott, H. Giordano, J. Sun, G.E. Konecny, R.L. Coleman, A.V. Tinker, D.M. O'Malley, R.S. Kristeleit, L. Ma, K.M. Bell-McGuinn, J.D. Brenton, J.M. Cragun, A. Oaknin, I. Ray-Coquard, M.I. Harrell, E. Mann, S.H. Kaufmann, A. Floquet, A. Leary, T.C. Harding, S. Goble, L. Maloney, J. Isaacson, A.R. Allen, L. Rolfe, R. Yelensky, M. Raponi and I.A. McNeish, **(2017)** *Rucaparib in relapsed, platinum-sensitive high-grade ovarian carcinoma (ARIEL2 Part 1): an international, multicentre, open-label, phase 2 trial.* Lancet Oncol, 18(1): p. 75-87.

199 J.K. Litton, H.S. Rugo, J. Ettl, S.A. Hurvitz, A. Goncalves, K.H. Lee, L. Fehrenbacher, R. Yerushalmi, L.A. Mina, M. Martin, H. Roche, Y.H. Im, R.G.W. Quek, D. Markova, I.C. Tudor, A.L. Hannah, W. Eiermann and J.L. Blum, **(2018)** *Talazoparib in Patients with Advanced Breast Cancer and a Germline BRCA Mutation.* N Engl J Med, 379(8): p. 753-763.

200 A. Gunjur, **(2018)** *Talazoparib for BRCA-mutated advanced breast cancer.* Lancet Oncol, 19(10): p. e511.

201 L.J. Barber, S. Sandhu, L. Chen, J. Campbell, I. Kozarewa, K. Fenwick, I. Assiotis, D.N. Rodrigues, J.S. Reis Filho, V. Moreno, J. Mateo, L.R. Molife, J. De Bono, S. Kaye, C.J. Lord and A. Ashworth, **(2013)** *Secondary mutations in BRCA2 associated with clinical resistance to a PARP inhibitor.* J Pathol, 229(3): p. 422-9.

202 S.M. Noordermeer, S. Adam, D. Setiaputra, M. Barazas, S.J. Pettitt, A.K. Ling, M. Olivieri, A. Alvarez-Quilon, N. Moatti, M. Zimmermann, S. Annunziato, D.B. Krastev, F. Song, I. Brandsma, J. Frankum, R. Brough, A. Sherker, S. Landry, R.K. Szilard, M.M. Munro, A. McEwan, T. Goullet de Rugy, Z.Y. Lin, T. Hart, J. Moffat, A.C. Gingras, A. Martin, H. van Attikum, J. Jonkers, C.J. Lord, S. Rottenberg and D. Durocher, **(2018)** *The shieldin complex mediates 53BP1-dependent DNA repair.* Nature, 560(7716): p. 117-121.

203 C.J. Lord and A. Ashworth, **(2013)** *Mechanisms of resistance to therapies targeting BRCA-mutant cancers.* Nat Med, 19(11): p. 1381-8.

204 P. Ter Brugge, P. Kristel, E. van der Burg, U. Boon, M. de Maaker, E. Lips, L. Mulder, J. de Ruiter, C. Moutinho, H. Gevensleben, E. Marangoni, I. Majewski, K. Jozwiak, W. Kloosterman, M. van Roosmalen, K. Duran, F. Hogervorst, N. Turner, M. Esteller, E. Cuppen, J. Wesseling and J. Jonkers, **(2016)** *Mechanisms of Therapy Resistance in Patient-Derived Xenograft Models of BRCA1-Deficient Breast Cancer.* J Natl Cancer Inst, 108(11): p.

205 J.J. Kim, S.Y. Lee, J.H. Choi, H.G. Woo, B. Xhemalce and K.M. Miller, **(2020)** *PCAF-Mediated Histone Acetylation Promotes Replication Fork Degradation by MRE11 and EXO1 in BRCA-Deficient Cells.* Mol Cell, 80(2): p. 327-344 e8.

206 A. Ray Chaudhuri, E. Callen, X. Ding, E. Gogola, A.A. Duarte, J.E. Lee, N. Wong, V. Lafarga, J.A. Calvo, N.J. Panzarino, S. John, A. Day, A.V. Crespo, B. Shen, L.M. Starnes, J.R. de Ruiter, J.A. Daniel, P.A. Konstantinopoulos, D. Cortez, S.B. Cantor, O. Fernandez-Capetillo, K. Ge, J. Jonkers, S. Rottenberg, S.K. Sharan and A. Nussenzweig, **(2016)** *Replication fork stability confers chemoresistance in BRCA-deficient cells.* Nature, 535(7612): p. 382-7.

207 J.E. Jaspers, A. Kersbergen, U. Boon, W. Sol, L. van Deemter, S.A. Zander, R. Drost, E. Wientjens, J. Ji, A. Aly, J.H. Doroshow, A. Cranston, N.M. Martin, A. Lau, M.J. O'Connor, S. Ganesan, P. Borst, J. Jonkers and S. Rottenberg, **(2013)** *Loss of 53BP1 causes PARP inhibitor resistance in Brca1-mutated mouse mammary tumors.* Cancer Discov, 3(1): p. 68-81.

208 H. Dev, T.W. Chiang, C. Lescale, I. de Krijger, A.G. Martin, D. Pilger, J. Coates, M. Sczaniecka-Clift, W. Wei, M. Ostermaier, M. Herzog, J. Lam, A. Shea, M. Demir, Q. Wu, F. Yang, B. Fu, Z. Lai, G. Balmus, R. Belotserkovskaya, V. Serra, M.J. O'Connor, A. Bruna, P. Beli, L. Pellegrini, C. Caldas, L. Deriano, J.J.L. Jacobs, Y. Galanty and S.P. Jackson, **(2018)** *Shieldin complex promotes DNA end-joining and counters homologous recombination in BRCA1-null cells.* Nat Cell Biol, 20(8): p. 954-965.

209 H. Ghezraoui, C. Oliveira, J.R. Becker, K. Bilham, D. Moralli, C. Anzilotti, R. Fischer, M. Deobagkar-Lele, M. Sanchiz-Calvo, E. Fueyo-Marcos, S. Bonham, B.M. Kessler, S. Rottenberg, R.J. Cornall, C.M. Green and J.R.

Chapman, **(2018)** *53BP1 cooperation with the REV7-shieldin complex underpins DNA structure-specific NHEJ.* Nature, 560(7716): p. 122-127.

210 R. Gupta, K. Somyajit, T. Narita, E. Maskey, A. Stanlie, M. Kremer, D. Typas, M. Lammers, N. Mailand, A. Nussenzweig, J. Lukas and C. Choudhary, **(2018)** *DNA Repair Network Analysis Reveals Shieldin as a Key Regulator of NHEJ and PARP Inhibitor Sensitivity.* Cell, 173(4): p. 972-988 e23.

211 R. Belotserkovskaya, E. Raga Gil, N. Lawrence, R. Butler, G. Clifford, M.D. Wilson and S.P. Jackson, **(2020)** *PALB2 chromatin recruitment restores homologous recombination in BRCA1-deficient cells depleted of 53BP1.* Nat Commun, 11(1): p. 819.

212 S.J. Pettitt, D.B. Krastev, I. Brandsma, A. Drean, F. Song, R. Aleksandrov, M.I. Harrell, M. Menon, R. Brough, J. Campbell, J. Frankum, M. Ranes, H.N. Pemberton, R. Rafiq, K. Fenwick, A. Swain, S. Guettler, J.M. Lee, E.M. Swisher, S. Stoynov, K. Yusa, A. Ashworth and C.J. Lord, **(2018)** *Genome-wide and high-density CRISPR-Cas9 screens identify point mutations in PARP1 causing PARP inhibitor resistance.* Nat Commun, 9(1): p. 1849.

213 M. Zimmermann, O. Murina, M.A.M. Reijns, A. Agathanggelou, R. Challis, Z. Tarnauskaite, M. Muir, A. Fluteau, M. Aregger, A. McEwan, W. Yuan, M. Clarke, M.B. Lambros, S. Paneesha, P. Moss, M. Chandrashekhar, S. Angers, J. Moffat, V.G. Brunton, T. Hart, J. de Bono, T. Stankovic, A.P. Jackson and D. Durocher, **(2018)** *CRISPR screens identify genomic ribonucleotides as a source of PARP-trapping lesions.* Nature, 559(7713): p. 285-289.

214 I. Bang, **(1910)** *Untersuchungen über die Guanylsäure.* Biochem. Z., 26: p. 293-311.

215 M. Gellert, M.N. Lipsett and D.R. Davies, **(1962)** *Helix formation by guanylic acid.* Proc Natl Acad Sci U S A, 48: p. 2013-8.

216 S. Arnott, R. Chandrasekaran and C.M. Marttila, **(1974)** *Structures for polyinosinic acid and polyguanylic acid.* Biochem J, 141(2): p. 537-43.

217 S.B. Zimmerman, G.H. Cohen and D.R. Davies, **(1975)** *X-ray fiber diffraction and model-building study of polyguanylic acid and polyinosinic acid.* J Mol Biol, 92(2): p. 181-92.

218 D. Sen and W. Gilbert, **(1988)** *Formation of parallel four-stranded complexes by guanine-rich motifs in DNA and its implications for meiosis.* Nature, 334(6180): p. 364-6.

219 W.I. Sundquist and A. Klug, **(1989)** *Telomeric DNA dimerizes by formation of guanine tetrads between hairpin loops.* Nature, 342(6251): p. 825-9.

220 J.R. Williamson, **(1994)** *G-quartet structures in telomeric DNA.* Annu Rev Biophys Biomol Struct, 23: p. 703-30.

221 J. Meyne, R.L. Ratliff and R.K. Moyzis, **(1989)** *Conservation of the human telomere sequence (TTAGGG)n among vertebrates.* Proc Natl Acad Sci U S A, 86(18): p. 7049-53.

222 W.E. Wright, V.M. Tesmer, K.E. Huffman, S.D. Levene and J.W. Shay, **(1997)** *Normal human chromosomes have long G-rich telomeric overhangs at one end.* Genes Dev, 11(21): p. 2801-9.

223 D. Sen and W. Gilbert, **(1990)** *A sodium-potassium switch in the formation of four-stranded G4-DNA.* Nature, 344(6265): p. 410-4.

224 J.T. Davis, **(2004)** *G-quartets 40 years later: from 5'-GMP to molecular biology and supramolecular chemistry.* Angew Chem Int Ed Engl, 43(6): p. 668-98.

225 D. Bhattacharyya, G. Mirihana Arachchilage and S. Basu, **(2016)** *Metal Cations in G-Quadruplex Folding and Stability.* Front Chem, 4: p. 38.

226 A. Kotar, B. Wang, A. Shivalingam, J. Gonzalez-Garcia, R. Vilar and J. Plavec, **(2016)** *NMR Structure of a Triangulenium-Based Long-Lived Fluorescence Probe Bound to a G-Quadruplex.* Angew Chem Int Ed Engl, 55(40): p. 12508-11.

227 W.J. Chung, B. Heddi, F. Hamon, M.P. Teulade-Fichou and A.T. Phan, **(2014)** *Solution structure of a G-quadruplex bound to the bisquinolinium compound Phen-DC(3).* Angew Chem Int Ed Engl, 53(4): p. 999-1002.

228 G. Wu, L. Chen, W. Liu and D. Yang, **(2019)** *Molecular Recognition of the Hybrid-Type G-Quadruplexes in Human Telomeres.* Molecules, 24(8): p.

229 C. Lin, G. Wu, K. Wang, B. Onel, S. Sakai, Y. Shao and D. Yang, **(2018)** *Molecular Recognition of the Hybrid-2 Human Telomeric G-Quadruplex by Epiberberine: Insights into Conversion of Telomeric G-Quadruplex Structures.* Angew Chem Int Ed Engl, 57(34): p. 10888-10893.

230 D. Yang, **(2019)** *G-Quadruplex DNA and RNA.* Methods Mol Biol, 2035: p. 1-24.

231 V. Dapic, V. Abdomerovic, R. Marrington, J. Peberdy, A. Rodger, J.O. Trent and P.J. Bates, **(2003)** *Biophysical and biological properties of quadruplex oligodeoxyribonucleotides.* Nucleic Acids Res, 31(8): p. 2097-107.

232 K. Guo, A. Pourpak, K. Beetz-Rogers, V. Gokhale, D. Sun and L.H. Hurley, **(2007)** *Formation of pseudosymmetrical G-quadruplex and i-motif structures in the proximal promoter region of the RET oncogene.* J Am Chem Soc, 129(33): p. 10220-8.

233 M.L. Gill, S.A. Strobel and J.P. Loria, **(2005)** *205Tl NMR methods for the characterization of monovalent cation binding to nucleic acids.* J Am Chem Soc, 127(47): p. 16723-32.

234 C. Wan, W. Fu, H. Jing and N. Zhang, **(2019)** *NMR solution structure of an asymmetric intermolecular leaped V-shape G-quadruplex: selective recognition of the d(G2NG3NG4) sequence motif by a short linear G-rich DNA probe.* Nucleic Acids Res, 47(3): p. 1544-1556.

235 J.L. Huppert, **(2008)** *Four-stranded nucleic acids: structure, function and targeting of G-quadruplexes.* Chem Soc Rev, 37(7): p. 1375-84.

236 G.N. Parkinson, M.P. Lee and S. Neidle, **(2002)** *Crystal structure of parallel quadruplexes from human telomeric DNA.* Nature, 417(6891): p. 876-80.

237 S. Haider, G.N. Parkinson and S. Neidle, **(2002)** *Crystal structure of the potassium form of an Oxytricha nova G-quadruplex.* J Mol Biol, 320(2): p. 189-200.

238 Y. Geng, C. Liu, B. Zhou, Q. Cai, H. Miao, X. Shi, N. Xu, Y. You, C.P. Fung, R.U. Din and G. Zhu, **(2019)** *The crystal structure of an antiparallel chair-type G-quadruplex formed by Bromo-substituted human telomeric DNA.* Nucleic Acids Res, 47(10): p. 5395-5404.

239 B. Heddi, V.V. Cheong, E. Schmitt, Y. Mechulam and A.T. Phan, **(2020)** *Recognition of different base tetrads by RHAU (DHX36): X-ray crystal structure of the G4 recognition motif bound to the 3'-end tetrad of a DNA G-quadruplex.* J Struct Biol, 209(1): p. 107399.

240 A.N. Lane, J.B. Chaires, R.D. Gray and J.O. Trent, **(2008)** *Stability and kinetics of G-quadruplex structures.* Nucleic Acids Res, 36(17): p. 5482-515.

241 G. Laughlan, A.I. Murchie, D.G. Norman, M.H. Moore, P.C. Moody, D.M. Lilley and B. Luisi, **(1994)** *The high-resolution crystal structure of a parallel-stranded guanine tetraplex.* Science, 265(5171): p. 520-4.

242 K. Phillips, Z. Dauter, A.I. Murchie, D.M. Lilley and B. Luisi, **(1997)** *The crystal structure of a parallel-stranded guanine tetraplex at 0.95 A resolution.* J Mol Biol, 273(1): p. 171-82.

243 M. Crnugelj, P. Sket and J. Plavec, **(2003)** *Small change in a G-rich sequence, a dramatic change in topology: new dimeric G-quadruplex folding motif with unique loop orientations.* J Am Chem Soc, 125(26): p. 7866-71.

244 R.H. Shafer and I. Smirnov, **(2000)** *Biological aspects of DNA/RNA quadruplexes.* Biopolymers, 56(3): p. 209-27.

245 A. Bugaut and S. Balasubramanian, **(2012)** *5'-UTR RNA G-quadruplexes: translation regulation and targeting.* Nucleic Acids Res, 40(11): p. 4727-41.

246 J.D. Beaudoin and J.P. Perreault, **(2013)** *Exploring mRNA 3'-UTR G-quadruplexes: evidence of roles in both alternative polyadenylation and mRNA shortening.* Nucleic Acids Res, 41(11): p. 5898-911.

247 M. Subramanian, F. Rage, R. Tabet, E. Flatter, J.L. Mandel and H. Moine, **(2011)** *G-quadruplex RNA structure as a signal for neurite mRNA targeting.* EMBO Rep, 12(7): p. 697-704.

248 S. Millevoi, H. Moine and S. Vagner, **(2012)** *G-quadruplexes in RNA biology.* Wiley Interdiscip Rev RNA, 3(4): p. 495-507.

249 M.M. Fay, S.M. Lyons and P. Ivanov, **(2017)** *RNA G-Quadruplexes in Biology: Principles and Molecular Mechanisms.* J Mol Biol, 429(14): p. 2127-2147.

250 K.W. Zheng, S. Xiao, J.Q. Liu, J.Y. Zhang, Y.H. Hao and Z. Tan, **(2013)** *Co-transcriptional formation of DNA:RNA hybrid G-quadruplex and potential function as constitutional cis element for transcription control.* Nucleic Acids Res, 41(10): p. 5533-41.

251 A.T. Phan and D.J. Patel, **(2003)** *Two-repeat human telomeric d(TAGGGTTAGGGT) sequence forms interconverting parallel and antiparallel G-quadruplexes in solution: distinct topologies, thermodynamic properties, and folding/unfolding kinetics.* J Am Chem Soc, 125(49): p. 15021-7.

252 A. Risitano and K.R. Fox, **(2004)** *Influence of loop size on the stability of intramolecular DNA quadruplexes.* Nucleic Acids Res, 32(8): p. 2598-606.

253 M. Cevec and J. Plavec, **(2005)** *Role of loop residues and cations on the formation and stability of dimeric DNA G-quadruplexes.* Biochemistry, 44(46): p. 15238-46.

254 G. Portella, M. Orozco and M. Vendruscolo, **(2020)** *Determination of a Structural Ensemble Representing the Dynamics of a G-Quadruplex DNA.* Biochemistry, 59(4): p. 379-388.

255 Y. Cheng, Y. Zhang, Z. Gong, X. Zhang, Y. Li, X. Shi, Y. Pei and H. You, **(2020)** *High Mechanical Stability and Slow Unfolding Rates Are Prevalent in Parallel-Stranded DNA G-Quadruplexes.* J Phys Chem Lett, 11(19): p. 7966-7971.

256 A. Piazza, M. Adrian, F. Samazan, B. Heddi, F. Hamon, A. Serero, J. Lopes, M.P. Teulade-Fichou, A.T. Phan and A. Nicolas, **(2015)** *Short loop length and high thermal stability determine genomic instability induced by G-quadruplex-forming minisatellites.* EMBO J, 34(12): p. 1718-34.

257 E. Puig Lombardi, A. Holmes, D. Verga, M.P. Teulade-Fichou, A. Nicolas and A. Londono-Vallejo, **(2019)** *Thermodynamically stable and genetically unstable G-quadruplexes are depleted in genomes across species.* Nucleic Acids Res, 47(12): p. 6098-6113.

258 J.L. Huppert and S. Balasubramanian, **(2005)** *Prevalence of quadruplexes in the human genome.* Nucleic Acids Res, 33(9): p. 2908-16.

259 A.K. Todd, M. Johnston and S. Neidle, **(2005)** *Highly prevalent putative quadruplex sequence motifs in human DNA.* Nucleic Acids Res, 33(9): p. 2901-7.

260 J.M. Garant, J.P. Perreault and M.S. Scott, **(2017)** *Motif independent identification of potential RNA G-quadruplexes by G4RNA screener.* Bioinformatics, 33(22): p. 3532-3537.

261 A.B. Sahakyan, V.S. Chambers, G. Marsico, T. Santner, M. Di Antonio and S. Balasubramanian, **(2017)** *Machine learning model for sequence-driven DNA G-quadruplex formation.* Sci Rep, 7(1): p. 14535.

262 E.P. Lombardi and A. Londono-Vallejo, **(2020)** *A guide to computational methods for G-quadruplex prediction.* Nucleic Acids Res: p.

263 A. Bedrat, L. Lacroix and J.L. Mergny, **(2016)** *Re-evaluation of G-quadruplex propensity with G4Hunter.* Nucleic Acids Res, 44(4): p. 1746-59.

264 G. Marsico, V.S. Chambers, A.B. Sahakyan, P. McCauley, J.M. Boutell, M.D. Antonio and S. Balasubramanian, **(2019)** *Whole genome experimental maps of DNA G-quadruplexes in multiple species.* Nucleic Acids Res, 47(8): p. 3862-3874.

265 J. Eddy and N. Maizels, **(2006)** *Gene function correlates with potential for G4 DNA formation in the human genome.* Nucleic Acids Res, 34(14): p. 3887-96.

266 J.L. Huppert and S. Balasubramanian, **(2007)** *G-quadruplexes in promoters throughout the human genome.* Nucleic Acids Res, 35(2): p. 406-13.

267 C. Schaffitzel, I. Berger, J. Postberg, J. Hanes, H.J. Lipps and A. Pluckthun, **(2001)** *In vitro generated antibodies specific for telomeric guanine-quadruplex*

DNA react with Stylonychia lemnae macronuclei. Proc Natl Acad Sci U S A, 98(15): p. 8572-7.

268 G. Biffi, D. Tannahill, J. McCafferty and S. Balasubramanian, **(2013)** *Quantitative visualization of DNA G-quadruplex structures in human cells.* Nat Chem, 5(3): p. 182-6.

269 A. Henderson, Y. Wu, Y.C. Huang, E.A. Chavez, J. Platt, F.B. Johnson, R.M. Brosh, Jr., D. Sen and P.M. Lansdorp, **(2014)** *Detection of G-quadruplex DNA in mammalian cells.* Nucleic Acids Res, 42(2): p. 860-9.

270 D. Sun, B. Thompson, B.E. Cathers, M. Salazar, S.M. Kerwin, J.O. Trent, T.C. Jenkins, S. Neidle and L.H. Hurley, **(1997)** *Inhibition of human telomerase by a G-quadruplex-interactive compound.* J Med Chem, 40(14): p. 2113-6.

271 R. Rodriguez, K.M. Miller, J.V. Forment, C.R. Bradshaw, M. Nikan, S. Britton, T. Oelschlaegel, B. Xhemalce, S. Balasubramanian and S.P. Jackson, **(2012)** *Small-molecule-induced DNA damage identifies alternative DNA structures in human genes.* Nat Chem Biol, 8(3): p. 301-10.

272 S.V. Lensing, G. Marsico, R. Hansel-Hertsch, E.Y. Lam, D. Tannahill and S. Balasubramanian, **(2016)** *DSBCapture: in situ capture and sequencing of DNA breaks.* Nat Methods, 13(10): p. 855-7.

273 H. Xu, M. Di Antonio, S. McKinney, V. Mathew, B. Ho, N.J. O'Neil, N.D. Santos, J. Silvester, V. Wei, J. Garcia, F. Kabeer, D. Lai, P. Soriano, J. Banath, D.S. Chiu, D. Yap, D.D. Le, F.B. Ye, A. Zhang, K. Thu, J. Soong, S.C. Lin, A.H. Tsai, T. Osako, T. Algara, D.N. Saunders, J. Wong, J. Xian, M.B. Bally, J.D. Brenton, G.W. Brown, S.P. Shah, D. Cescon, T.W. Mak, C. Caldas, P.C. Stirling, P. Hieter, S. Balasubramanian and S. Aparicio, **(2017)** *CX-5461 is a DNA G-quadruplex stabilizer with selective lethality in BRCA1/2 deficient tumours.* Nat Commun, 8: p. 14432.

274 Q. Li, J.F. Xiang, Q.F. Yang, H.X. Sun, A.J. Guan and Y.L. Tang, **(2013)** *G4LDB: a database for discovering and studying G-quadruplex ligands.* Nucleic Acids Res, 41(Database issue): p. D1115-23.

275 A.R. Duarte, E. Cadoni, A.S. Ressurreicao, R. Moreira and A. Paulo, **(2018)** *Design of Modular G-quadruplex Ligands.* ChemMedChem, 13(9): p. 869-893.

276 T. Simonsson, P. Pecinka and M. Kubista, **(1998)** *DNA tetraplex formation in the control region of c-myc.* Nucleic Acids Res, 26(5): p. 1167-72.

277 A. Siddiqui-Jain, C.L. Grand, D.J. Bearss and L.H. Hurley, **(2002)** *Direct evidence for a G-quadruplex in a promoter region and its targeting with a small molecule to repress c-MYC transcription.* Proc Natl Acad Sci U S A, 99(18): p. 11593-8.

278 S. Cogoi and L.E. Xodo, **(2006)** *G-quadruplex formation within the promoter of the KRAS proto-oncogene and its effect on transcription.* Nucleic Acids Res, 34(9): p. 2536-49.

279 G.R. Vandenbark, C.M. deCastro, H. Taylor, S. Dew-Knight and R.E. Kaufman, **(1992)** *Cloning and structural analysis of the human c-kit gene.* Oncogene, 7(7): p. 1259-66.

280 S. Rankin, A.P. Reszka, J. Huppert, M. Zloh, G.N. Parkinson, A.K. Todd, S. Ladame, S. Balasubramanian and S. Neidle, **(2005)** *Putative DNA quadruplex formation within the human c-kit oncogene.* J Am Chem Soc, 127(30): p. 10584-9.

281 G.R. Clark, P.D. Pytel, C.J. Squire and S. Neidle, **(2003)** *Structure of the first parallel DNA quadruplex-drug complex.* J Am Chem Soc, 125(14): p. 4066-7.

282 J. Dai, M. Carver, L.H. Hurley and D. Yang, **(2011)** *Solution structure of a 2:1 quindoline-c-MYC G-quadruplex: insights into G-quadruplex-interactive small molecule drug design.* J Am Chem Soc, 133(44): p. 17673-80.

283 W.J. Chung, B. Heddi, M. Tera, K. Iida, K. Nagasawa and A.T. Phan, **(2013)** *Solution structure of an intramolecular (3 + 1) human telomeric G-quadruplex bound to a telomestatin derivative.* J Am Chem Soc, 135(36): p. 13495-501.

284 W. Liu, Y.F. Zhong, L.Y. Liu, C.T. Shen, W. Zeng, F. Wang, D. Yang and Z.W. Mao, **(2018)** *Solution structures of multiple G-quadruplex complexes induced by a platinum(II)-based tripod reveal dynamic binding.* Nat Commun, 9(1): p. 3496.

285 H.J. Sullivan, B. Chen and C. Wu, **(2020)** *Molecular Dynamics Study on the Binding of an Anticancer DNA G-Quadruplex Stabilizer, CX-5461, to Human*

Telomeric, c-KIT1, and c-Myc G-Quadruplexes and a DNA Duplex. J Chem Inf Model, 60(10): p. 5203-5224.

286 J. Jamroskovic, M. Doimo, K. Chand, I. Obi, R. Kumar, K. Brannstrom, M. Hedenstrom, R. Nath Das, A. Akhunzianov, M. Deiana, K. Kasho, S. Sulis Sato, P.L. Pourbozorgi, J.E. Mason, P. Medini, D. Ohlund, S. Wanrooij, E. Chorell and N. Sabouri, **(2020)** *Quinazoline Ligands Induce Cancer Cell Death through Selective STAT3 Inhibition and G-Quadruplex Stabilization.* J Am Chem Soc, 142(6): p. 2876-2888.

287 J.S.A. Spiegel, S.; Balasubramanian, S., **(2019)** *The Structure and Function of DNA G-Quadruplexes.* Trends in chemistry, Vol. 2, No.2: p.

288 M. Fry and L.A. Loeb, **(1999)** *Human werner syndrome DNA helicase unwinds tetrahelical structures of the fragile X syndrome repeat sequence d(CGG)n.* J Biol Chem, 274(18): p. 12797-802.

289 P. Mohaghegh, J.K. Karow, R.M. Brosh, Jr., V.A. Bohr and I.D. Hickson, **(2001)** *The Bloom's and Werner's syndrome proteins are DNA structure-specific helicases.* Nucleic Acids Res, 29(13): p. 2843-9.

290 M.D. Huber, D.C. Lee and N. Maizels, **(2002)** *G4 DNA unwinding by BLM and Sgs1p: substrate specificity and substrate-specific inhibition.* Nucleic Acids Res, 30(18): p. 3954-61.

291 S. Lee, J. Kim, S. Han and C.J. Park, **(2020)** *Recognition and Unfolding of c-MYC and Telomeric G-Quadruplex DNAs by the RecQ C-Terminal Domain of Human Bloom Syndrome Helicase.* ACS Omega, 5(24): p. 14513-14522.

292 T.B. London, L.J. Barber, G. Mosedale, G.P. Kelly, S. Balasubramanian, I.D. Hickson, S.J. Boulton and K. Hiom, **(2008)** *FANCJ is a structure-specific DNA helicase associated with the maintenance of genomic G/C tracts.* J Biol Chem, 283(52): p. 36132-9.

293 Y. Wu, K. Shin-ya and R.M. Brosh, Jr., **(2008)** *FANCJ helicase defective in Fanconia anemia and breast cancer unwinds G-quadruplex DNA to defend genomic stability.* Mol Cell Biol, 28(12): p. 4116-28.

294 C. Ribeyre, J. Lopes, J.B. Boule, A. Piazza, A. Guedin, V.A. Zakian, J.L. Mergny and A. Nicolas, **(2009)** *The yeast Pif1 helicase prevents genomic*

instability caused by G-quadruplex-forming CEB1 sequences in vivo. PLoS Genet, 5(5): p. e1000475.

295 F. Foury and J. Kolodynski, **(1983)** *pif mutation blocks recombination between mitochondrial rho+ and rho- genomes having tandemly arrayed repeat units in Saccharomyces cerevisiae.* Proc Natl Acad Sci U S A, 80(17): p. 5345-9.

296 J.B. Boule, L.R. Vega and V.A. Zakian, **(2005)** *The yeast Pif1p helicase removes telomerase from telomeric DNA.* Nature, 438(7064): p. 57-61.

297 K. Paeschke, J.A. Capra and V.A. Zakian, **(2011)** *DNA replication through G-quadruplex motifs is promoted by the Saccharomyces cerevisiae Pif1 DNA helicase.* Cell, 145(5): p. 678-91.

298 K. Paeschke, M.L. Bochman, P.D. Garcia, P. Cejka, K.L. Friedman, S.C. Kowalczykowski and V.A. Zakian, **(2013)** *Pif1 family helicases suppress genome instability at G-quadruplex motifs.* Nature, 497(7450): p. 458-62.

299 N. van Wietmarschen, S. Merzouk, N. Halsema, D.C.J. Spierings, V. Guryev and P.M. Lansdorp, **(2018)** *BLM helicase suppresses recombination at G-quadruplex motifs in transcribed genes.* Nat Commun, 9(1): p. 271.

300 M.C. Chen, R. Tippana, N.A. Demeshkina, P. Murat, S. Balasubramanian, S. Myong and A.R. Ferre-D'Amare, **(2018)** *Structural basis of G-quadruplex unfolding by the DEAH/RHA helicase DHX36.* Nature, 558(7710): p. 465-469.

301 W.F. Chen, S. Rety, H.L. Guo, Y.X. Dai, W.Q. Wu, N.N. Liu, D. Auguin, Q.W. Liu, X.M. Hou, S.X. Dou and X.G. Xi, **(2018)** *Molecular Mechanistic Insights into Drosophila DHX36-Mediated G-Quadruplex Unfolding: A Structure-Based Model.* Structure, 26(3): p. 403-415 e4.

302 A. Piazza, J.B. Boule, J. Lopes, K. Mingo, E. Largy, M.P. Teulade-Fichou and A. Nicolas, **(2010)** *Genetic instability triggered by G-quadruplex interacting Phen-DC compounds in Saccharomyces cerevisiae.* Nucleic Acids Res, 38(13): p. 4337-48.

303 W. Lin, S. Sampathi, H. Dai, C. Liu, M. Zhou, J. Hu, Q. Huang, J. Campbell, K. Shin-Ya, L. Zheng, W. Chai and B. Shen, **(2013)** *Mammalian DNA2*

helicase/nuclease cleaves G-quadruplex DNA and is required for telomere integrity. EMBO J, 32(10): p. 1425-39.

304 P. Sarkies, P. Murat, L.G. Phillips, K.J. Patel, S. Balasubramanian and J.E. Sale, **(2012)** *FANCJ coordinates two pathways that maintain epigenetic stability at G-quadruplex DNA.* Nucleic Acids Res, 40(4): p. 1485-98.

305 J.K. Karow, R.K. Chakraverty and I.D. Hickson, **(1997)** *The Bloom's syndrome gene product is a 3'-5' DNA helicase.* J Biol Chem, 272(49): p. 30611-4.

306 M.D. Gray, J.C. Shen, A.S. Kamath-Loeb, A. Blank, B.L. Sopher, G.M. Martin, J. Oshima and L.A. Loeb, **(1997)** *The Werner syndrome protein is a DNA helicase.* Nat Genet, 17(1): p. 100-3.

307 W.L. Bridge, C.J. Vandenberg, R.J. Franklin and K. Hiom, **(2005)** *The BRIP1 helicase functions independently of BRCA1 in the Fanconi anemia pathway for DNA crosslink repair.* Nat Genet, 37(9): p. 953-7.

308 R.J. Gibbons, D.J. Picketts, L. Villard and D.R. Higgs, **(1995)** *Mutations in a putative global transcriptional regulator cause X-linked mental retardation with alpha-thalassemia (ATR-X syndrome).* Cell, 80(6): p. 837-45.

309 D. Clynes and R.J. Gibbons, **(2013)** *ATRX and the replication of structured DNA.* Curr Opin Genet Dev, 23(3): p. 289-94.

310 N. Shioda, Y. Yabuki, K. Yamaguchi, M. Onozato, Y. Li, K. Kurosawa, H. Tanabe, N. Okamoto, T. Era, H. Sugiyama, T. Wada and K. Fukunaga, **(2018)** *Targeting G-quadruplex DNA as cognitive function therapy for ATR-X syndrome.* Nat Med, 24(6): p. 802-813.

311 M.J. Law, K.M. Lower, H.P. Voon, J.R. Hughes, D. Garrick, V. Viprakasit, M. Mitson, M. De Gobbi, M. Marra, A. Morris, A. Abbott, S.P. Wilder, S. Taylor, G.M. Santos, J. Cross, H. Ayyub, S. Jones, J. Ragoussis, D. Rhodes, I. Dunham, D.R. Higgs and R.J. Gibbons, **(2010)** *ATR-X syndrome protein targets tandem repeats and influences allele-specific expression in a size-dependent manner.* Cell, 143(3): p. 367-78.

312 Y. Wang, J. Yang, A.T. Wild, W.H. Wu, R. Shah, C. Danussi, G.J. Riggins, K. Kannan, E.P. Sulman, T.A. Chan and J.T. Huse, **(2019)** *G-quadruplex*

DNA drives genomic instability and represents a targetable molecular abnormality in ATRX-deficient malignant glioma. Nat Commun, 10(1): p. 943.

313 D. Clynes, C. Jelinska, B. Xella, H. Ayyub, S. Taylor, M. Mitson, C.Z. Bachrati, D.R. Higgs and R.J. Gibbons, **(2014)** *ATRX dysfunction induces replication defects in primary mouse cells.* PLoS One, 9(3): p. e92915.

314 D. Clynes, D.R. Higgs and R.J. Gibbons, **(2013)** *The chromatin remodeller ATRX: a repeat offender in human disease.* Trends Biochem Sci, 38(9): p. 461-6.

315 E. Fouquerel, D. Parikh and P. Opresko, **(2016)** *DNA damage processing at telomeres: The ends justify the means.* DNA Repair (Amst), 44: p. 159-168.

316 A.M. Zahler, J.R. Williamson, T.R. Cech and D.M. Prescott, **(1991)** *Inhibition of telomerase by G-quartet DNA structures.* Nature, 350(6320): p. 718-20.

317 J.B. Vannier, V. Pavicic-Kaltenbrunner, M.I. Petalcorin, H. Ding and S.J. Boulton, **(2012)** *RTEL1 dismantles T loops and counteracts telomeric G4-DNA to maintain telomere integrity.* Cell, 149(4): p. 795-806.

318 D.L. Croteau, V. Popuri, P.L. Opresko and V.A. Bohr, **(2014)** *Human RecQ helicases in DNA repair, recombination, and replication.* Annu Rev Biochem, 83: p. 519-52.

319 M. Zimmermann, T. Kibe, S. Kabir and T. de Lange, **(2014)** *TRF1 negotiates TTAGGG repeat-associated replication problems by recruiting the BLM helicase and the TPP1/POT1 repressor of ATR signaling.* Genes Dev, 28(22): p. 2477-91.

320 A.L. Moye, K.C. Porter, S.B. Cohen, T. Phan, K.G. Zyner, N. Sasaki, G.O. Lovrecz, J.L. Beck and T.M. Bryan, **(2015)** *Telomeric G-quadruplexes are a substrate and site of localization for human telomerase.* Nat Commun, 6: p. 7643.

321 K. Takahama, A. Takada, S. Tada, M. Shimizu, K. Sayama, R. Kurokawa and T. Oyoshi, **(2013)** *Regulation of telomere length by G-quadruplex*

telomere DNA- and TERRA-binding protein TLS/FUS. Chem Biol, 20(3): p. 341-50.

322 K.B. Marcu, S.A. Bossone and A.J. Patel, **(1992)** *myc function and regulation.* Annu Rev Biochem, 61: p. 809-60.

323 K.B. Wang, M.S.A. Elsayed, G. Wu, N. Deng, M. Cushman and D. Yang, **(2019)** *Indenoisoquinoline Topoisomerase Inhibitors Strongly Bind and Stabilize the MYC Promoter G-Quadruplex and Downregulate MYC.* J Am Chem Soc, 141(28): p. 11059-11070.

324 J.M. Santos-Pereira and A. Aguilera, **(2015)** *R loops: new modulators of genome dynamics and function.* Nat Rev Genet, 16(10): p. 583-97.

325 M.L. Duquette, P. Handa, J.A. Vincent, A.F. Taylor and N. Maizels, **(2004)** *Intracellular transcription of G-rich DNAs induces formation of G-loops, novel structures containing G4 DNA.* Genes Dev, 18(13): p. 1618-29.

326 A. De Magis, S.G. Manzo, M. Russo, J. Marinello, R. Morigi, O. Sordet and G. Capranico, **(2019)** *DNA damage and genome instability by G-quadruplex ligands are mediated by R loops in human cancer cells.* Proc Natl Acad Sci U S A, 116(3): p. 816-825.

327 C.Y. Lee, C. McNerney, K. Ma, W. Zhao, A. Wang and S. Myong, **(2020)** *R-loop induced G-quadruplex in non-template promotes transcription by successive R-loop formation.* Nat Commun, 11(1): p. 3392.

328 B.P. Belotserkovskii, J.H. Soo Shin and P.C. Hanawalt, **(2017)** *Strong transcription blockage mediated by R-loop formation within a G-rich homopurine-homopyrimidine sequence localized in the vicinity of the promoter.* Nucleic Acids Res, 45(11): p. 6589-6599.

329 B.P. Belotserkovskii, R. Liu, S. Tornaletti, M.M. Krasilnikova, S.M. Mirkin and P.C. Hanawalt, **(2010)** *Mechanisms and implications of transcription blockage by guanine-rich DNA sequences.* Proc Natl Acad Sci U S A, 107(29): p. 12816-21.

330 E.A. Raiber, R. Kranaster, E. Lam, M. Nikan and S. Balasubramanian, **(2012)** *A non-canonical DNA structure is a binding motif for the transcription factor SP1 in vitro.* Nucleic Acids Res, 40(4): p. 1499-508.

331 A. Kerkour, J. Marquevielle, S. Ivashchenko, L.A. Yatsunyk, J.L. Mergny and G.F. Salgado, **(2017)** *High-resolution three-dimensional NMR structure of the KRAS proto-oncogene promoter reveals key features of a G-quadruplex involved in transcriptional regulation.* J Biol Chem, 292(19): p. 8082-8091.

332 N. Kim, **(2019)** *The Interplay between G-quadruplex and Transcription.* Curr Med Chem, 26(16): p. 2898-2917.

333 J.L. Huppert, A. Bugaut, S. Kumari and S. Balasubramanian, **(2008)** *G-quadruplexes: the beginning and end of UTRs.* Nucleic Acids Res, 36(19): p. 6260-8.

334 G.S. Wilkie, K.S. Dickson and N.K. Gray, **(2003)** *Regulation of mRNA translation by 5'- and 3'-UTR-binding factors.* Trends Biochem Sci, 28(4): p. 182-8.

335 A. Gross, J.M. McDonnell and S.J. Korsmeyer, **(1999)** *BCL-2 family members and the mitochondria in apoptosis.* Genes Dev, 13(15): p. 1899-911.

336 R. Shahid, A. Bugaut and S. Balasubramanian, **(2010)** *The BCL-2 5' untranslated region contains an RNA G-quadruplex-forming motif that modulates protein expression.* Biochemistry, 49(38): p. 8300-6.

337 S.Q. Mao, A.T. Ghanbarian, J. Spiegel, S. Martinez Cuesta, D. Beraldi, M. Di Antonio, G. Marsico, R. Hansel-Hertsch, D. Tannahill and S. Balasubramanian, **(2018)** *DNA G-quadruplex structures mold the DNA methylome.* Nat Struct Mol Biol, 25(10): p. 951-957.

338 P. Prorok, M. Artufel, A. Aze, P. Coulombe, I. Peiffer, L. Lacroix, A. Guedin, J.L. Mergny, J. Damaschke, A. Schepers, C. Cayrou, M.P. Teulade-Fichou, B. Ballester and M. Mechali, **(2019)** *Involvement of G-quadruplex regions in mammalian replication origin activity.* Nat Commun, 10(1): p. 3274.

339 E. Butovskaya, P. Solda, M. Scalabrin, M. Nadai and S.N. Richter, **(2019)** *HIV-1 Nucleocapsid Protein Unfolds Stable RNA G-Quadruplexes in the Viral Genome and Is Inhibited by G-Quadruplex Ligands.* ACS Infect Dis, 5(12): p. 2127-2135.

340 T. de Lange, **(2005)** *Shelterin: the protein complex that shapes and safeguards human telomeres.* Genes Dev, 19(18): p. 2100-10.

341 D. Gomez, T. Wenner, B. Brassart, C. Douarre, M.F. O'Donohue, V. El Khoury, K. Shin-Ya, H. Morjani, C. Trentesaux and J.F. Riou, **(2006)** *Telomestatin-induced telomere uncapping is modulated by POT1 through G-overhang extension in HT1080 human tumor cells.* J Biol Chem, 281(50): p. 38721-9.

342 A.J. Zaug, E.R. Podell and T.R. Cech, **(2005)** *Human POT1 disrupts telomeric G-quadruplexes allowing telomerase extension in vitro.* Proc Natl Acad Sci U S A, 102(31): p. 10864-9.

343 P. Phatak, J.C. Cookson, F. Dai, V. Smith, R.B. Gartenhaus, M.F. Stevens and A.M. Burger, **(2007)** *Telomere uncapping by the G-quadruplex ligand RHPS4 inhibits clonogenic tumour cell growth in vitro and in vivo consistent with a cancer stem cell targeting mechanism.* Br J Cancer, 96(8): p. 1223-33.

344 A. Saharia, L. Guittat, S. Crocker, A. Lim, M. Steffen, S. Kulkarni and S.A. Stewart, **(2008)** *Flap endonuclease 1 contributes to telomere stability.* Curr Biol, 18(7): p. 496-500.

345 G. Guilbaud, P. Murat, B. Recolin, B.C. Campbell, A. Maiter, J.E. Sale and S. Balasubramanian, **(2017)** *Local epigenetic reprogramming induced by G-quadruplex ligands.* Nat Chem, 9(11): p. 1110-1117.

346 C. Papadopoulou, G. Guilbaud, D. Schiavone and J.E. Sale, **(2015)** *Nucleotide Pool Depletion Induces G-Quadruplex-Dependent Perturbation of Gene Expression.* Cell Rep, 13(11): p. 2491-2503.

347 E. Besnard, A. Babled, L. Lapasset, O. Milhavet, H. Parrinello, C. Dantec, J.M. Marin and J.M. Lemaitre, **(2012)** *Unraveling cell type-specific and reprogrammable human replication origin signatures associated with G-quadruplex consensus motifs.* Nat Struct Mol Biol, 19(8): p. 837-44.

348 A.M. Burger, F. Dai, C.M. Schultes, A.P. Reszka, M.J. Moore, J.A. Double and S. Neidle, **(2005)** *The G-quadruplex-interactive molecule BRACO-19 inhibits tumor growth, consistent with telomere targeting and interference with telomerase function.* Cancer Res, 65(4): p. 1489-96.

349 K.I. McLuckie, M. Di Antonio, H. Zecchini, J. Xian, C. Caldas, B.F. Krippendorff, D. Tannahill, C. Lowe and S. Balasubramanian, **(2013)** *G-*

quadruplex DNA as a molecular target for induced synthetic lethality in cancer cells. J Am Chem Soc, 135(26): p. 9640-3.

350 T.M. Abdel-Fatah, A. Arora, P. Moseley, C. Coveney, C. Perry, K. Johnson, C. Kent, G. Ball, S. Chan and S. Madhusudan, **(2014)** *ATM, ATR and DNA-PKcs expressions correlate to adverse clinical outcomes in epithelial ovarian cancers.* BBA Clin, 2: p. 10-7.

351 L. Deriano, O. Guipaud, H. Merle-Beral, J.L. Binet, M. Ricoul, G. Potocki-Veronese, V. Favaudon, Z. Maciorowski, C. Muller, B. Salles, L. Sabatier and J. Delic, **(2005)** *Human chronic lymphocytic leukemia B cells can escape DNA damage-induced apoptosis through the nonhomologous end-joining DNA repair pathway.* Blood, 105(12): p. 4776-83.

352 W. Li, C. Xie, Z. Yang, J. Chen and N.H. Lu, **(2013)** *Abnormal DNA-PKcs and Ku 70/80 expression may promote malignant pathological processes in gastric carcinoma.* World J Gastroenterol, 19(40): p. 6894-901.

353 E. Willmore, S.L. Elliott, T. Mainou-Fowler, G.P. Summerfield, G.H. Jackson, F. O'Neill, C. Lowe, A. Carter, R. Harris, A.R. Pettitt, C. Cano-Soumillac, R.J. Griffin, I.G. Cowell, C.A. Austin and B.W. Durkacz, **(2008)** *DNA-dependent protein kinase is a therapeutic target and an indicator of poor prognosis in B-cell chronic lymphocytic leukemia.* Clin Cancer Res, 14(12): p. 3984-92.

354 S.J. Harnor, A. Brennan and C. Cano, **(2017)** *Targeting DNA-Dependent Protein Kinase for Cancer Therapy.* ChemMedChem, 12(12): p. 895-900.

355 D. Davidson, L. Amrein, L. Panasci and R. Aloyz, **(2013)** *Small Molecules, Inhibitors of DNA-PK, Targeting DNA Repair, and Beyond.* Front Pharmacol, 4: p. 5.

356 I. Beuvink, A. Boulay, S. Fumagalli, F. Zilbermann, S. Ruetz, T. O'Reilly, F. Natt, J. Hall, H.A. Lane and G. Thomas, **(2005)** *The mTOR inhibitor RAD001 sensitizes tumor cells to DNA-damaged induced apoptosis through inhibition of p21 translation.* Cell, 120(6): p. 747-59.

357 R.A. Izzard, S.P. Jackson and G.C. Smith, **(1999)** *Competitive and noncompetitive inhibition of the DNA-dependent protein kinase.* Cancer Res, 59(11): p. 2581-6.

358 S. Boulton, S. Kyle, L. Yalcintepe and B.W. Durkacz, **(1996)** *Wortmannin is a potent inhibitor of DNA double strand break but not single strand break repair in Chinese hamster ovary cells.* Carcinogenesis, 17(11): p. 2285-90.

359 C.J. Vlahos, W.F. Matter, K.Y. Hui and R.F. Brown, **(1994)** *A specific inhibitor of phosphatidylinositol 3-kinase, 2-(4-morpholinyl)-8-phenyl-4H-1-benzopyran-4-one (LY294002).* J Biol Chem, 269(7): p. 5241-8.

360 I.R. Hardcastle, X. Cockcroft, N.J. Curtin, M.D. El-Murr, J.J. Leahy, M. Stockley, B.T. Golding, L. Rigoreau, C. Richardson, G.C. Smith and R.J. Griffin, **(2005)** *Discovery of potent chromen-4-one inhibitors of the DNA-dependent protein kinase (DNA-PK) using a small-molecule library approach.* J Med Chem, 48(24): p. 7829-46.

361 L. Hu, C. Zaloudek, G.B. Mills, J. Gray and R.B. Jaffe, **(2000)** *In vivo and in vitro ovarian carcinoma growth inhibition by a phosphatidylinositol 3-kinase inhibitor (LY294002).* Clin Cancer Res, 6(3): p. 880-6.

362 S. Semba, N. Itoh, M. Ito, M. Harada and M. Yamakawa, **(2002)** *The in vitro and in vivo effects of 2-(4-morpholinyl)-8-phenyl-chromone (LY294002), a specific inhibitor of phosphatidylinositol 3'-kinase, in human colon cancer cells.* Clin Cancer Res, 8(6): p. 1957-63.

363 Y. Zhao, H.D. Thomas, M.A. Batey, I.G. Cowell, C.J. Richardson, R.J. Griffin, A.H. Calvert, D.R. Newell, G.C. Smith and N.J. Curtin, **(2006)** *Preclinical evaluation of a potent novel DNA-dependent protein kinase inhibitor NU7441.* Cancer Res, 66(10): p. 5354-62.

364 S. Kalepu and V. Nekkanti, **(2015)** *Insoluble drug delivery strategies: review of recent advances and business prospects.* Acta Pharm Sin B, 5(5): p. 442-53.

365 F.T. Zenke, A. Zimmermann, C. Sirrenberg, H. Dahmen, L. Vassilev, U. Pehl, T. Fuchss and A. Blaukat, **(2016)** *Abstract 1658: M3814, a novel investigational DNA-PK inhibitor: enhancing the effect of fractionated radiotherapy leading to complete regression of tumors in mice.* 76(14 Supplement): p. 1658-1658.

366 I.S. Mohiuddin and M.H. Kang, **(2019)** *DNA-PK as an Emerging Therapeutic Target in Cancer.* Front Oncol, 9: p. 635.

367 Q. Ding, Y.V. Reddy, W. Wang, T. Woods, P. Douglas, D.A. Ramsden, S.P. Lees-Miller and K. Meek, **(2003)** *Autophosphorylation of the catalytic subunit of the DNA-dependent protein kinase is required for efficient end processing during DNA double-strand break repair.* Mol Cell Biol, 23(16): p. 5836-48.

368 D. White, I.U. Rafalska-Metcalf, A.V. Ivanov, A. Corsinotti, H. Peng, S.C. Lee, D. Trono, S.M. Janicki and F.J. Rauscher, 3rd, **(2012)** *The ATM substrate KAP1 controls DNA repair in heterochromatin: regulation by HP1 proteins and serine 473/824 phosphorylation.* Mol Cancer Res, 10(3): p. 401-14.

369 R. Baskar, K.A. Lee, R. Yeo and K.W. Yeoh, **(2012)** *Cancer and radiation therapy: current advances and future directions.* Int J Med Sci, 9(3): p. 193-9.

370 K. Nurgali, R.T. Jagoe and R. Abalo, **(2018)** *Editorial: Adverse Effects of Cancer Chemotherapy: Anything New to Improve Tolerance and Reduce Sequelae?* Front Pharmacol, 9: p. 245.

371 R. Rodriguez, S. Muller, J.A. Yeoman, C. Trentesaux, J.F. Riou and S. Balasubramanian, **(2008)** *A novel small molecule that alters shelterin integrity and triggers a DNA-damage response at telomeres.* J Am Chem Soc, 130(47): p. 15758-9.

372 S. Muller, S. Kumari, R. Rodriguez and S. Balasubramanian, **(2010)** *Small-molecule-mediated G-quadruplex isolation from human cells.* Nat Chem, 2(12): p. 1095-8.

373 S. Muller, D.A. Sanders, M. Di Antonio, S. Matsis, J.F. Riou, R. Rodriguez and S. Balasubramanian, **(2012)** *Pyridostatin analogues promote telomere dysfunction and long-term growth inhibition in human cancer cells.* Org Biomol Chem, 10(32): p. 6537-46.

374 Y. Pommier, M.J. O'Connor and J. de Bono, **(2016)** *Laying a trap to kill cancer cells: PARP inhibitors and their mechanisms of action.* Sci Transl Med, 8(362): p. 362ps17.

375 J. Zimmer, *Roles of BRCA1 and BRCA2 in DNA Replication and Genome Stability*, in *Department of Oncology.* **(2017)**, University of Oxford.

376 J. Gu, H. Lu, B. Tippin, N. Shimazaki, M.F. Goodman and M.R. Lieber, **(2007)** *XRCC4:DNA ligase IV can ligate incompatible DNA ends and can ligate across gaps.* EMBO J, 26(4): p. 1010-23.

377 G.C. Smith and S.P. Jackson, **(1999)** *The DNA-dependent protein kinase.* Genes Dev, 13(8): p. 916-34.

378 J. Nacson, J.J. Krais, A.J. Bernhardy, E. Clausen, W. Feng, Y. Wang, E. Nicolas, K.Q. Cai, R. Tricarico, X. Hua, D. DiMarcantonio, E. Martinez, D. Zong, E.A. Handorf, A. Bellacosa, J.R. Testa, A. Nussenzweig, G.P. Gupta, S.M. Sykes and N. Johnson, **(2018)** *BRCA1 Mutation-Specific Responses to 53BP1 Loss-Induced Homologous Recombination and PARP Inhibitor Resistance.* Cell Rep, 24(13): p. 3513-3527 e7.

379 D. Zong, S. Adam, Y. Wang, H. Sasanuma, E. Callen, M. Murga, A. Day, M.J. Kruhlak, N. Wong, M. Munro, A. Ray Chaudhuri, B. Karim, B. Xia, S. Takeda, N. Johnson, D. Durocher and A. Nussenzweig, **(2019)** *BRCA1 Haploinsufficiency Is Masked by RNF168-Mediated Chromatin Ubiquitylation.* Mol Cell, 73(6): p. 1267-1281 e7.

380 M. Barazas, A. Gasparini, Y. Huang, A. Kucukosmanoglu, S. Annunziato, P. Bouwman, W. Sol, A. Kersbergen, N. Proost, R. de Korte-Grimmerink, M. van de Ven, J. Jonkers, G.R. Borst and S. Rottenberg, **(2019)** *Radiosensitivity Is an Acquired Vulnerability of PARPi-Resistant BRCA1-Deficient Tumors.* Cancer Res, 79(3): p. 452-460.

381 E.M. Tacconi, S. Badie, G. De Gregoriis, T. Reislander, X. Lai, M. Porru, C. Folio, J. Moore, A. Kopp, J. Baguna Torres, D. Sneddon, M. Green, S. Dedic, J.W. Lee, A.S. Batra, O.M. Rueda, A. Bruna, C. Leonetti, C. Caldas, B. Cornelissen, L. Brino, A. Ryan, A. Biroccio and M. Tarsounas, **(2019)** *Chlorambucil targets BRCA1/2-deficient tumours and counteracts PARP inhibitor resistance.* EMBO Mol Med, 11(7): p. e9982.

382 C. Cruz, M. Castroviejo-Bermejo, S. Gutierrez-Enriquez, A. Llop-Guevara, Y.H. Ibrahim, A. Gris-Oliver, S. Bonache, B. Morancho, A. Bruna, O.M. Rueda, Z. Lai, U.M. Polanska, G.N. Jones, P. Kristel, L. de Bustos, M. Guzman, O. Rodriguez, J. Grueso, G. Montalban, G. Caratu, F. Mancuso, R. Fasani, J. Jimenez, W.J. Howat, B. Dougherty, A. Vivancos, P. Nuciforo, X. Serres-Creixams, I.T. Rubio, A. Oaknin, E. Cadogan, J.C. Barrett, C. Caldas, J. Baselga, C. Saura, J. Cortes, J. Arribas, J. Jonkers, O. Diez, M.J.

O'Connor, J. Balmana and V. Serra, **(2018)** *RAD51 foci as a functional biomarker of homologous recombination repair and PARP inhibitor resistance in germline BRCA-mutated breast cancer.* Ann Oncol, 29(5): p. 1203-1210.

383 H.C. Lee, H. Wang, V. Baladandayuthapani, H. Lin, J. He, R.J. Jones, I. Kuiatse, D. Gu, Z. Wang, W. Ma, J. Lim, S. O'Brien, J. Keats, J. Yang, R.E. Davis and R.Z. Orlowski, **(2017)** *RNA Polymerase I Inhibition with CX-5461 as a Novel Therapeutic Strategy to Target MYC in Multiple Myeloma.* Br J Haematol, 177(1): p. 80-94.

384 S. Rottenberg, A.O. Nygren, M. Pajic, F.W. van Leeuwen, I. van der Heijden, K. van de Wetering, X. Liu, K.E. de Visser, K.G. Gilhuijs, O. van Tellingen, J.P. Schouten, J. Jonkers and P. Borst, **(2007)** *Selective induction of chemotherapy resistance of mammary tumors in a conditional mouse model for hereditary breast cancer.* Proc Natl Acad Sci U S A, 104(29): p. 12117-22.

385 I.M. Ward, X. Wu and J. Chen, **(2001)** *Threonine 68 of Chk2 is phosphorylated at sites of DNA strand breaks.* J Biol Chem, 276(51): p. 47755-8.

386 Q. Sun, Y. Guo, X. Liu, F. Czauderna, M.I. Carr, F.T. Zenke, A. Blaukat and L.T. Vassilev, **(2019)** *Therapeutic Implications of p53 Status on Cancer Cell Fate Following Exposure to Ionizing Radiation and the DNA-PK Inhibitor M3814.* Mol Cancer Res, 17(12): p. 2457-2468.

387 J.J. Leahy, B.T. Golding, R.J. Griffin, I.R. Hardcastle, C. Richardson, L. Rigoreau and G.C. Smith, **(2004)** *Identification of a highly potent and selective DNA-dependent protein kinase (DNA-PK) inhibitor (NU7441) by screening of chromenone libraries.* Bioorg Med Chem Lett, 14(24): p. 6083-7.

388 S. Liu, S.O. Opiyo, K. Manthey, J.G. Glanzer, A.K. Ashley, C. Amerin, K. Troksa, M. Shrivastav, J.A. Nickoloff and G.G. Oakley, **(2012)** *Distinct roles for DNA-PK, ATM and ATR in RPA phosphorylation and checkpoint activation in response to replication stress.* Nucleic Acids Res, 40(21): p. 10780-94.

389 A.K. Ashley, M. Shrivastav, J. Nie, C. Amerin, K. Troksa, J.G. Glanzer, S. Liu, S.O. Opiyo, D.D. Dimitrova, P. Le, B. Sishc, S.M. Bailey, G.G. Oakley and J.A. Nickoloff, **(2014)** *DNA-PK phosphorylation of RPA32 Ser4/Ser8*

regulates replication stress checkpoint activation, fork restart, homologous recombination and mitotic catastrophe. DNA Repair (Amst), 21: p. 131-9.

390 C.M. Simbulan-Rosenthal, D.S. Rosenthal, S. Iyer, A.H. Boulares and M.E. Smulson, **(1998)** *Transient poly(ADP-ribosyl)ation of nuclear proteins and role of poly(ADP-ribose) polymerase in the early stages of apoptosis.* J Biol Chem, 273(22): p. 13703-12.

391 A.H. Boulares, A.G. Yakovlev, V. Ivanova, B.A. Stoica, G. Wang, S. Iyer and M. Smulson, **(1999)** *Role of poly(ADP-ribose) polymerase (PARP) cleavage in apoptosis. Caspase 3-resistant PARP mutant increases rates of apoptosis in transfected cells.* J Biol Chem, 274(33): p. 22932-40.

392 A.G. Thorsell, T. Ekblad, T. Karlberg, M. Low, A.F. Pinto, L. Tresaugues, M. Moche, M.S. Cohen and H. Schuler, **(2017)** *Structural Basis for Potency and Promiscuity in Poly(ADP-ribose) Polymerase (PARP) and Tankyrase Inhibitors.* J Med Chem, 60(4): p. 1262-1271.

393 B. Wang, D. Chu, Y. Feng, Y. Shen, M. Aoyagi-Scharber and L.E. Post, **(2016)** *Discovery and Characterization of (8S,9R)-5-Fluoro-8-(4-fluorophenyl)-9-(1-methyl-1H-1,2,4-triazol-5-yl)-2,7,8,9-te trahydro-3H-pyrido[4,3,2-de]phthalazin-3-one (BMN 673, Talazoparib), a Novel, Highly Potent, and Orally Efficacious Poly(ADP-ribose) Polymerase-1/2 Inhibitor, as an Anticancer Agent.* J Med Chem, 59(1): p. 335-57.

394 E. Sanij, K.M. Hannan, J. Xuan, S. Yan, J.E. Ahern, A.S. Trigos, N. Brajanovski, J. Son, K.T. Chan, O. Kondrashova, E. Lieschke, M.J. Wakefield, D. Frank, S. Ellis, C. Cullinane, J. Kang, G. Poortinga, P. Nag, A.J. Deans, K.K. Khanna, L. Mileshkin, G.A. McArthur, J. Soong, E. Berns, R.D. Hannan, C.L. Scott, K.E. Sheppard and R.B. Pearson, **(2020)** *CX-5461 activates the DNA damage response and demonstrates therapeutic efficacy in high-grade serous ovarian cancer.* Nat Commun, 11(1): p. 2641.

395 R. Biehs, M. Steinlage, O. Barton, S. Juhasz, J. Kunzel, J. Spies, A. Shibata, P.A. Jeggo and M. Lobrich, **(2017)** *DNA Double-Strand Break Resection Occurs during Non-homologous End Joining in G1 but Is Distinct from Resection during Homologous Recombination.* Mol Cell, 65(4): p. 671-684 e5.

396 J.V. Forment, R.V. Walker and S.P. Jackson, **(2012)** *A high-throughput, flow cytometry-based method to quantify DNA-end resection in mammalian cells.* Cytometry A, 81(10): p. 922-8.

397 A.C. Vitor, P. Huertas, G. Legube and S.F. de Almeida, **(2020)** *Studying DNA Double-Strand Break Repair: An Ever-Growing Toolbox.* Front Mol Biosci, 7: p. 24.

398 A. Gunn and J.M. Stark, **(2012)** *I-SceI-based assays to examine distinct repair outcomes of mammalian chromosomal double strand breaks.* Methods Mol Biol, 920: p. 379-91.

399 P. Roidos, S. Sungalee, S. Benfatto, O. Sercin, A.M. Stutz, A. Abdollahi, J. Mauer, F.T. Zenke, J.O. Korbel and B.R. Mardin, **(2020)** *A scalable CRISPR/Cas9-based fluorescent reporter assay to study DNA double-strand break repair choice.* Nat Commun, 11(1): p. 4077.

400 S. Ray, D. Tillo, R.E. Boer, N. Assad, M. Barshai, G. Wu, Y. Orenstein, D. Yang, J.S. Schneekloth, Jr. and C. Vinson, **(2020)** *Custom DNA Microarrays Reveal Diverse Binding Preferences of Proteins and Small Molecules to Thousands of G-Quadruplexes.* ACS Chem Biol, 15(4): p. 925-935.

401 T.C. Chou, **(2010)** *Drug combination studies and their synergy quantification using the Chou-Talalay method.* Cancer Res, 70(2): p. 440-6.

402 V.M. Vassin, R.W. Anantha, E. Sokolova, S. Kanner and J.A. Borowiec, **(2009)** *Human RPA phosphorylation by ATR stimulates DNA synthesis and prevents ssDNA accumulation during DNA-replication stress.* J Cell Sci, 122(Pt 22): p. 4070-80.

403 C.T. Olivieri M, Álvarez-Quilón A, Li K, Schellenberg MJ, Zimmermann M, Hustedt N, Rossi SE, Adam S, Melo H, Heijink AM, Sastre-Moreno G, Moatti N, Szilard R, McEwan A, Ling AK, Serrano-Benitez A, Ubhi T, Delgado-Sainz I, Ferguson MW, Brown GW, Cortés-Ledesma F, Williams RS, Martin A, Xu D, Durocher D, **(2019)** *A genetic map of the response to DNA damage in human cells.* bioRxiv: p.

404 P.M. Bruno, M. Lu, K.A. Dennis, H. Inam, C.J. Moore, J. Sheehe, S.J. Elledge, M.T. Hemann and J.R. Pritchard, **(2020)** *The primary mechanism*

of cytotoxicity of the chemotherapeutic agent CX-5461 is topoisomerase II poisoning. Proc Natl Acad Sci U S A, 117(8): p. 4053-4060.

405 V. Quennet, A. Beucher, O. Barton, S. Takeda and M. Lobrich, **(2011)** *CtIP and MRN promote non-homologous end-joining of etoposide-induced DNA double-strand breaks in G1.* Nucleic Acids Res, 39(6): p. 2144-52.

406 A. Cristini, J.H. Park, G. Capranico, G. Legube, G. Favre and O. Sordet, **(2016)** *DNA-PK triggers histone ubiquitination and signaling in response to DNA double-strand breaks produced during the repair of transcription-blocking topoisomerase I lesions.* Nucleic Acids Res, 44(3): p. 1161-78.

407 J.M. Wheeler, N.E. Beck, H.C. Kim, I.P. Tomlinson, N.J. Mortensen and W.F. Bodmer, **(1999)** *Mechanisms of inactivation of mismatch repair genes in human colorectal cancer cell lines: the predominant role of hMLH1.* Proc Natl Acad Sci U S A, 96(18): p. 10296-301.

408 S.A. Lujan, J.S. Williams, A.R. Clausen, A.B. Clark and T.A. Kunkel, **(2013)** *Ribonucleotides are signals for mismatch repair of leading-strand replication errors.* Mol Cell, 50(3): p. 437-43.

409 A. Vaisman, J.P. McDonald, D. Huston, W. Kuban, L. Liu, B. Van Houten and R. Woodgate, **(2013)** *Removal of misincorporated ribonucleotides from prokaryotic genomes: an unexpected role for nucleotide excision repair.* PLoS Genet, 9(11): p. e1003878.

410 F. Coquel, M.J. Silva, H. Techer, K. Zadorozhny, S. Sharma, J. Nieminuszczy, C. Mettling, E. Dardillac, A. Barthe, A.L. Schmitz, A. Promonet, A. Cribier, A. Sarrazin, W. Niedzwiedz, B. Lopez, V. Costanzo, L. Krejci, A. Chabes, M. Benkirane, Y.L. Lin and P. Pasero, **(2018)** *SAMHD1 acts at stalled replication forks to prevent interferon induction.* Nature, 557(7703): p. 57-61.

411 T. Reislander, E.P. Lombardi, F.J. Groelly, A. Miar, M. Porru, S. Di Vito, B. Wright, H. Lockstone, A. Biroccio, A. Harris, A. Londono-Vallejo and M. Tarsounas, **(2019)** *BRCA2 abrogation triggers innate immune responses potentiated by treatment with PARP inhibitors.* Nat Commun, 10(1): p. 3143.

412 B.A. Weaver, **(2014)** *How Taxol/paclitaxel kills cancer cells.* Mol Biol Cell, 25(18): p. 2677-81.

413 C. Zierhut, N. Yamaguchi, M. Paredes, J.D. Luo, T. Carroll and H. Funabiki, **(2019)** *The Cytoplasmic DNA Sensor cGAS Promotes Mitotic Cell Death.* Cell, 178(2): p. 302-315 e23.

414 V. Dieras, H.S. Han, B. Kaufman, H. Wildiers, M. Friedlander, J.P. Ayoub, S.L. Puhalla, I. Bondarenko, M. Campone, E.H. Jakobsen, M. Jalving, C. Oprean, M. Palacova, Y.H. Park, Y. Shparyk, E. Yanez, N. Khandelwal, M.G. Kundu, M. Dudley, C.K. Ratajczak, D. Maag and B.K. Arun, **(2020)** *Veliparib with carboplatin and paclitaxel in BRCA-mutated advanced breast cancer (BROCADE3): a randomised, double-blind, placebo-controlled, phase 3 trial.* Lancet Oncol, 21(10): p. 1269-1282.

415 S.M. Domchek, S. Postel-Vinay, S.A. Im, Y.H. Park, J.P. Delord, A. Italiano, J. Alexandre, B. You, S. Bastian, M.G. Krebs, D. Wang, S.N. Waqar, M. Lanasa, J. Rhee, H. Gao, V. Rocher-Ros, E.V. Jones, S. Gulati, A. Coenen-Stass, I. Kozarewa, Z. Lai, H.K. Angell, L. Opincar, P. Herbolsheimer and B. Kaufman, **(2020)** *Olaparib and durvalumab in patients with germline BRCA-mutated metastatic breast cancer (MEDIOLA): an open-label, multicentre, phase 1/2, basket study.* Lancet Oncol, 21(9): p. 1155-1164.

416 M.L. Telli, **(2020)** *BROCADE3: a challenge to the treatment paradigm in BRCA breast cancer?* Lancet Oncol, 21(10): p. 1254-1255.

417 G. Gallo-Oller, R. Ordonez and J. Dotor, **(2018)** *A new background subtraction method for Western blot densitometry band quantification through image analysis software.* J Immunol Methods, 457: p. 1-5.

7 Appendix

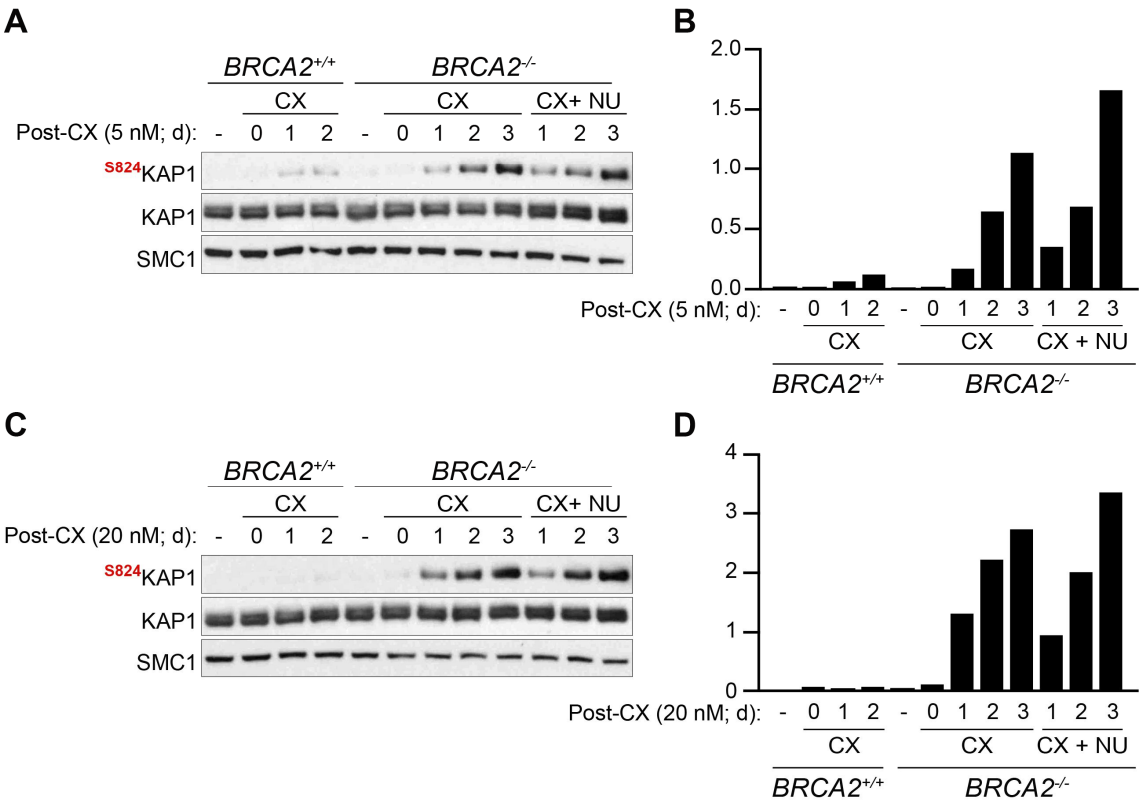
List of supplementary figures

Supplementary Figure 1: Effect of DNA-PKcs inhibitor NU7441 on BRCA2-deficient cells upon CX5461 treatment 143

Supplementary Figure 2: Recovery of BRCA-deficient mouse cells upon PDS and olaparib treatment 144

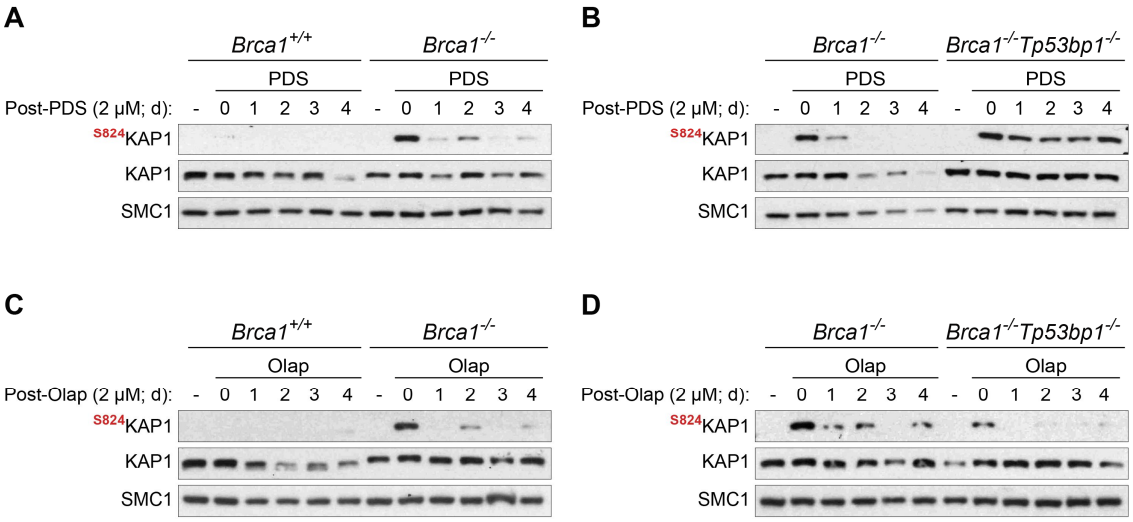
Supplementary Figure 3: Recovery of BRCA-deficient mouse cells upon PDS and olaparib treatment 145

Supplementary Figure 4: Effect of CtIP depletion on BRCA1-/ 53BP1-deficient cells upon PDS treatment 146



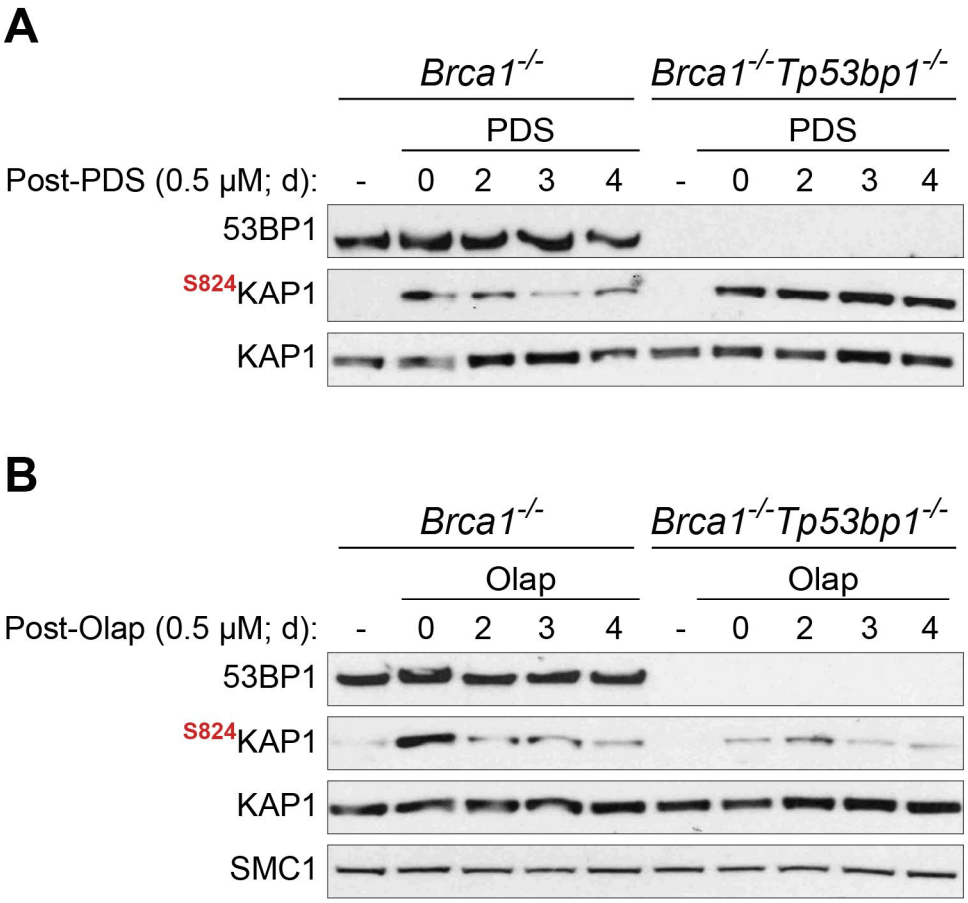
Supplementary Figure 1: Effect of DNA-PKcs inhibitor NU7441 on BRCA2-deficient cells upon CX5461 treatment

(A, C) Human DLD1 cells BRCA2-proficient incubated with 5 or 20 nM CX5461 for 24 hours and released into growth medium with 0.25 M NU7441 or fresh growth medium. Cells were then treated daily with 0.25 M NU7441 or supplemented with fresh growth medium for indicated time. Whole-cell extracts were prepared after treatment and immunoblotted as indicated. SMC1 was used as loading control. (B, D) Quantitative graph of (A) and (C) respectively.



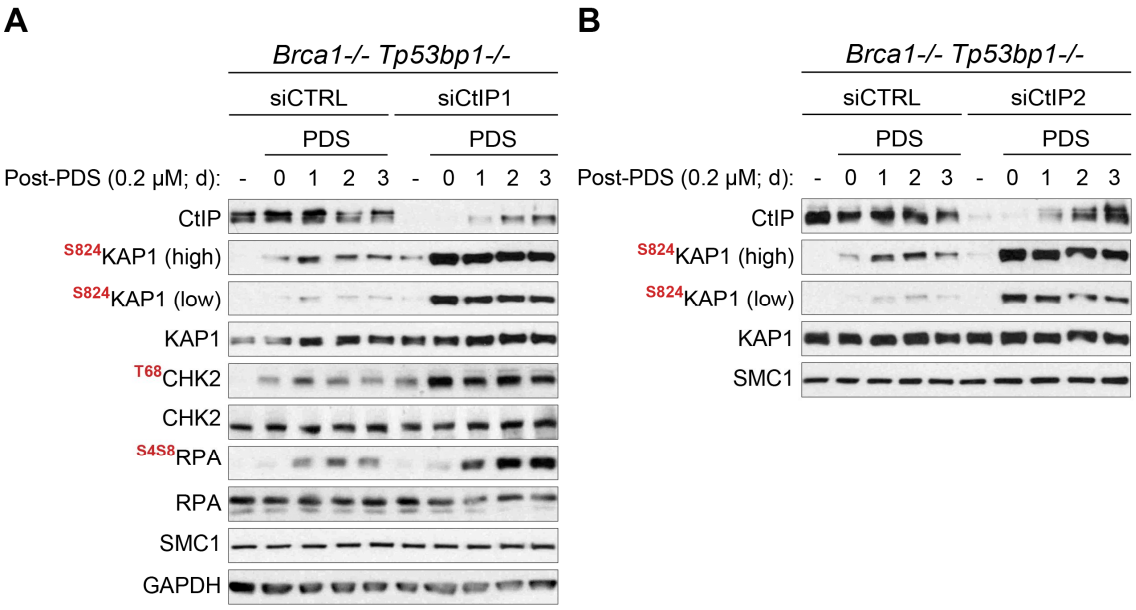
Supplementary Figure 2: Recovery of BRCA-deficient mouse cells upon PDS and olaparib treatment

(A, B) Mouse BRCA-proficient (*Brca1*$^{+/+}$), BRCA1-deficient (*Brca1*$^{-/-}$), (B, D) BRCA1-/ 53BP1-deficient (*Brca1*$^{-/-}$ *Tp53bp1*$^{-/-}$) cells were incubated with 2 µM PDS (A, B) or 2 M olaparib (C, D) for 24 hours and released into fresh growth medium for indicated time. Whole-cell extracts were prepared after treatment and immunoblotted as indicated. SMC1 was used as loading control.



Supplementary Figure 3: Recovery of BRCA-deficient mouse cells upon PDS and olaparib treatment

(A) Mouse BRCA1-deficient (*Brca1*$^{-/-}$), BRCA1-/ 53BP1-deficient (*Brca1*$^{-/-}$ *Tp53bp1*$^{-/-}$) cells were incubated with 0.5 µM PDS (A) or 0.5 M olaparib (B) for 24 hours then released into fresh growth medium for indicated time. Whole-cell extracts were prepared after treatment and immunoblotted as indicated. KAP1 or SMC1 was used as loading control.



Supplementary Figure 4: Effect of CtIP depletion on BRCA1-/ 53BP1-deficient cells upon PDS treatment

(A, B) Mouse BRCA1-/ 53BP1-deficient (*Brca1*$^{-/-}$ *Tp53bp1*$^{-/-}$) cells were treated with siRNAs against CtIP or siCTRL then incubated with 0.2 µM PDS for 24 hours and released into fresh growth medium. Whole-cell extracts were prepared after treatment and immunoblotted as indicated. SMC1 and GAPDH were used as loading controls. (high) and (low) refer to a long and short exposure to chemiluminescent reagent.